THÈSE

En vue de l'obtention du

DOCTORAT DE L'UNIVERSITÉ DE TOULOUSE

Délivré par *Université Toulouse 3 Paul Sabatier (UT3 Paul Sabatier)*
Discipline ou spécialité : *Génie Electrique*

Présentée et soutenue par *Yuan ZHANG*
Le *jeudi 4 décembre 2014*

Titre :
A new flat dark discharge lamp for backlight applications based on electron–excited– phosphor luminescence

---

JURY
Jean-Marc Bauchire, Prof.
Ray-Lee Lin, Prof.
Christian Glaize, Prof.
Yann Cressault, Maître des Conférences HdR.

Ecole doctorale : *ED GEET*
Unité de recherche : *Laboratoire plasma et conversion d'énergie*
Directeur(s) de Thèse : *Georges ZISSIS*
Rapporteurs : *Jean-Marc Bauchire, Prof. Ray-Lee Lin, Prof.*

Acknowledgements

First of all, I would like to express my deepest gratitude to Professor Georges Zissis, my research supervisor, for his patient guidance, enthusiastic encouragement and useful critiques of this research work. He has deep insight into the lighting and light sources industry, and is quite sensitive to the new trends in the technology development. Every discussion with him will inspire me with many new ideas. He is always confident and optimistic in the face of difficulty. What I learn from him is not only about the knowledge but also the attitude to the future life.

I would like to thank Dr. Sounil BHOSLE for his guide and help with the vacuum system and the glass work, and Dr. Spiros Kitsinelis for his advice and assistance on the experiment and my paper work. My grateful thanks are also extended to all the teachers and technicians in our group: such as Mr. David BUSO, Mr. Laurent CANALE, Mr. Pascal DUPUIS, Mr. Manuel LOPES, Mr. Marc TERNISIEN, Mr. Cédric RENAUD, Mr. Jean-Luc, Mr. Gérald LEDRU and etc, for their kind and patient suggestions, without which I could have not complete my thesis.

My sincere appreciation goes to my dear colleagues: Lydie AREXIS BOISSON, Arezki TOUMI, Ikbal MARGHAD, Laure BARREYRE-PANDELE, Angel BARROSO, Sovannarith LENG, Alaa ALCHADDOUD, Feng TIAN, and Ahmad Nazri Dagang. Your warmheartedness and kindness support my daily life and study in France.

I wish to appreciate the help provided by Prof. M.C. Liu and and his group from Energy and Environment Research Laboratories of Industrial Technology Research Institute in Taiwan, who participated this study with great cooperation. And I would like to acknowledge the generous help from Prof. Shanduan ZHANG and other faculties and friends in Fudan University too.

I would also like to extend my thanks to all the members in laboratory Laplace and all my dear friends in France and China for their encouragement and support. It is indeed my pleasure to meet and cooperate with them.

Finally, I wish to thank my parents for their support and encouragement throughout my study and life.

Table of contents

General introduction

Since the first practical incandescent lamp was manufactured by Edison, electrical light sources have been developed for more than 100 years. There are three generation light sources: incandescent lamp, discharge lamp and solid state lamp. Incandescent lamps produce light by heating a filament until it glows. Discharge lamps produce light by ionizing a gas through electric discharge inside the lamp. Solid-state lamps (SSL) use a phenomenon called electroluminescence (when electrons transit between the specific energy levels of different materials in semiconductor under the external electric field, the extra energy between the band gap could be emitted by means of photons) to convert electrical energy directly to light. The normal incandescent lamps have been banned in many countries (such as USA from 2014) due to its low luminance efficacy, since the commercial CFL and SSL products could perfectly take their place by the good lighting performance and energy saving. Although LEDs and OLEDs as typical SSL have promising future in lighting and display industry, the gas discharge lamps are still dominating the most indoor or outdoor applications nowadays.

The flat dark discharge lamp (FDDL) studied in this thesis is a new kind of discharge lamp in which no mercury is used. The visible emission is coming from the phosphor instead of the discharged buffer gas, so called dark discharge lamp. It borrows the ideas from the general low pressure discharge lamp and the cathode ray tube. As a lamp its lighting mechanism is brand new compared with the traditional discharge lamps which generally work in the glow or arc discharge regime. It employs the CL phosphor ($ZnS:Cu,Al+In_2O_3$) which is widely applied in the CRT, without which lamp could be dark. The gas pressure is about 0.2 mbar which is lower than the general low pressure mercury lamp and higher than that in the CRT or FED. This pressure can maintain high lamp voltage to accelerate electrons to excite the phosphor while the ionization of gas atoms produces electrons in the space.

Traditional discharge lamps work under glow or arc discharge regimes, while the FDDL we studied functions in the regime between Townsend discharge regimes and glow discharge region. Its gas pressure is higher than the field emission display device and its lamp voltage is higher than that of normal low pressure mercury discharge lamp or PDP. Visible radiation directly from the gas discharge is quite limited in such high E/n value ($\sim 10^5$ Td, reduced electric field, E is electric field, n is the density of gas), but due to the high energy initial and

secondary electrons will contribute to the light emission. As a new candidate for the green backlight application, a better understanding needs to be explored.

The manuscript is organized in 3 chapters as follows: **the first chapter** presents the family of artificial electrical light sources, including incandescent lamp, discharge lamp and solid state lamp. Their history, working mechanism and development are introduced in this part. Further introduction of our lamp and some basic numerical calculation are introduced in **the second chapter**, in which the excitation and ionization mean free paths are used to analyze qualitatively the physics behind the threshold pressure for the FDDL. The lighting mechanism of FDDL is also introduced and compared with that of traditional FL, HID and CRT in this chapter. **The third part** shows our experiment results. The tests on the sample lamps explore some feathers of FDDL. And the experiment results of FDDL at different pressure filled with Neon and Xenon are also presented and discussed in this chapter.

This thesis work has been done in LM (Lumière et Matière) group of LAPLACE (LAboratoire PLAsma et Conversion d'Energie) with the collaboration of Prof. M.C. Liu and his group from energy and environment research laboratories in industrial technology research institute in Taiwan.

CHAPTER I:

Introduction- Electrical Light Sources

Human has the inner interest for brightness. Life without light is unimaginable. In the modern times electrical light sources allow us to extend our activities, such as working, travel and entertainment, beyond the daylight hours. Factories and office buildings are designed with no possibility of ever being adequately illuminated by daylight. Worldwide communication would be impossible if half the world could not dispel the darkness by turning on the light at the flick of a switch. Electrical light sources are very important in present daily life.

The electric light sources, called lamps and used for providing illumination, can be divided into three general classes: incandescent, discharge, and solid-state lamps. Incandescent lamps produce light by heating a filament until it glows. Discharge lamps produce light by ionizing a gas through electric discharge inside the lamp. Solid-state lamps use a phenomenon called electroluminescence to convert electrical energy directly to light.

I.1 Incandescent Lamps

The incandescent lamp is one of the longest existing electro-technical products, its history comprises about 200 years. The essential start of this history is the experiment of Sir Humphrey Davy in 1802 whereby a Pt wire was heated to incandescence by the passage of current from a Voltaic pile. The first historic milestone was reached with the carbon filament lamp of Edison in 1879. And in 1912 the gas-filled tungsten filament lamp came to the world. In 1959 the halogen lamp was invented [1].

Incandescent lamp technology uses electric current to heat a coiled tungsten filament to incandescence. The glass envelope contains a mixture of nitrogen and a small amount of other inert gases such as argon. Some incandescent lamps, such as some flashlight lamps, also contain xenon. Thomas Edison’s first carbon filament lamp had a life of about 40 hours.

Today, commonly available incandescent lamps have average lives of between 750 and 2000 hours. Figure 1.1 shows the construction of a typical incandescent lamp.

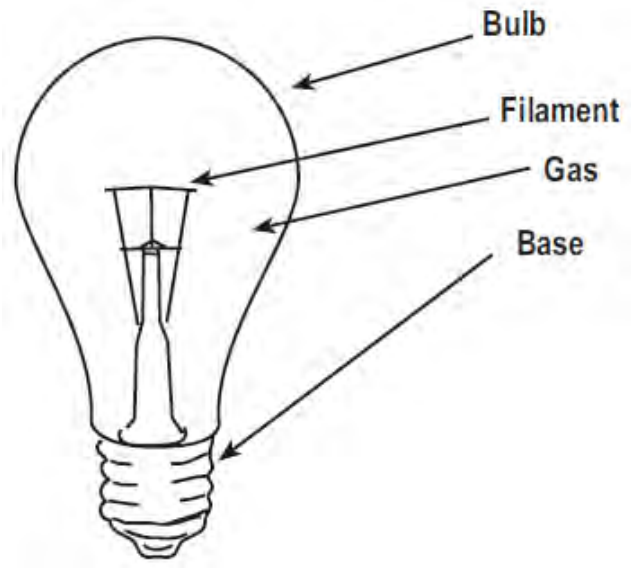

Fig.1.1 Construction of a Incandescent lamp

Incandescent lamps are strongly affected by input voltage. For example, reducing input voltage from the normal to 95% can double the life of a standard incandescent lamp, while increasing voltage to just 105% of normal can halve its life. Voltage variations also affect light output (lumens), power (watts), and efficacy (lumens per watt).

Halogen Lamps Unlike normal incandescent lamps, halogen lamps use a halogen gas fill (typically iodine or bromine), to produce what is called a "halogen cycle" inside the lamp. In the chemical formula 1.1 W is tungsten, X is halogen atom, and n is the number of atoms involved. When the temperature is low (near the bulb wall) the positive process happens (from left to right). When the temperature is high (near the filament), it goes to the opposite way (from right to left).

$$(near\ the\ filament)W + \mathrm{nX} \leftrightarrow \mathrm{WXn}(\text{near the bulb}) \qquad (1.1)$$

Halogen gas combines with the tungsten that evaporates from the lamp filament, eventually re-depositing the tungsten on the filament instead of allowing it to accumulate on the bulb wall as it does in standard incandescent lamps. The tungsten- halogen lamp has several differences from incandescent lamps: ·

1. The lamps have a longer life (2000-3500 hours). ·

2. The bulb wall remains cleaner, because the evaporated tungsten is constantly redeposited on the filament by the halogen cycle. This allows the lamp to maintain lumen output throughout its life.
3. The higher operating temperature of the filament improves luminous efficacy. ·
4. The lamp produces a "whiter" or "cooler" light, which has a higher correlated color temperature (CCT) than standard incandescent lamps. ·
5. The bulbs are more compact, offering opportunities for better optical control.

Halogen lamps are sometimes called "quartz" lamps because their higher temperature requires quartz envelopes instead of the softer glass used for other incandescent lamps.

I.2 Mechanism of Discharge Lamps

The principle of a gas discharge lamp is based on the conversion of electric power into radiation by means of an electrical discharge in the gas medium in the lamp. In such lamps weakly or moderately ionized plasma is created. Plasma is an ionized gas and consists of electrons, ions, neutrals and excited particles and is on average neutral. The gas is located, in general, in a discharge tube with two electrodes [2].

I.2.1 Brief history of the gas discharge research

Gas discharge is a basic physical phenomenon in the nature. Leaving lightning alone, the first observation on man-made electric discharges can date back to 17th century, when the researcher saw the friction charged insulated conductors lose their charge. Coulomb proved experimentally in 1785 that charge leaks through air. We understand now that the cause of leakage is the non-self-sustaining discharge.

The history of gas-discharge lamps began in 1675 when French astronomer Jean-Felix Picard observed that the empty space in his mercury barometer glowed as the mercury jiggled while he was carrying the barometer [3]. Hauksbee first demonstrated a gas-discharge lamp in 1750 [4]. He showed that an evacuated or partially evacuated glass globe, in which he placed a small amount of mercury, while charged by static electricity could produce a light bright enough to read by.

After the first battery (the voltaic pile) was developed by A. Volta in 1800, the sufficiently powerful electric batteries were developed, and this allows the discovery of arc discharge

which was first reported by V. V. Petrov in Russia in 1803. Several years later Humphrey Davy in Britain produced and studied the arc in air. This type of discharge became known as ‘arc’ because its bright horizontal column between two electrodes bends up and arches the middle owing to the Archimedes’s force. Since then, discharge light sources have been researched because they create light from electricity considerably more efficiently than incandescent light bulbs.

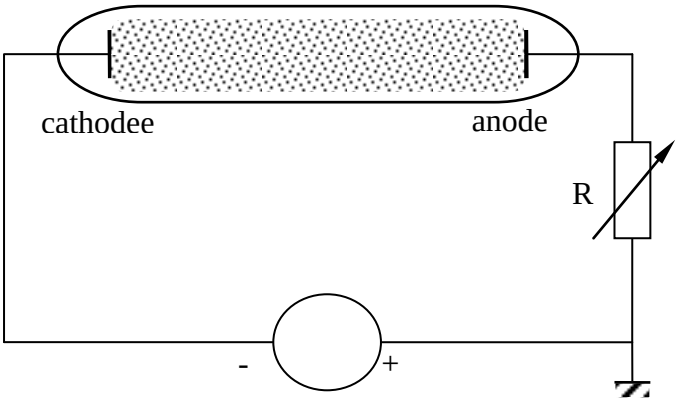

Fig. 1.2: Classical experimental setup for the typical gas discharge tube

The glow discharge was first discovered and studied by Faraday in thirties of 19th century. Faraday worked with tubes evacuated to a pressure about 1 Torr and applied voltage up to 1000V. In 1855, with the work of Heinrich Geissler [4], the first evacuated (~103 Pa) glass tubes (seen in Fig. 1.2) became available for scientific research and made it easy to study discharges in a more controlled environment.

Later it was discovered that the arc discharge could be optimized by using an inert gas instead of air as a medium. Therefore noble gases neon, argon, krypton or xenon was used, as well as carbon dioxide historically.

In 1889 [5], Friedrich Paschen published his work in which he investigated the minimum potential that is necessary to generate a spark in the gap between the two electrodes in gas discharge tubes. Curves of this potential as a function of pressure and the gap distance are nowadays called Paschen curves (see Fig. 1.3 (a)).

At the beginning of 1900 [6], J. S. E. Townsend proposed the theory of ionization by collision to explain the development of currents in gases, by which many phenomena in connection with the discharge through gas can be explained, including Paschen’s observations. He introduced a coefficient α to describe the average number of electrons produced by one

electron moving through a unit length of centimeter in gas. This so-called ionization coefficient is widely used in the study of various discharge phenomena, including the work performed in this thesis. Numerous experimental results were gradually accumulated on cross sections of various electron-atom collisions, drift velocities of electrons and ions, their recombination coefficients, etc. These works built the foundations of the current reference sources, without which no research in discharge physics would be possible. The concept of plasma was first introduced by I. Langmuir and L. Tonks in 1928 [7], [8]. Langmuir also made many important contributions to the physics of gas discharge, including probe techniques [9] of plasma diagnostics.

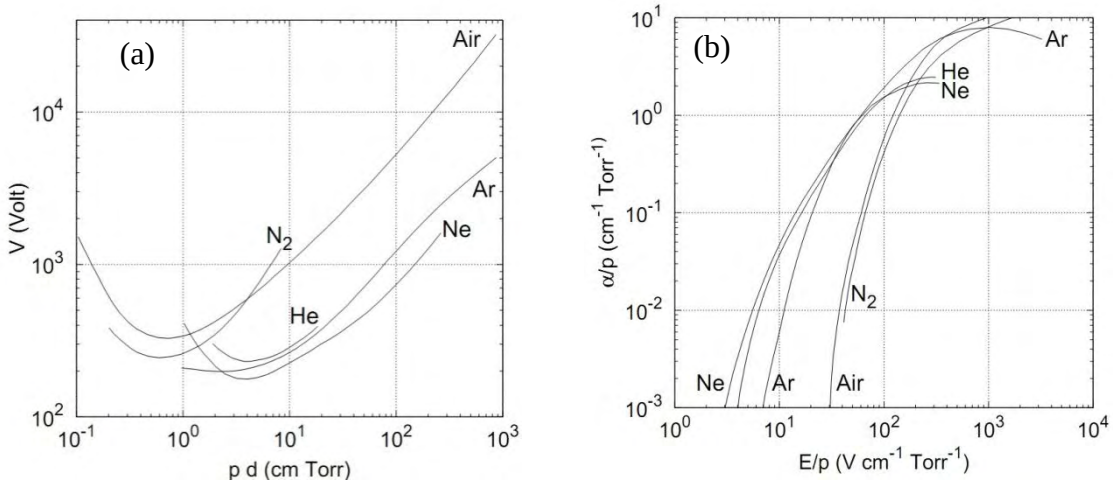

Fig. 1.3: (a) The Paschen curves for different gases [10], the minimum in the curve is called Stolevtov's point; (b) the dependence of α/p on the reduced electric field E/p for various gases [11] .

Most of the observations and studies of gas discharges in the late 19th and early 20th centuries were performed in the context of atomic physics research. After William Crookes' cathode ray experiments, which were also preformed with glass discharge tubes, and J. J. Thomson's measurements of the e/m ratio, it became clear that the current in gases is mostly carried by electrons. A great deal of information on elementary processes involving electrons, ions, atoms, and light fields was obtained by studying phenomena in gas discharge tubes.

The introduction of the metal vapor lamp, including various metals within the discharge tube, was a later advance. The heat of the gas discharge vaporized some of the metal and the discharge is then produced almost exclusively by the metal vapor. The usual metals are sodium and mercury owing to their visible spectrum emission.

One hundred years of research later led to lamps without electrodes which are instead energized by microwave or radio frequency sources. In addition, light sources of much lower output have been created, extending the applications of discharge lighting to home or indoor use.

I.2.2 Voltage- current characteristic curve of discharge lamp

Fig.1.4 shows the voltage- current characteristic curve of discharge lamp. It is measured with the equipment like that in Fig.1.2. Though it may be not exactly same when some parameters (such as geometry of the electrodes, the gas used, the pressure and the electrode material) change, it would be fit for most condition [12]. Generally the discharge can be divided into

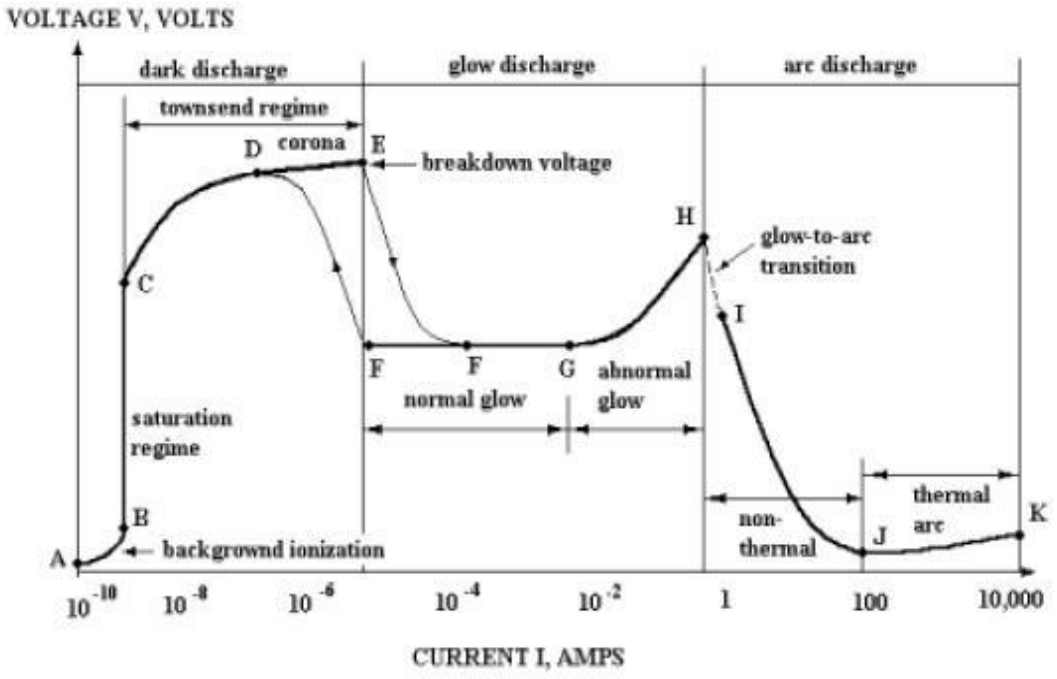

Figure 1.4. Voltage vs. current plot of discharge [13].

dark discharge, glow discharge and arc discharge.

Dark Discharge

In the regime between A and E on the outline the discharge progress is almost invisible. So it is called dark discharge.

A – B This is the background ionization stage. As a voltage is applied upon the electrodes the electrical field will move these seldom free spacial charges to their destined electrode. The

weak current come from movement of the space free electrons or charged particles. The population of these free charges is depended on background radiation from cosmic rays, radioactive minerals, or other sources. Increasing voltage sweeps out an increasing fraction of these ions and electrons. So the current will increase as the voltage rises.

B – C This is a current saturation region. The current stays constant when the voltage rises up. Because all the free special charges have been involved in the charge transportation between the electrodes, the increasing voltage cannot create more free electrons into the space. But this saturated current value is sensitive to the ionization radiation, which could be used to measure the intensity of radioactivity and is the mechanism of Geiger counter.

C – E This is the Townsend discharge region. When the applied voltage is high enough, the initial free electrons could be accelerated to high velocity before they arrive at the electrode or collide with the gas atoms or molecular. These high kinetic energy electrons could ionize the neutral gas atoms and produce another ions and electrons. At the same time the ions would also acquire energy from the electrical field. When the high energy ions hit on the cathode, the electrons may escape from the cathode material. This is called secondary electron emission process and mainly determined by the character of the cathode material. New electrons make the current rise exponentially. When the new electrons yielded from collision ionization and cathode emission could compensate the loss of electrons at the electrodes. The discharge will sustain by itself. As the electric field becomes even stronger, the secondary electron may also ionize another neutral atom leading to an avalanche of electron and ion production.

D – E This is corona discharge which occurs in regions of high electric field near sharp points, edges, or wires in gases. Charges tend to place in the part with big curvity, which is easy to create high electrical field around. This would help the filamentary or streamer discharge to happen. If the current is large enough it could also be seen such as the electrical lightening ball in the scientific museum.

E This is the breakdown voltage point. At this voltage the avalanche of electrons yield more and more new electrons in the space between the electrodes, and the current might increase by a factor of 10^4 to 10^8, which is usually limited only by the resistor in the circuit. At this time we can find that the lamp voltage falls while the current rises, which is called negative resistance characteristics. So ballasts would be required to limit the current of the lamp. For the DC voltage resistors are often chosen as ballast, while for the AC voltage magnetic or

electronic ballasts are usually better choice. The breakdown voltage for a particular gas and electrode material depends on the product of the pressure and the distance between the electrodes, pd, as expressed in Paschen's law [5].

Glow Discharge

In this region the discharge is not invisible any longer. The large amount of electrons provides the possibility of excitation collision. The electrons or ions with proper energy would excite the atoms from low energy levels to high levels during the inelastic collision process. The atom at high level is generally not stable. When they are back to ground level, the energy would come in the form of radiation. Some of the radiation wavelengths are in the range of visible light. So we can see the glow.

F – G This is the normal glow region, in which the voltage is almost independent of the current over several orders of magnitude in the discharge current. The electrode current density is kind of saturated and independent of the total current. So the effective surface area on the cathode which is response to the current cross section will decide the current value. When the current arrive at point G, the entire cathode surface has contributed to the plasma current.

G – H This is the abnormal glow regime, and the voltage increases significantly with the increasing total current in order to force the cathode current density above its natural value and provide the desired current. If we try to decrease current from point G to E, a form of hysteresis is observed in the voltage-current characteristics, which makes the point F' is at the left side of F. Because the discharge is able to maintains itself at considerably lower currents and current densities than that at point F if the gas has been broken down. When the breakdown happened in the volume, large amount of free special charges are created. The energy necessary for maintain the discharge is lower than that needed for striking the gas.

Arc Discharges

H – K This is the arc discharge region. The cathode is hot enough to emit electrons into the plasma. The plasma is hot too, which turns the uniform dispersive glow into bright concentrated arc. We can find the negative resistance characteristics again from I to J, and after that the voltage increases slowly as the current increases.

I.2.3 Discharge Lamps

Discharge lamps produce light by passing an electric current through a gas that emits light when ionized by the current. An auxiliary device known as a ballast supplies voltage to the lamp's electrodes, which have been coated with a mixture of alkaline earth oxides to enhance electron emission. Two general categories of discharge lamps are used to provide illumination: high-intensity discharge and fluorescent lamps.

Four types of high-intensity discharge (HID) lamps are most widely available on today's market: high-pressure mercury vapor lamps, metal-halide lamps, high-pressure sodium lamps, and xenon lamps.

In a high-pressure mercury vapor lamp, light is produced by an electric discharge through gaseous mercury. The mercury, typically along with argon gas, is contained within a quartz arc tube, which is surrounded by an outer bulb of borosilicate glass. Xenon may also be used in high-pressure mercury vapor lamps to aid starting time, and does not significantly change the visible spectrum of the lamp.

A metal-halide lamp (MHL) is a mercury vapor lamp with other metal compounds (known as halides) added to the arc tube to improve both color and luminous efficacy.

Light is produced in a high-pressure sodium (HPS) lamp by an electric discharge through combined vapors of mercury and sodium, with the sodium radiation dominating the spectral emission. The hard glass outer bulb may be clear, or its inner surface may be coated with a diffuse powder to reduce the brightness of the arc tube.

Unlike the other three HID lamps described here, xenon lamps do not contain mercury vapor. They contain xenon gas, kept at a pressure of several atmospheres. Xenon lamps are available in wattages from 5 to 32,000 watts.

The fluorescent lamp is a gas discharge source that contains mercury vapor at low pressure, with a small amount of inert gas for starting. Once an arc is established, the mercury vapor emits ultraviolet radiation. Fluorescent powders (phosphors) coating the inner walls of the glass bulb respond to this ultraviolet radiation by emitting wavelengths in the visible region of the spectrum.

Linear fluorescent lamps range in length from six inches to eight feet, and in diameter from 2/8 inch (T2) to 2-1/8 inches (T17). Their power ranges from 14 to 215 watts.

Compact Fluorescent Lamps (CFLs) produce light in the same manner as linear fluorescent lamps. Their tube diameter is usually 5/8 inch (T5) or smaller. CFL power ranges from 5 to 55 watts.

Ballasts, which are required by both fluorescent and HID lamps, provide the necessary circuit conditions (voltage, current, and wave form) to start and operate the lamps.

I.2.4. Mercury problem for discharge lamp

As introduction above, except the high pressure Xenon lamp, almost all the other discharge lamps would employ mercury as essential ingredient. Mercury has two important characters: 1. It is the only metal that is liquid at standard conditions for temperature and pressure. At general room temperature there is mercury vapor inside the lamp, which makes it easier to acquire energy from the excited inert gas atoms by collisions. It will help a lot to offer the extra electrons in the breakdown procedure. 2. Its resonance spectral radiation at 253.7nm is efficient to excite phosphor which is the base of normal fluorescent lamp especially at low pressure. And at medium or high pressure its radiation near 400nm (404.7nm and 435.8 nm) will contribute blue component to the light output.

However mercury is very toxic to both human and environment. Mercury is bound to the cell walls or membranes of microorganisms. Mercury poisoning can damage the brain, kidney, and lungs [14] and result in several diseases, including acrodynia (pink disease) [15], Hunter-Russell syndrome, and Minamata disease [16]. As inorganic mercury is liquid at normal condition, it is easy to transport and distribute in the globe scope by the atmospheric circulation. A wide variety of physiological, reproductive and biochemical abnormalities have been reported in fish exposed to sublethal concentrations of mercury. Birds fed inorganic mercury show a reduction in food intake and consequent poor growth. Other (more subtle) effects in avian receptors have been reported (i.e., increased enzyme production, decreased cardiovascular function, blood parameter changes, immune response, kidney function and structure, and behavioral changes) [17].

I.2.5 Lighting Mechanism

The basic process that occurs in the discharge can be described as follows. The electrons are accelerated by an externally imposed electric field, their directed velocity will be scattered into random directions by elastic and inelastic collisions with heavy particles. The result of this ohmic heating is a high electron temperature. In the case of inelastic collisions, part the kinetic energy of the electrons is transformed into the internal energy of atoms. These inelastic collisions are essential for chemical processes, such as excitation, ionization and dissociation and the generation of radiation. The internal energy of the atoms is released as

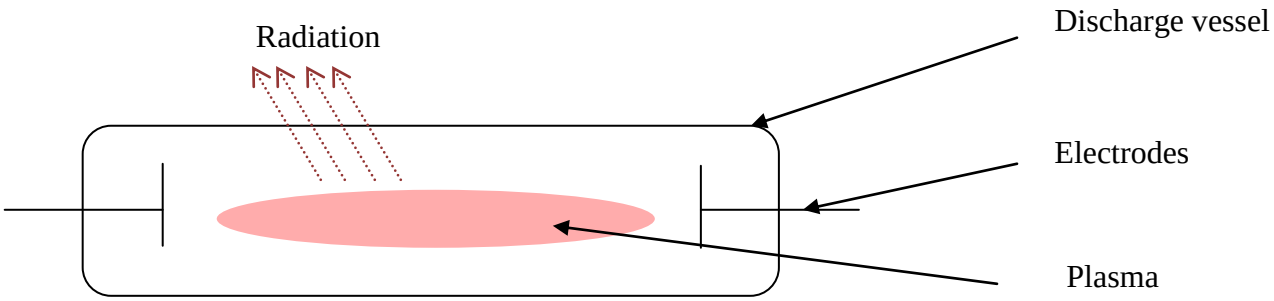

Figure.1.5 simple structure of a discharge chamber

electromagnetic radiation as the atoms relax back to their lower energy states. The radiation may come from each species of metal and inert gas atoms.

When the pressure is medium or high (generally from hundreds of Torr to several atmospheres, such as HID lamps), there are enough inert gas particles involve in the elastic and inelastic collision. More energy could be transferred to the plasma gas, which makes the discharge near the arc discharge regime, and the heat makes the physical or chemical changes of metal or metal halide happen. The pressure or collision broadening effect helps to emit continuous spectrum in the visible radiation range (from 380nm to 780nm), which really does

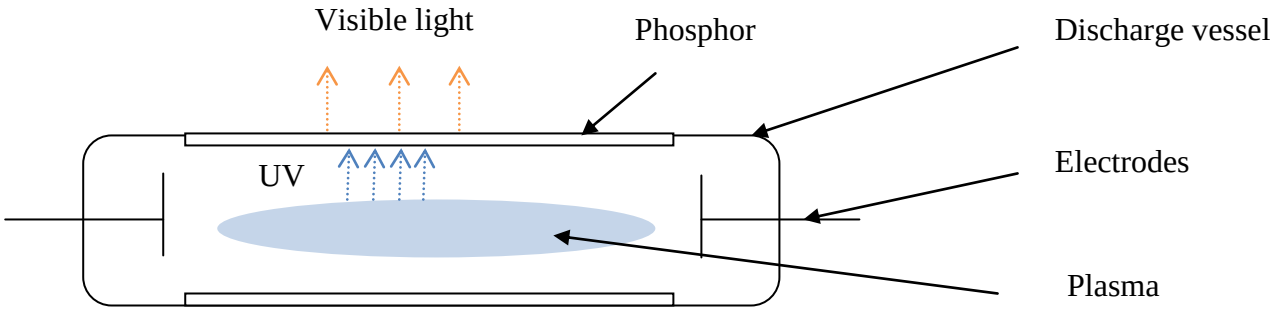

Figure.1.6 typical structure of a fluorescent lamp

great favor to increase the color rendering index (CRI) of the HID (especially the HPS lamp). The metal atoms give out their characteristic spectral line at blue part, green part or red part. By applicable mixture of the tri-stimulus value, white light is produced such as MHL. HID

can directly radiate visible light. Fig.1.5 shows the simple structure of HID‘s discharge chamber. Outside the chamber, HID lamps are generally equipped with a glass outer bulb for safety and elimination of the UV radiation.

When the pressure is low (i.e. several Torr), the particles in the plasma is rare, which limits the temperature of the plasma and the input power. Low pressure lamps mainly work at glow discharges regime. The characteristic spectral line of metals could be the only radiation from the discharge plasma as the pressure broadening could be neglected. The light efficacy may be acceptable while CRI of lamp is poor such as low pressure sodium lamp. For the low pressure mercury lamp the directly visible radiation is negligible, but the ultraviolet (UV) emission at 185nm and 254nm is strong. UV at 185nm has great applications such as ozone generator and sterilization except lighting. The UV phosphor can turn the UV radiation at 254 nm to visible light or white light, seeing Fig1.6. Some narrow tube cold cathode fluorescent lamp (CCFL) are wildly used as the backlight of the liquid crystal display (LCD)

I.3. Solid-state Lamps (SSL)

I.3.1 LED

LEDs (Light-Emitting Diodes) are respective solid-state semiconductor devices that convert electrical energy directly into light. LEDs can be extremely small and durable; some LEDs can provide much longer lamp life than other sources. LEDs produce narrow-spectrum light when DC voltage is applied. The light-generating chip is quite small, considered as point light source in the luminaries and lighting design. Light is generated inside the chip, a solid crystal material, when current flows across the junctions of different materials. The composition of the materials determines the wavelength and therefore the color of light.

In solids, the valence band is the highest range of electron energies in which electrons are normally present at absolute zero temperature and the conduction band is the range of electron energies enough to free an electron from binding with its atom to move freely within the atomic lattice of the material as a 'delocalized electron'. The conduction ability could be explained from Fig.1.7. In a metal the various energy bands overlap to give a single band of energies that is only partially full of electrons. The electrons in the outer level are free to move. In semiconductor materials (such as GaN or AlInGaP) the free electron in the conduction band and the hole – positive charge (an electron vacant position) can wander

around the crystal and contribute to the crystal conductivity. Electrons in the conduction band of the material and lower-energy sites (‘holes’) in the valence band into which they can fall, will create the photons when the recombination happens shown in Fig. 1.8. The energy of the photons will correspond to the energy gap between the conduction band and valence band, also called the band gap. However in insulator, the band gap is so large that seldom electrons could pass through it and move freely in conduction gap. A light-emitting diode is an electronic device integrating electrical access to the band gap structure and allowing for efficient light generation.

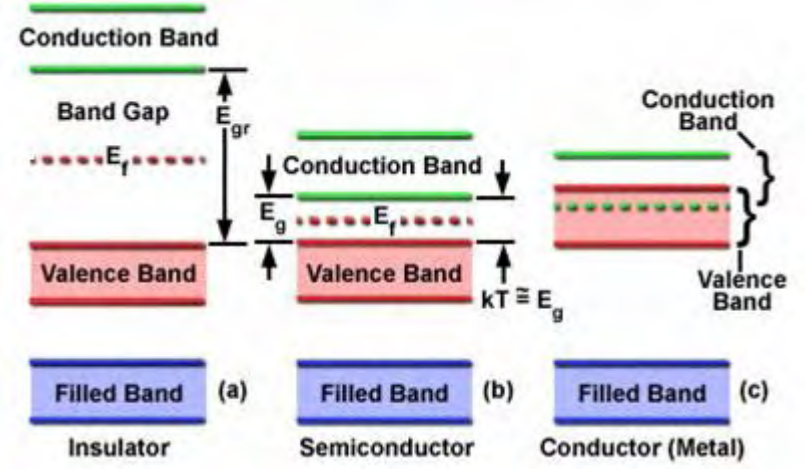

Fig.1.7 Energy band gaps in materials

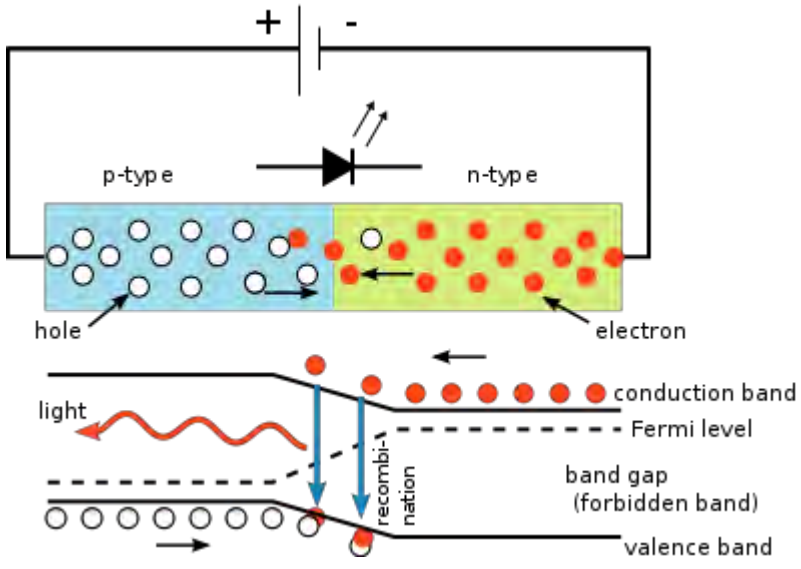

Fig. 1.8 Schematic diagrams of Light Emitting Diodes (LED)

N – type semiconductors: By adding pentavalent impurities (donor impurity) such as arsenic in silicon we can obtain a semiconductor in which the electron concentration is larger than the

hole concentration. P – type semiconductors: By adding trivalent impurity (acceptor) such as boron in silicon we can obtain a semiconductor in which the hole concentration is larger than the electron one.

LEDs essentially consist of three different types of materials layered on top of each other. The bottom layer is n-type semiconductor followed by multiple alternating thin layers (1–30 nm) of material with a smaller band gap (such as InGaN/GaN), also called quantum wells. Above that, there is a p-type semiconductor layer. The sandwiching of a smaller band gap material (InGaN) between layers of larger band gap material (GaN) creates a well that spatially traps electrons and holes, allowing them to recombine efficiently, generating light with the wavelength of the smaller band gap material. The p side is on the surface from which light is emitted, and narrow so photons will not be absorbed by the material. N region is heavily doped with suitable impurities to ensure that most of recombination takes place closer to the p region.

Although the LED was invented in the 1920s, a practical visible-light version (red) was not developed until the early 1960s [18]. These early devices were of very low power and were usable only as indicator lamps. Until recently, the only high-luminosity LEDs available emitted red light. Through the 1970s, developments continued, and shorter wavelengths (orange, yellow, and green) came onto the market. Early attempts to produce blue-emitting semiconductors focused on SiC, but these devices proved inefficient (0.03% efficiency [19]) owing to the material's indirect band gap. GaN was first investigated as a potential material for LEDs in the late 1960s by Paul Maruska and Jacques Pankove (Radio Corporation of America) and in later years additionally by Isamu Akasaki and co-workers (Nagoya University in Japan) and by Shuji Nakamura (Nichia Corporation) [20]. GaN is a direct-band gap semiconductor material with a 3.45-eV band gap, which corresponds to near-ultraviolet light (364 nm). The GaN revolution has provided efficient ultraviolet, violet and blue light emitters. The first practical blue LED was developed in 1993 [21], and in 1996, a phosphor coating was applied to a blue LED to create the world's first white LED.

The difference between the direct-band gap and the indirect-band gap is shown in Fig. 1.9. Direct band gap semiconductor: the minima of the conduction band and the maxima of the valence band occur at the same value of k, so an electron making the smallest energy transition from the conduction band to the valence band can do so without a change in k (the momentum). Indirect band gap semiconductor: the minima of the conduction band and the

maxima of the valence band occur for different values of k, thus, the smallest energy transition for an electron requires a change in momentum. Recombination probability for direct band gap semiconductors is much higher than that for indirect band gap semiconductors.

Direct band gap semiconductors give up the energy released during this transition (Ebg) in the form of light. Recombination in indirect band gap semiconductors occurs through some defect states within the band gap, and the energy is released in the form of heat given to the lattice.

As white light is a kind of continuous spectrum, two or more wavelengths are required to generate a broad spectrum of light that is a better approximation of a blackbody radiation, such as that of the Sun. One way to produce additional colors is to use a phosphor that absorbs light of one wavelength and emits at longer wavelength, such as rare-earth-doped yttrium aluminium garnets (YAG:RE). For example, cerium-doped YAG can absorb blue and ultraviolet light and emit yellow light relatively efficiently [22]. Crucial to this process is the fact that higher-energy light (for example ultraviolet or blue) is converted to lower energy (for example yellow or red). Therefore, LEDs emitting red light cannot be used for white-light generation using phosphors; instead a short-wavelength ultraviolet, violet or blue LED is required. That is why the first white LED came after the development of efficient GaN LED.

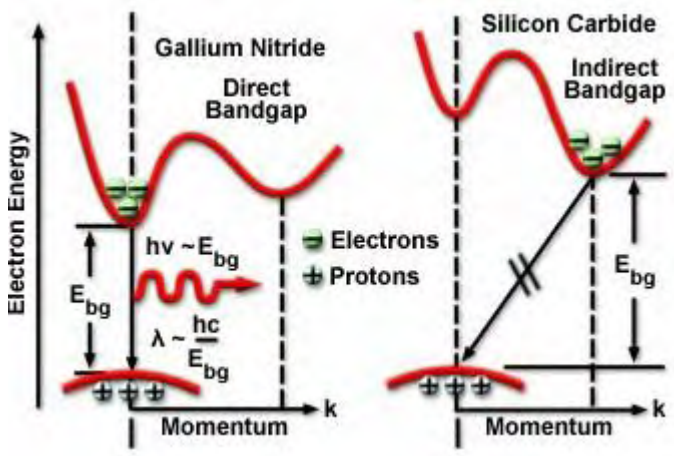

Fig. 1.9 semiconductor energy levels

The three most popular approaches are shown in Fig. 1.10 [20]. These are a blue LED with yellow phosphors; an ultraviolet LED with blue and yellow phosphors (or red, green and blue phosphors); and a device that combines red, green and blue LEDs.

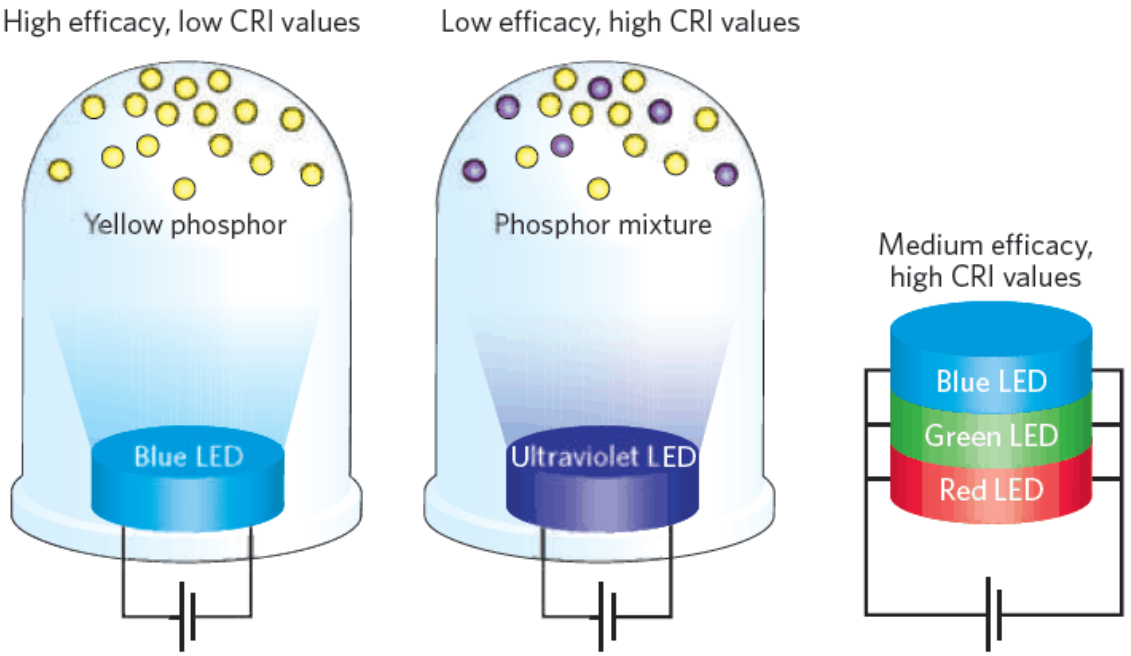

Fig.1.10 Three dominant ways to produce white light based on LEDs

Each scheme has its advantages and disadvantages. The advantage to using a blue LED and a yellow phosphor is its high theoretical efficacy, which is attractive for the creation of a cheap, bright white-light source. However, this benefit comes at the expense of a lower value for the color-rendering index (describing the ability to reproduce colors of an object as seen under an ideal white-light source, such as the Sun.), which is typically so low that such devices are undesirable for indoor use. Ultraviolet LEDs with phosphor mixtures provide a better CRI value and are suitable for indoor applications but at the expense of poorer efficacy. To control white light dynamically, the third approach, a combination of three (or more) LEDs of different wavelengths is attractive, and may lead to higher efficacies than the ultraviolet–phosphor LEDs, but will generally be the most expensive option until further advances are made. Fig.1.11 [20] presents the spectra for two phosphor-based white LEDs and sunlight. The historic development of luminous efficacy for the most common white-light sources is shown in Fig. 1.12.

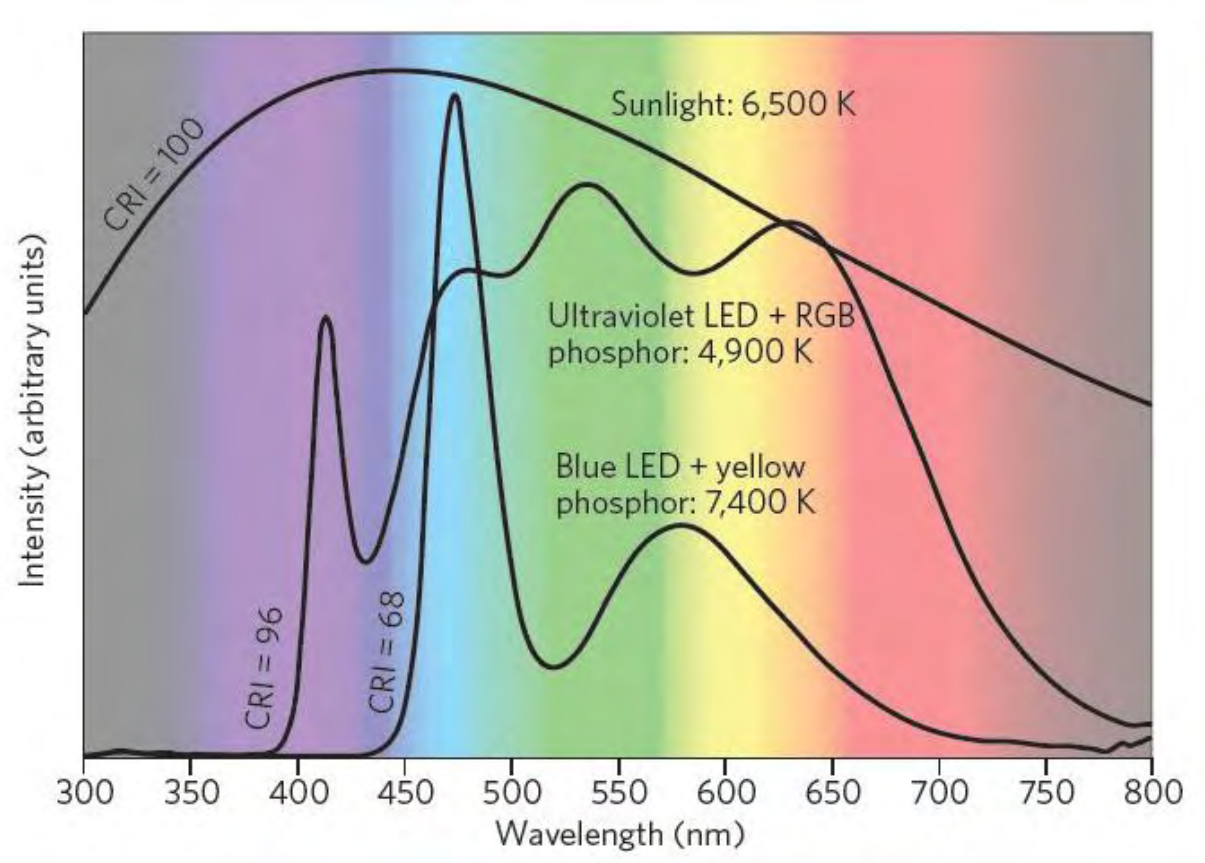

Fig. 1.11 Comparison of the spectrum of ideal sunlight with twoLED-based white-light sources

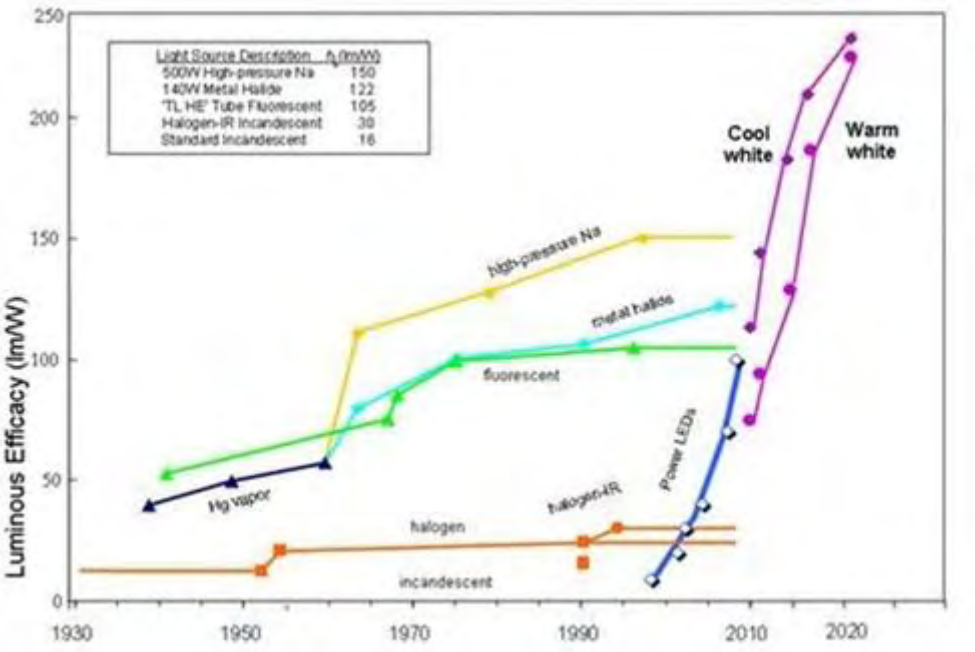

Fig. 1.12 Evolution of LED efficacy from PHILIPS. These values are for the LED and not the lamp or luminaire.

Semiconductor (active layer)	λ [nm]	Comment
GaAs	870–900	Infrared (IR)
Al_xGa_{1-x} As (0 < x < 0.4)	640–870	Red to IR
$In_{1-x}Ga_xAs_yP_{1-y}$ (y ≈ 2.20x, 0 < x < 0.47)	1–1.6 μm	LEDs in communications
InGaN alloys	430–460	Blue
	500–530	Green
InGaN/GaN quantum well	450–530	Blue–green
SiC	460–470	Blue. Low efficacy
$In_{0.49}Al_x$ $Ga_{0.51-x}$ P	590–630	Amber, green, red
$GaAs_{1-y}P_y$ (y < 0.45)	630–870	Red–IR
$GaAs_{1-y}P_y$ (y > 0.45) (N or Zn, O doping)	560–700	Red, orange, yellow
GaP (Zn–O)	700	Red
GaP (N)	565	Green

Table 1.1 Selected LED semiconductor materials, wavelengths of emission in commercial LEDs.

Nowadays LEDs can generate red, yellow, green, blue or white light (semiconductors referring to the colors shown in Table 1.1[23]), have a life up to 50,000 hours, and are widely used in traffic signals and for decorative purposes. White light LEDs are a recent advance and may have a great potential market for some general lighting applications. Their efficacy have already compared with the main commercial lamp products, as shown in Fig. 1.13. Some commercial LED products are shown in Fig. 1.14, which are Diall Spotlight, Philips E14 Spotlight, TOSHIBA Spotlight, Philips Stdr Bulb, Apollo SITA Spotlight, LG Bulb and their main commercial parameters are measured in the lab as shown in Table 1.2. They have become quite good substitute for the incandescent lamp and gas discharge lamp in low power application, such as indoor lighting applications or headlights of vehicles. Although initial costs may seem high to a customer, LED products are actually already a cheaper solution considering their long life and high efficacy. It is clear that LEDs would help to reduce the energy cost for lighting. It is said that 22% of the electricity power in the United States is consumed in lighting and related applications and if the LEDs could substitute for all

conventional white light sources in the world, energy consumption could be reduced by around 1,000 TWh per year, as well as reducing greenhouse gas emission by about 200 million tonnes [24].

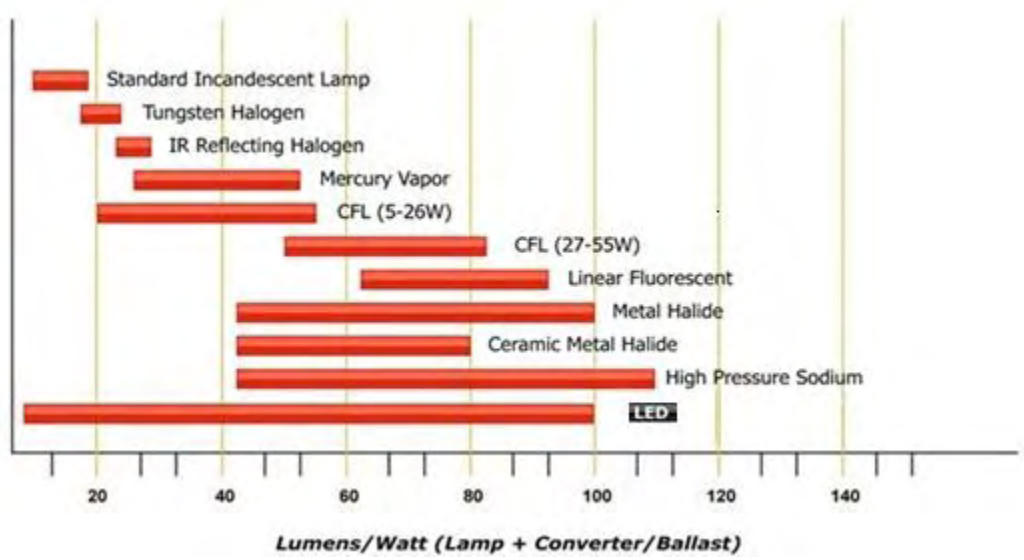

Fig. 1.13 Efficacy comparison of light sources

Fig. 1.14 Some LED bulbs and spot lights in the market.

Brand	Socket	light output [lm]	Power [W]	power factor	Efficacy [lm/W]	Color temperature [K]	CRI	lifetime declared [h]
Diall LED	GU10	342	6,5	0,45	53	2841	78	25000-50000
Philips	E14	212	4,0	0,67	53	2625	80	
Toshiba	GU10	293	6,0	0,95	49	3069	82	
Philips LED stdr	E27	696	9,5	0,60	73	2697	79	
Apollo	GU10	196	2,9	0,34	68	2977	70	
LG Innov	E27	487	7,6	0,98	64	2746	81	

Table 1.2 The main parameter of the LED samples

As the well known Moore's law (which predicts by Moore in 1965 that the performance of microprocessors would double every two years), a similar prediction for LEDs was made by Roland Haitz (2006). It is based on historical data in Fig. 1.15. As currently stated, it predicts that the luminous output of individual LED devices is increasing at a compound rate of 35% per year and that the cost per lumen is decreasing at 20% per year. To the extent that current manufacturers seem to have settled on 3 W as the maximum practical power in a small device, we can read this as also meaning an increase in efficacy of 35% per year. [25]

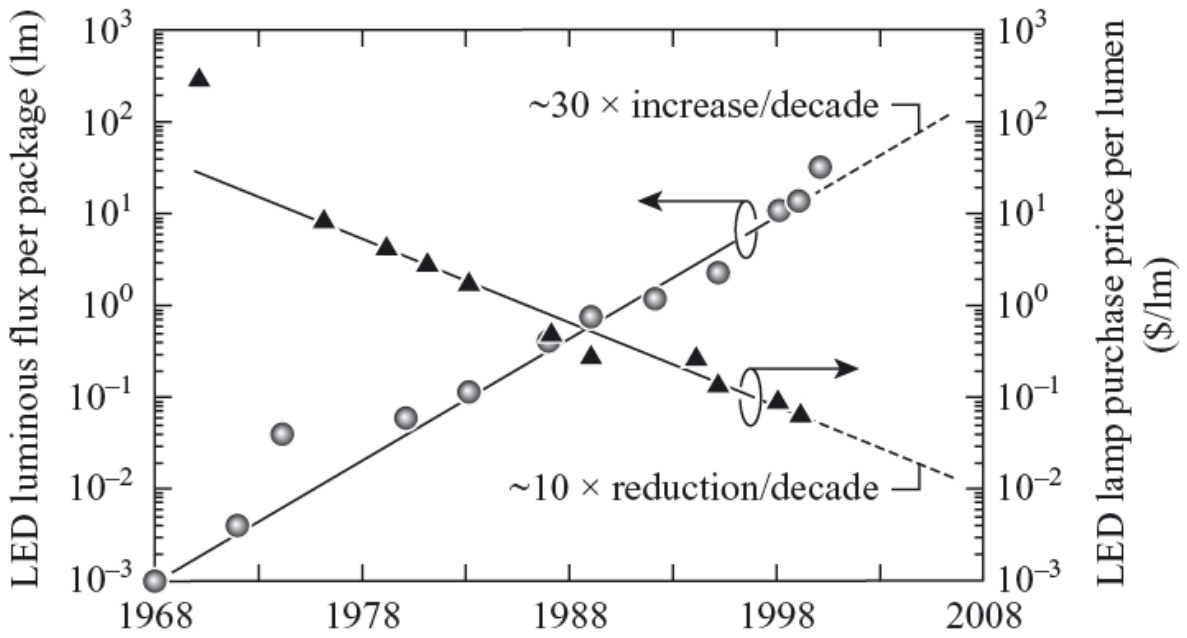

Fig.1.15 Haitz's Law.

However, there may be two kinds of physical limits for white LED's efficacy rise. For the white LED using phosphor, phosphor conversion of white light from LEDs would be limited to about 238 Lm/W (for an acceptable CRI) [25]. Note that since fluorescent tubes are also phosphor-converted, but starting from 235 nm rather than 435 nm, their ultimate efficacy is considerably lower than that of LEDs. Ultimately LEDs will be more efficient than fluorescent lighting. For the white LED combining two or more colors without phosphor, direct emission can be more efficient, because there is no absorption and reemission involved. But since colors other than green are needed to get acceptable CRI, white light cannot be made at higher efficacy than about 350 Lm/W [25]. After the efficacy limit is reached, Haitz's law may still apply to the cost per lumen. The figure shows that after 2015 the cost per lumen of LEDs will approach that of 60 W incandescent bulbs.

The total LED efficacy is also described as the external quantum efficiency (EQE), which is defined as below:

EQE=IE*IQE*EE*CE

where IE is the injection efficiency, IQE is the internal quantum efficiency, EE is the extraction efficiency and CE is the conversion efficiency of the phosphor. The IE is the ratio of electrons being injected into the quantum wells to those provided by the power source, the IQE is the ratio of photons generated to the number of electron–hole recombination, and the extraction efficiency is the ratio of photons leaving the LED to those generated. In the case of white-light generation using phosphors, the CE is the ratio of emitted longer-wavelength photons to shorter-wavelength absorbed photons. It could be one for the LED without phosphor. The improvement of EQE is mainly focused on increasing IQE and EE.

The IQE of today's best LEDs is at least 75% [26] and may even be approaching 80%. To make further improvements, firstly nonradiative recombination centres, which help to convert the bang gap energy to heat, need to be eliminated. More importantly, a shift is needed in growing the LEDs, from polar to nonpolar or semipolar crystallographic directions instead, to eliminate strain induced electric polarization fields seen within the quantum wells [27].

When it comes to the extraction efficiency, because of large differences in the refractive indices of air and the semiconductor, such as GaN, a considerable fraction (90–95%) of the generated photons within the LED are trapped by total internal reflection. A popular method is to increase the amount of light hitting the LED–air interface at near-perpendicular values to

reduce the occurrence of total internal reflections. For example, as shown in Fig. 1.16 [28], internal reflections can be reduced and hence more light can be collected by shaping the semiconductor into a dome so that the angles of incidence at the semiconductor-air surface are smaller than the critical angle. An economic method of allowing more light to escape from the LED is to encapsulate it in a transparent plastic dome.

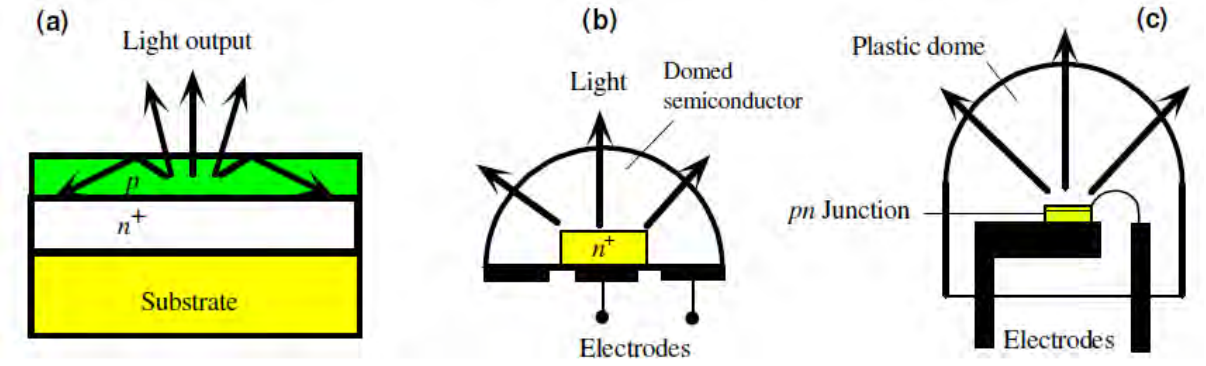

Fig. 1.16 (a) normal semiconductor with total internal reflection. (b) domed semiconductor. (c) encapsulation

Generally speaking, increasing the exterior power will give more luminous flux for LEDs except for operating at higher current densities (over 10 Acm^{-2}). When the current through the LED is too high, the EQE would decrease. Although the exact cause has not yet been determined, it is believed that using thicker quantum wells and altering the structure to lessen carrier overflow will reduce this to the point that it will be possible to operate at higher efficacies and currents.

LEDs produce more light per electrical watt than incandescent lamps with the latest devices rivaling fluorescent tubes in energy efficiency. They are solid-state devices, which are much more robust than any glass-envelope lamp and contain no hazardous materials like fluorescent lamps. LEDs also have a much longer lifetime than incandescent, fluorescent, and high-density discharge lamps

Although LEDs possess many advantages over traditional light sources, a total system approach must be considered when designing an LED-based lighting system. LEDs do not radiate heat directly, but do produce heat that must be removed to ensure maximum performance and lifetime. LEDs require a constant-current DC power source rather than a standard AC line voltage. Finally, because LEDs are directional light sources, external optics may be necessary to produce the desired light distribution [29].

Nowadays the discharge lamps based on plasma technology are still the take the governing position in the lighting industry. The low luminance efficiency has leaded the incandescent lamp to restrictive governmental legislation [30]. SSLs, in the near future, prove to be a good alternative in some cases, especially as a replacement for incandescent and possibly fluorescent lamps. However, even if LED technology is advancing as rapidly as predicted, electrical discharges will have to supply the major share of light sources for at least another two decades [31], [32], [33]. In any case it is expected that the gas-discharge lamps are mostly qualified for the general illumination of large areas such as sports arenas, buildings and roads.

I.3.1 OLED

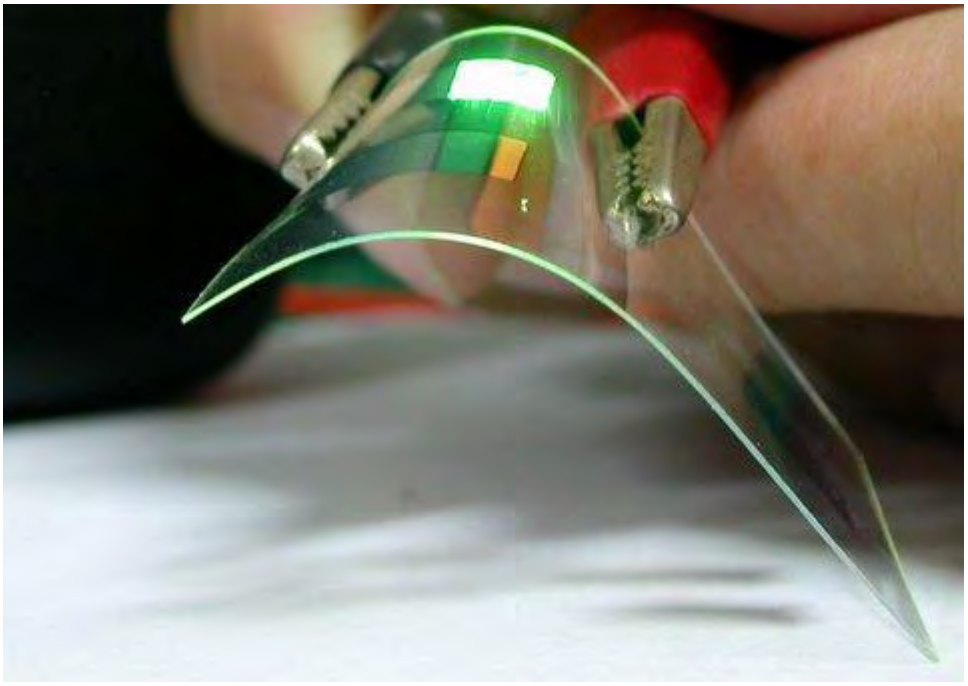

Fig. 1.17 OLED Early Product

OLED is the acronym of organic light-emitting diode, as shown in Fig. 1.17. It's really still an LED in which the emissive electroluminescent layer is a film of organic compound which emits light when the current is passing. This layer of organic semiconductor is located between two electrodes and at least one of these electrodes is transparent so that the light comes out from the active layer. The typical structure of an OLED is shown in Fig. 1.18[34]. A common device structure comprises a glass substrate coated with indium tin oxide (ITO) as transparent anode and a thin, opaque metal film as cathode. Several thin – film layers are deposited on each other and each layer performs a defined function such as generation of specific color or the transportation of electronic charge away from the electrodes towards the organic dopants. The collective aim is to maximize the recombination of electrons and holes and cause organic molecules to emit light. The organic stack including the electrodes is usually thinner than 1 μm. Two classes of organic materials are commonly used for organic light-emitting devices: polymeric substances and so-called "small molecule materials" which do not exhibit any orientating property and therefore form amorphous films.

One interesting aspect of organics-based optoelectronics is the possibility to use simple screen printing or wet deposition techniques for cost-effective fabrication of large-area devices. Nowadays, this applies only to polymeric organics, whereas evaporating techniques still have to be applied for small molecules.

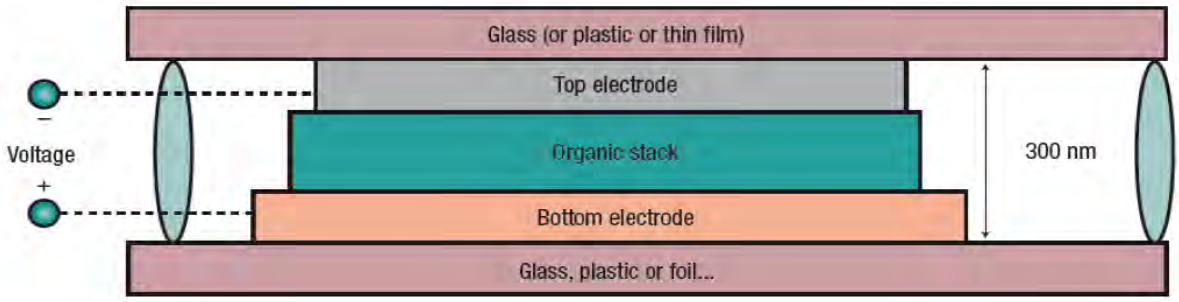

Fig. 1.18 The typical structure of an OLED.

When a DC bias is applied to the electrodes, the injected electrons and holes can recombine in the organic layers and emit light of a certain color depending on the properties of the organic material. These materials have conductivity levels ranging from insulators to conductors, and are therefore considered organic semiconductors. Since charge carrier transport in organic semiconductors relies on individual hopping processes between more or less isolated molecules or along polymer chains (Fig.1.19 [34]), the conductivity of organic semiconductors is several orders of magnitude lower than that of their inorganic counterparts. Furthermore, the concept of energetic bands is not applicable to organic electronics. Instead of "valence band" and "conduction band", the relevant terms are "HOMO level" (highest occupied molecular orbital level) and "LUMO level" (lowest unoccupied molecular orbital level). A current of electrons flows through the device from cathode to anode, as electrons are injected into the LUMO of the organic layer at the cathode and withdrawn from the HOMO at the anode. This latter process may also be described as the injection of electron holes into the HOMO. Before actually decaying radiatively, an electron-hole pair will form an exciton in an intermediate step, a bound state of the electron and hole, which will eventually emit light when it decays. This happens closer to the emissive layer, because in organic semiconductors holes are generally more mobile than electrons. The frequency of this radiation depends on the band gap of the material, in this case the difference in energy between the HOMO and LUMO.

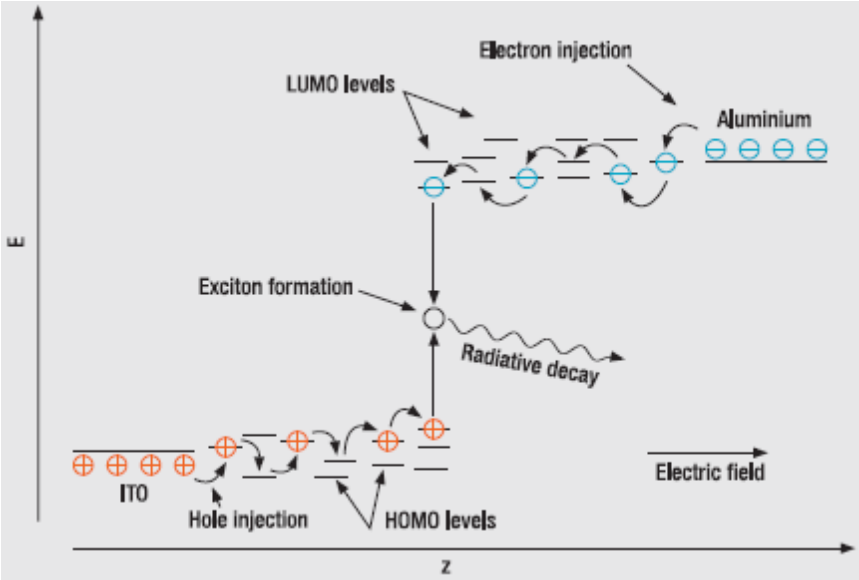

Fig. 1.19 Diagram of OLED light emission mechanism

As electrons and holes are fermions with half integer spin, an exciton may either be in a singlet state or a triplet state depending on how the spins of the electron and hole have been combined. Statistically three triplet excitons will be formed for each singlet exciton. Decay from triplet states (phosphorescence) is spin forbidden, increasing the timescale of the transition and limiting the internal efficiency of fluorescent devices. Depending on its chemical structure, a dye molecule can be either a fluorescent or a phosphorescent emitter. Only in the latter, all excitons–singlets and triplets are allowed to decay radiatively. Typically, a polymer such as poly (n-vinylcarbazole) is used as a host material to which an organometallic complex is added as a dopant. The heavy metal atom at the centre of these complexes exhibits strong spin-orbit coupling. Phosphorescent organic light-emitting diodes make use of spin–orbit interactions to facilitate intersystem crossing between singlet and triplet states, thus obtaining emission from both singlet and triplet states and improving the internal efficiency. In the former, however, three quarters of all excitons(the triplet excitons) do not emit any light. Fluorescent emitters therefore have a maximum intrinsic efficiency of only 25 % and their application is avoided if possible. However, up to now, the lifetimes of phosphorescent emitters, especially at a short wavelength (blue), are inferior to those of fluorescent ones.

Originally, the most basic polymer OLEDs consisted of a single organic layer (such as polyphenylene vinylene). However multilayer OLEDs can be fabricated with two or more layers in order to improve device efficiency as well as conductive properties. Different

materials may be chosen to aid charge injection at electrodes, as shown in Fig.1.20 [35]. The emissive layer (EML) is the source of the light. Other layers that comprise the organic compound are the electron transport layer (ETL), hole transport layer (HTL), and hole injection layer (HIL). Their role is to optimize the flow of the electric current so that the EML's light emission is maximized.

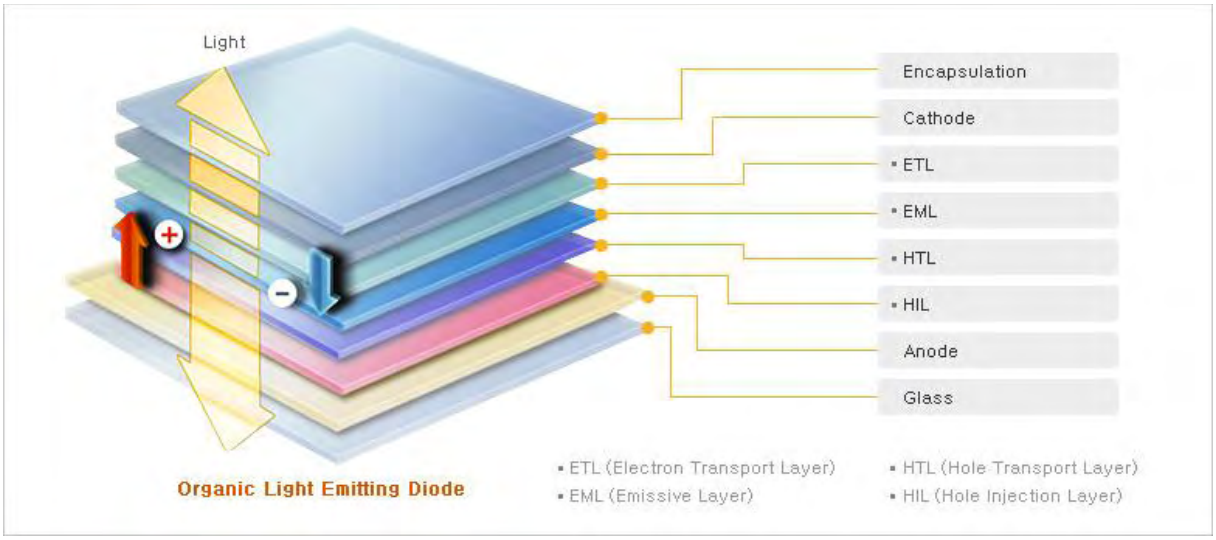

Fig. 1.20 Multilayer OLEDs scheme

Indium tin oxide (ITO) is commonly used as the anode material. It is transparent to visible light and has a high work function which promotes injection of holes into the HOMO level of the organic layer. A typical conductive layer may consist of PEDOT:PSS (which is a polymer mixture of two ionomers : sodium polystyrene sulfonate carrying negative charges ; poly(3,4-ethylenedioxythiophene) carries positive charges) [36] as the HOMO level of this material generally lies between the work function of ITO and the HOMO of other commonly used polymers, reducing the energy barriers for hole injection. Besides ITO's conductivity is lower than the metal's, which is about two orders of magnitude lower than that of aluminium. This leads to a significant voltage drop across the transparent electrode and causes variations in the local driving voltage of the active layers depending on the distance to the electrical contacts. Consequently, the emission intensity decreases from the periphery of the device towards its center. In order to lower the lateral voltage drop, thin metal bus lines can be deposited on top of the ITO anode, which increases the mean conductivity of the anode, while shadowing only a minor fraction of the active area and thus yielding a more uniform luminance pattern. Metals such as barium and calcium are often used for the cathode as they have low work

functions which are good for injection of electrons into the LUMO of the organic layer [37]. Such metals are reactive, so they require a capping layer of aluminium to avoid degradation.

Experimental research has proven that the properties of the anode, specifically the anode/hole transport layer (HTL) interface topography plays a major role in the efficiency, performance, and lifetime of organic light emitting diodes. Imperfections in the surface of the anode decrease anode-organic film interface adhesion, increase electrical resistance, and allow for more frequent formation of non-emissive dark spots in the OLED material adversely affecting lifetime. Mechanisms to decrease anode roughness for ITO/glass substrates include the use of thin films and self-assembled monolayers. Also, alternative substrates and anode materials are being considered to increase OLED performance and lifetime. Possible examples include single crystal sapphire substrates treated with gold (Au) film anodes yielding lower work functions, operating voltages, electrical resistance values, and increasing lifetime of OLEDs [38].

In organic semiconductor technology, electrical doping is used to increase the conductivity of the material and to enhance the carrier injection from the electrodes into the organic materials. This allows for the design of devices with intrinsically undoped active layers embedded in p-type and n-type-doped layers, which are therefore referred to as “PIN diodes”. In addition to an improved electrical performance, such a design also provides the opportunity to increase the thickness of the device while maintaining the operating voltage almost constant. The overall thickness of the device between the electrodes should amount to some hundred nanometers to provide sufficient protection against electrical short-circuits. These are often caused by the presence of particles on the substrate during evaporation of the organic layers or by the roughness of the substrate.

Doping also enables a series connection of several active layers in a higher-stacked structure (Fig.1.21[34]). An intermediate PN junction operated in reverse direction behaves like a tunnel contact: the carriers can directly pass from the HOMO level of one layer to the LUMO level of the adjacent layer. In the OLED community, these junctions are often called “charge generation layers (CGLs)” because electron-hole pairs are created at the interface and separated by the field. The equivalent circuit of a large-area device is a series connection of three resistors, representing the anode, the organic layers and the cathode. The higher the differential resistivity of the organic layers at the operating point, the lower is the voltage drop across the electrodes which results in an enhanced uniformity. As stacked device architectures

have a much higher differential resistivity, stacking is a way to increase the uniformity and output of large-area devices without having to apply bus lines.

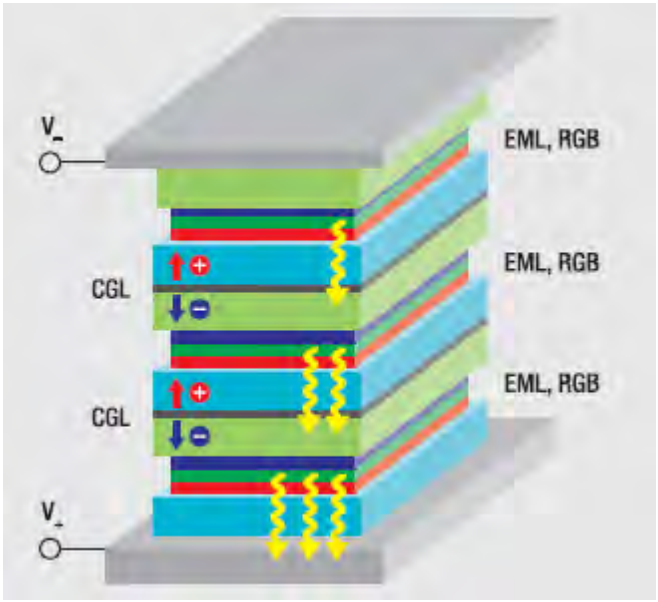

Fig. 1.21 Stacked device architecture

A device structure with immanent series connection is referred to as “stacking”. A twofold white stacked device, for example, can basically achieve the same luminance levels as a simple device – at half the current, since there are two emitting units, but at twice the voltage. Compared with simple PIN devices, stacked device architectures offer several advantages in terms of lifetime, optical performance etc.

The organic layers have to be protected against air as they are sensitive to moisture and oxygen and decompose when exposed. A possible encapsulation technique is shown in Fig. 1.22[34]. A thin but dense amorphous oxide layer is deposited onto the cathode, which provides a sufficient permeation barrier. Due to its thinness, this thin-film encapsulation (TFE) has to be protected from mechanical damage, for example by laminating an additional glass layer onto it, by applying a lacquer coating etc.

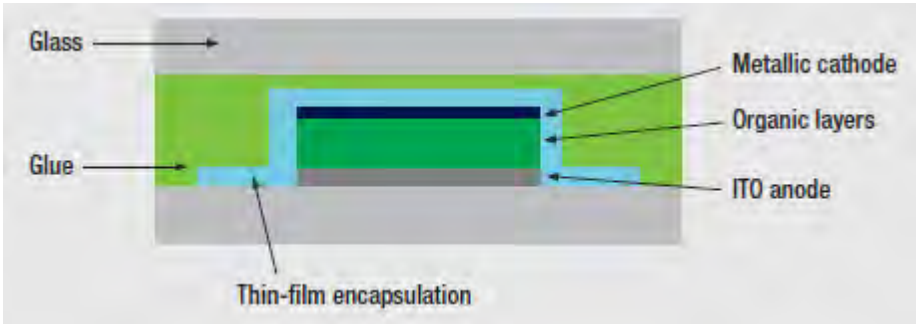

Fig. 1.22 Thin film encapsulation

Typical emission spectra of organic molecules are broad (as shown in Fig.1.23 [34]). As stated before, the emission color is a material property. Thus, the total emission can be tuned to virtually any color, including white at any color temperature, by stacking several different emitting layers in a single device. This is possible since the organic layers are almost transparent in the visible spectral range. Most white OLEDs contain a red, a green and a blue emission layer to create high-quality white light.

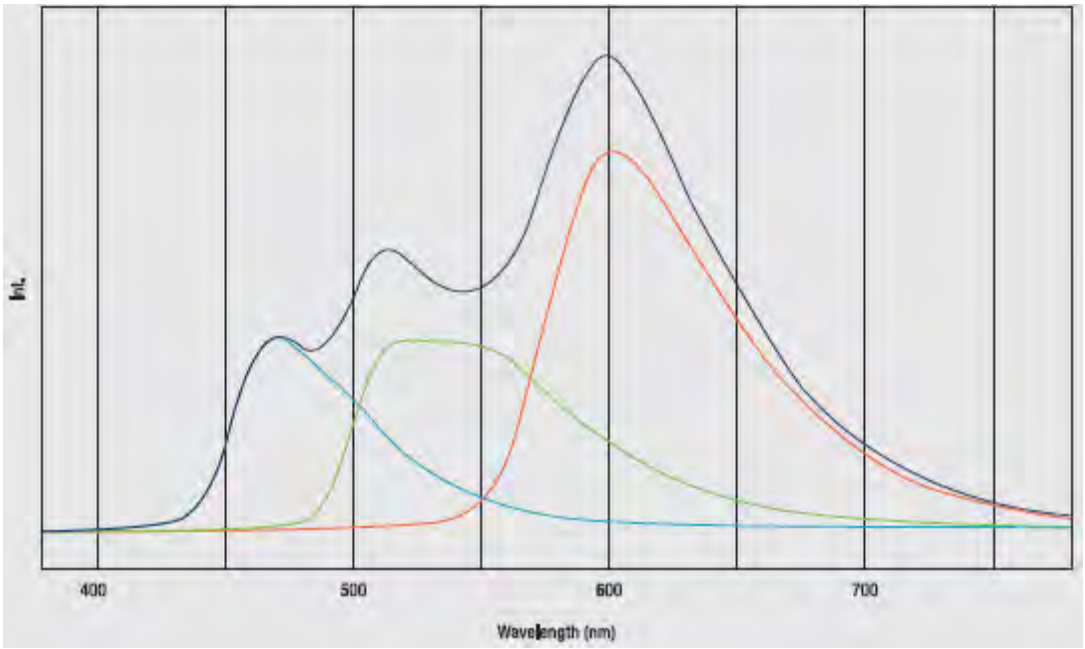

Fig.1.23: Typical emission spectra of organic materials. The diagram shows spectra of red, green and blue emitters and their superposition which yields white emission at a high color rendering index.

During the lifetime of an OLED, the luminance will decrease monotonically at constant current. The resistivity and thus the operating voltage will increase accordingly. The lifetime scales super-linearly with both the emitted radiation intensity (or current density) and the

temperature. The temperature, in particular, has to be considered when designing OLED based luminaires. At high luminance levels, large-area devices may have considerably elevated temperatures during operation and the possibility of heat exchange with the surroundings should be provided in order to ensure a long lifetime of the device. In this case, stacked device architectures once again offer the possibility to lower the individual emission of each unit, thus slowing down their aging mechanisms, while keeping the overall emission constant.

OLEDs are very good flexible glare-free area light sources with high color quality. When turned off, they can be transparent or have either a mirror-like or milky appearance. They can be very thin and lightweight, and turned on instantly. OLEDs have the potential to be equally or more efficient and long-living than fluorescent lamps, while being 100 % mercury-free and no UV and IR radiation. As a kind organic material it is easy to realize the low cost production as the other plastic film. However, on the other hand, organic materials are not as robust as the inorganic material and degrade by the water and the oxygen, which always limits the performance and the lifetime of OLEDs. Besides faster degradation is occurring in the blue OLEDs that are required to be used in company with the red and green OLED in order to produce white light.

In the near future, OLEDs could be wild used displays devices, such as television screens, computer monitors, and portable systems. An OLED display works without a backlight; thus, it can display deep black levels and can be thinner and lighter than a liquid crystal display (LCD) [39].

I.4 The Work of This Thesis

The subject of our work is a mercury free gas discharge lamp, the flat dark discharge lamp (FDDL). It is filled with lower pressure gases (below 1 Torr), and operated with voltages in the range of 1.7 - 4 kV DC and currents of 0.5 - 1 mA. When it works normally no obvious visible light comes from the discharge chamber and only the luminance of cathodoluminescent (CL) phosphor could be observed (so called dark discharge lamp). It would be convenient to work as the backlight for the LCD owing to its shape. Fewer gas atoms or molecules cannot support a saturate propagation of electron and ion production, which limit the capability of charge transportation and keep the voltage higher and current lower than the normal fluorescent lamp. But with high lamp voltage and few collisions

electrons could be accelerated to high velocity and make phosphor bright. After breakdown progress the population of electrons rises exponentially, and the FDDL turns on.

Further introduction of our lamp and some basic numerical calculation are introduced in Chapter II, in which the excitation and ionization mean free paths are used to analyze the physics behind the threshold pressure for the FDDL. Traditional discharge lamps work under glow or arc discharge regimes, while the lamp we studied functions in the regime between Townsend discharge regimes and glow discharge region. Further introduction to the special characteristics of FDDL are present in chapter II.2.

In such a narrow gap and low pressure, there may be no adequate collisions happening before charged particles reach electrodes. The mean free path, diffusion model and Townsend discharge theory are introduced in chapter II.3. Fluid equations and Townsend discharge theory could help to understand physics insides and give the possible space charge distribution. Mean free path presents the collision possibility, which helps to explain the special working condition for this application in chapter II.4. As the cross sections distribution of excitation and ionization are different, when the discharge gap is limited, there would be some condition which is good for ionization and bad for excitation.

Some feathers of the sample lamps are explored in chapter III. And the experiment result of FDDL at different pressure filled with Neon and Xenon are also present and discussed in that chapter. Experiments are operated on the sample and empty FDDLs. From the sample tests, some characteristics of the FDDL have been revealed in chapter III.2 including the phosphor performance (the response of the phosphor to different wave length incident photons) and the uniformity of the lamp. It will help to fully understand the characteristics of this type of brand new light sources. In chapter III.3, the empty lamps are filled with different pressure neon to present the lamp behavior with different pressures and input powers. Low pressure and high input power would help to improve the lamp application. Xenon is also filled as buffer gas to compare the turn on voltage with that of Neon. The V-I plot could help to prove its difference from the field emission. In the commentary chapter, some failures and problems are revealed and possible reasons are discussed.

I.5 Summary

Electrical light sources have been developed for about 200 years. There are three generation light source: incandescent lamp, discharge lamp and solid state lamp. The incandescent lamp

employs tungsten wire heated by current to produce light, which is simple and cheap. It has high color rendering index (CRI) but low lifetime and energy efficiency. Halogen lamp is a developed incandescent lamp, in which a “halogen cycle” could help the filament working at higher temperature. When gas is broken down in a discharge vessel, charged particles such as electrons and ions are produced and accelerated. When they collide with other atoms or molecular, some energy may radiate in photons. This is the basic lighting mode for all the discharge lamps. Many metal elements are added inside to contribute their characteristic spectrum, among which mercury is most important and widely used. The discharge lamp has good efficiency and large luminance flux, so they are the popular commercial choice for most indoor and outdoor lighting applications. The solid state lamp uses the recombination of electrons and holes in the inorganic or organic semiconductor materials to give light. It has high efficiency and long life, and is quite mature in many low power commercial applications. They may develop quite fast in the near future.

The FDDL lamp studied in this thesis is a new kind of discharge lamp in which no mercury is used. As a new candidate for the green backlight application, an optimum working condition needs to be explored.

References

[1] Wim van den Hoek, Notes on the history of incandescent lamps, *Proceedings of the 12th international symposium on the science and technology of light sources and the 3rd international conference on white LEDs and Solid state lighting*, July 11-16, 2010, Eindhoven, Netherlands

[2] J R Coaton, A M Marsden, *Lamps and Lighting*, Arnold, London, 4th edition, 1997

[3] J. Cusson, Académie des inscriptions et belles-lettres. *Le Journal des sçavans*. 1665.

[4] Waymouth, F.John, *Electric Discharge Lamps* (October 15, 1971).

[5] F. Paschen. Ueber die zum Funkenübergang in Luff, Wasserstoff und Kohlensäure bei verschiedenen Drucken erforderliche Potentialdifferenz. *Wied. Ann*., 37:69-96, 1889.

[6] J. S. Townsend. *The Theory of Ionization of Gases by Collision*. Constable & Company Ltd., London, 1910.

[7] I. Langmuir. The Interaction of Electron and Positive Ion Space Charges in Cathode Sheaths. *Phys. Rev*. 33, 954–989 (1929)

[8] L. Tonks and I. Langmuir. A General Theory of the Plasma of an Arc. *Phys. Rev*. 34, 876–922 (1929)

[9] H. M. Mott-Smith and I. Langmuir. The Theory of Collectors in Gaseous Discharges. *Phys. Rev*. 28, 727–763 (1926)

[10] Yu. P. Raizer. *Gas Discharge Physics*. (Springer, Berlin, 1991).

[11] W. Bartholomeyczyk. Über den Mechanismus der Zündung langer Entladungsrohre. *Ann. der Physik*, 5:485–520, 1939.

[12] X.Xu. *Gas Discharge Physics*. Fudan University Press, Shanghai, 1996. ISBN7-309-01669-6/O.165

[13] *Structure of a Glow Discharge*, Princeton Plasma Physics Laboratory

[14] Clifton II, Jack C. Mercury Exposure and Public Health, *Pediatric Clinics of North America* 54, no. 2 (avril 2007): 237.e1-237.e45.

[15] G Bjørklund, Mercury and Acrodynia. *Journal of Orthomolecular Medicine* 10 (3 & 4): 145–146.

[16] Davidson, W Philip, Gary J Myers, Bernard Weiss. Mercury exposure and child development outcomes . *Pediatrics* 113, no. 4 Suppl (avril 2004): 1023-1029.

[17] Boening, Dean W. Ecological effects, transport, and fate of mercury: a general review . *Chemosphere* 40, no. 12 (juin 2000): 1335-1351.

[18] N.Zheludev, The life and times of the LED — A 100-year history. *Nature Photonics* 1:189–192. 2007.

[19] Edmond, John A., Hua-Shuang Kong, Calvin H. Carter Jr. Blue LEDs, UV photodiodes and high-temperature rectifiers in 6H-SiC . *Physica B: Condensed Matter* 185, no 1-4 (avril 1993): 453-460. doi:10.1016/0921-4526(93)90277-D.

[20] Pimputkar, Siddha, James S. Speck, Steven P. DenBaars, Shuji Nakamura. Prospects for LED Lighting. *Nature Photonics* 3, no 4 (avril 2009): 180-182. doi:10.1038/nphoton.2009.32.

[21] Nakamura et al. 1996. Light emitting gallium nitride-based compound semiconductor device. U.S. Patent 5,578,839, filed Nov. 17, 1993 and issued Nov. 26, 1996.

[22] Allen, Steven C., et Andrew J. Steckl. A nearly ideal phosphor-converted white light-emitting diode. *Applied Physics Letters* 92, no 14 (7 avril 2008): 143309. doi:10.1063/1.2901378.

[23] Thomas G. Brown. *The Optics Encyclopedia: Basic Foundations and Practical Applications.* Wiley-VCH, 2004.

[24 Krames, M.R., O.B. Shchekin, Regina Mueller-Mach, Gerd O. Mueller, Ling Zhou, G. Harbers, et M.G. Craford. Status and Future of High-Power Light-Emitting Diodes for Solid-State Lighting . *Journal of Display Technology* 3, no 2 (juin 2007): 160-175. doi:10.1109/JDT.2007.895339.

[25]Lenk, Ron, et Carol Lenk. *Practical Lighting Design with LEDs*. John Wiley & Sons, 2011.

[26] Narukawa, Yukio, Masahiko Sano, Takahiko Sakamoto, Takao Yamada, et Takashi Mukai. Successful Fabrication of White Light Emitting Diodes by Using Extremely High

External Quantum Efficiency Blue Chips. *Physica Status Solidi* (a) 205, no 5 (1 mai 2008): 1081-1085. doi:10.1002/pssa.200778428.

[27] Waltereit, P., O. Brandt, A. Trampert, H. T. Grahn, J. Menniger, M. Ramsteiner, M. Reiche, et K. H. Ploog. Nitride Semiconductors Free of Electrostatic Fields for Efficient White Light-Emitting Diodes . *Nature* 406, no 6798 (24 août 2000): 865-868. doi:10.1038/35022529.

[28] Kasap, Safa O. Optoelectronics . *In The Optics Encyclopedia*. Wiley-VCH Verlag GmbH & Co. KGaA, 2007.

[29] Bourget, C. Michael. An Introduction to Light-emitting Diodes. *HortScience* 43, no. 7 (janvier 12, 2008): 1944-1946.

[30] *Official Journal of the European Union* 24-3-2009 L 76/3 Comission Regulation 244/2009 18 march 2009. See also: http//ec.europa.eu/energy/efficiency/ecodesign/lumen/doc/incandescent-bulbs-en.pdf.

[31] *Solid-State Lighting Research and Development Portfolio*, Navigant Consulting, 2006 http://apps1.eere.energy.gov/buildings/publications/pdfs/ssl/ssl_multiyear_plan.pdf

[32] M. Krames, Progress in High power light-emitting diodes for solid state lighting, *Proc. 11th Int. Symp on the Science and Technol. of Light Sources*, May 2007, Shanghai, ed. M.Q. Liu and R. Devonshire, p571-573

[33] Stoffels W W, Nimalasuriya T, Flikweert A J, Mulders H C J, 2008 Plasma physics and controlled fusion, special issue, invited papers form the *34th european physical society conference on plasma physics*, Warsaw, Poland, 2-6 July 2007, accepted for publication.

[34] *Introduction to OLED technology*, OSRAM. http://www.osram.ch/media/resource/HIRES/331488/1982902/einfhrung-in-die-oled-technologie-gb.pdf

[35] *OLED Light*, LG Chem. http://www.lgchem.com/global/green-energy/oled-lighting.

[36]Carter, S. A., M. Angelopoulos, S. Karg, P. J. Brock, et J. C. Scott. Polymeric anodes for improved polymer light-emitting diode performance. *Applied Physics Letters* 70, no 16 (21 avril 1997): 2067-2069. doi:10.1063/1.118953.

[37] Friend, R. H., R. W. Gymer, A. B. Holmes, J. H. Burroughes, R. N. Marks, C. Taliani, D. D. C. Bradley, et al. Electroluminescence in Conjugated Polymers. *Nature* 397, no 6715 (14 janvier 1999): 121-128. doi:10.1038/16393.

[38] Spintronic OLEDs could be brighter and more efficient. *Engineer* (Online Edition): 1. 16 July 2012.

[39] *OLED*. Wikipedia, the Free Encyclopedia, http://en.wikipedia.org/w/index.php?title=OLED&oldid=617757366.

CHAPTER II:

Theoretical Analysis on the FDDL

II.1 Introduction

Traditional discharge lamps work under glow or arc discharge regimes, while the lamp we studied functions in the regime between Townsend discharge regimes and glow discharge region. Its gas pressure is higher than the field emission display device and its lamp voltage is lower than that of normal low pressure mercury discharge lamp or PDP. Visible radiation directly from the gas discharge is quite limited in such high E/n value (~10^5 Td, reduced electric field, E is electric field, n is the density of gas), but due to the high energy initial and secondary electrons will contribute to the light emission [1]. The secondary emission electrons may not obligatorily come from cathode material. Further introduction to the special characteristics of FDDL are present in chapter II.2.

In such a narrow gap and low pressure, there may be no adequate collisions happening before charged particles reach electrodes. The mean free path, diffusion model and Townsend discharge theory are introduced in chapter II.3. Fluid equations and Townsend discharge theory could help to understand physics insides and give the possible space charge distribution. Mean free path presents the collision possibility, which helps to explain the special working condition for this application in chapter II.4. As the cross sections distribution of excitation and ionization are different, when the discharge gap is limited, there would be some condition which is good for ionization and bad for excitation.

II.2 Speciality of the Flat Dark Discharge Lamp (FDDL)

II.2.1 Introduction to FDDL

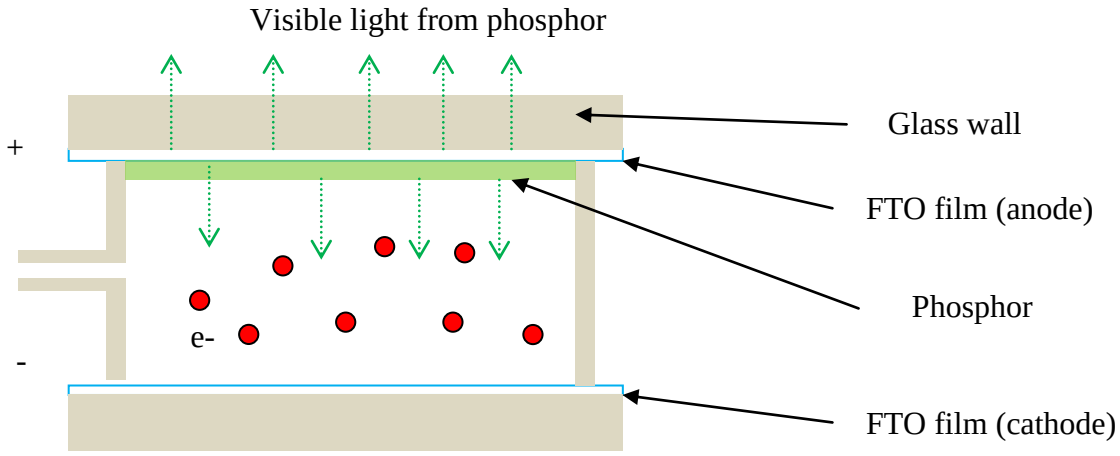

Fig. 2.1 Construction of our flat lamp (side view)

The main work in this thesis bases on a kind of flat dark discharge lamp (or FDDL) as showed in Fig. 2.1 and Fig. 2.2. No mercury is employed in the discharge vessel. It works under DC voltage. A layer of transparent and conductive fluorine-doped tin-oxide (FTO) film is coated on the inner side of top glass wall as an electrode. The electrode deposited by phosphor will work as the anode. The discharge would happen between the two planer electrodes and the distance between them is 1cm. The device utilizes electron beams induced by gas discharge to hit and excite the phosphor at the anode. The spectrum of the emitted light depends entirely on the phosphor materials coated on the anode. Ultraviolet is not required and the usage of mercury can be avoided. The features of double-side lighting indicate that the flat dark discharge lamp (FDDL) might become potential candidate for the next-generation green lighting source [2].

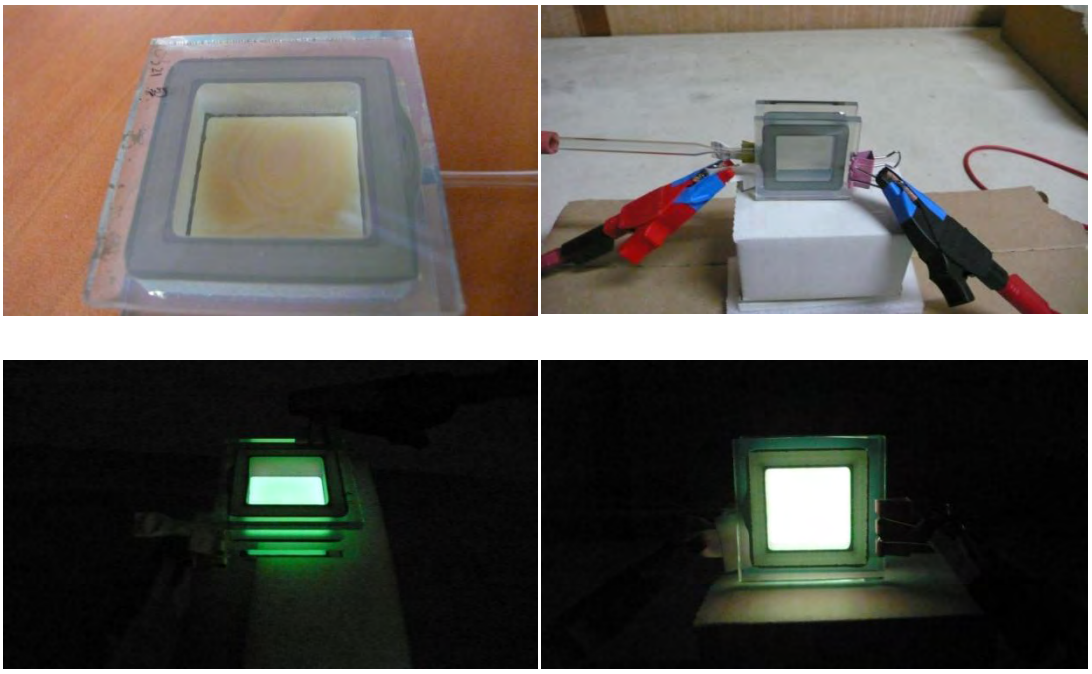

Fig. 2.2 Photos of the lamps

II.2.2 Comparison with the similar applications

The mechanism of the lamp is brand new compared with the traditional discharge lamps.

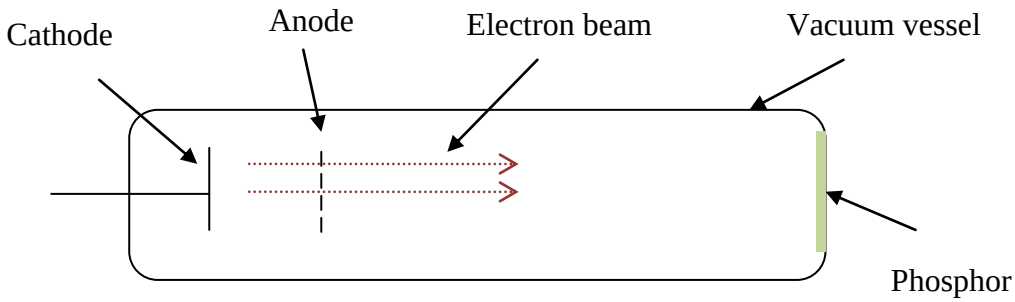

Fig. 2.3 simple structure of a CRT

The mechanism of FDDL is similar with that of cathode ray tube (CRT).CRT is a vacuum tube containing an electron gun (a source of electrons or electron emitter) and a fluorescent screen used to view images. The pressure (about 0.1-0.01 Pa) is lower than the FDDL. Hot cathode could emit electrons, which are accelerated by the high voltage between electrodes and bombard the CL phosphor (seen in Fig. 2.3). It is often used as traditional screens and the equipment is often big and heavy. Nowadays it could be also applied in the lighting industry. Charles E. Hunt has applied the mechanism in general lighting by proposing an electron stimulated luminescence (ESL) lamps [3]. Their R30 bulb has entered American retail market

with the target specifications as 500 lumens, 3200K, CRI 90+, R9 > 85, 19 Watts and 10000-hour lifetime (seen in Fig. 2.4). It is proved to be a good substitution for incandescent, but not a good backlighting source.

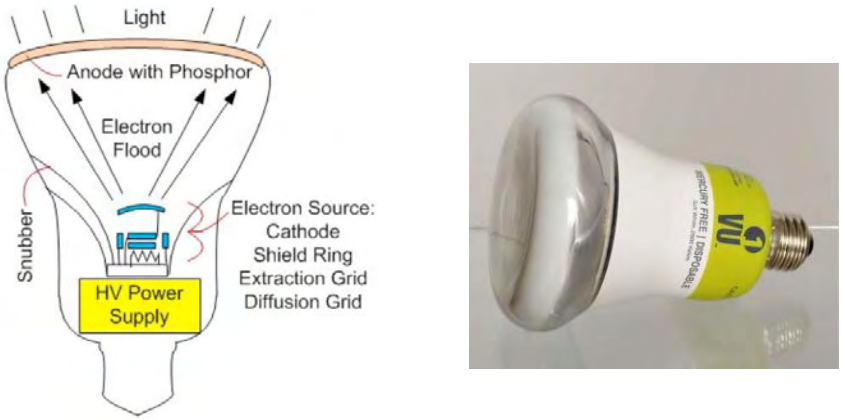

Fig. 2.4 Conceptual depiction of the ESL™ Configuration (left) and the photo of their R30 reflector bulb (right)

The lighting mechanism of FDDL is different from other normal flat panel display modes too, such as plasma display panel (PDP) and field emission display (FED). Figure 2.5 shows the structure of PDP. A panel typically has millions of tiny cells in compartmentalized space between two panels of glass. These compartments or "cells" hold a mixture of noble gases and an amount of mercury. The long stripe electrodes are arrayed between the cells and the glass plates. The electrodes are covered by insulating protective layers [4]. What happen inside the cell is same with that in a fluorescent lamp: voltage between the electrodes breakdown the inert gases. The inelastic collisions between electrons, ions and atoms make the mercury atoms emit UV photons, which excite the red, green or blue UV phosphor coating inside the cells. And then the visible light comes out [5],[6]. Each pixel in a plasma display is made up of three cells comprising the primary colors of visible light. Varying the voltage of the signals to the cells thus allows different perceived colors. Eden and group in university of Illinois develop their micro channel plasma device and produce lighting sheets as large as 30 x 30 cm^2 [7]. Though the configuration of the microchannel is not exactly same with that of PDP and their discharge procedure is dielectric barrier discharge (DBD), the lighting mechanism is similar.

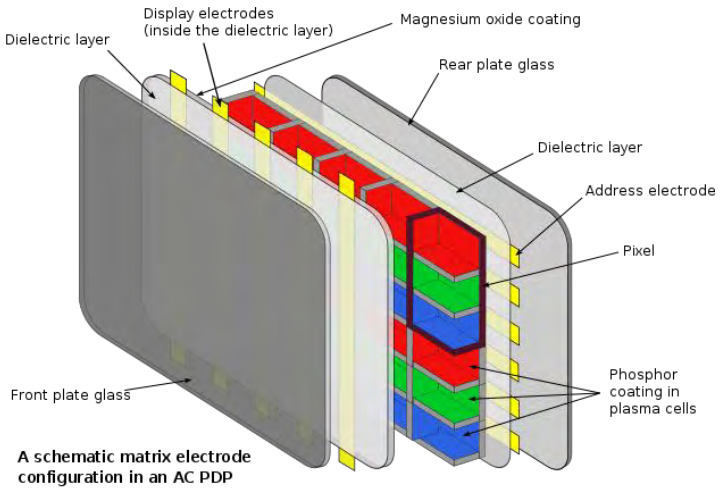

Fig. 2.5 Simple composition of the alternating current plasma display panel with matrix electrode design.

The FED uses large-area field electron emission sources to provide electrons that strike colored CL phosphor to produce a color image as an electronic visual display. Its lighting mechanism is close to CRT. In the high vacuum (could be lower than 10^{-6} Torr [8]) and high voltage (several kV), the cathode material could emit electrons. FED just like a matrix of cathode ray tubes, each tube producing a single sub-pixel, grouped in threes to form red-green-blue (RGB) pixels. The FE lamp published by Mitchell M. Cao and Charles E. Hunt could reach a peak luminance of 11830 Cd/m^2 at an applied voltage of 6.4 kV [8].

II.2.3 Characteristics of FDDL

For flat dark discharge lamp, as electric field is strong enough and density of particles is low, electrons can be accelerated to high speed between collisions. The energy is high enough to make the molecular and atoms ionized rather than excited. This can explain the phenomenon in the experiment [9], shown in Fig 2.6. When the working gas is nitrogen, if the population density inside is uniform, we could get the mean free path as about 0.31 cm. It means an electron will collide with N_2 for about 3 times when it travels from cathode to anode.

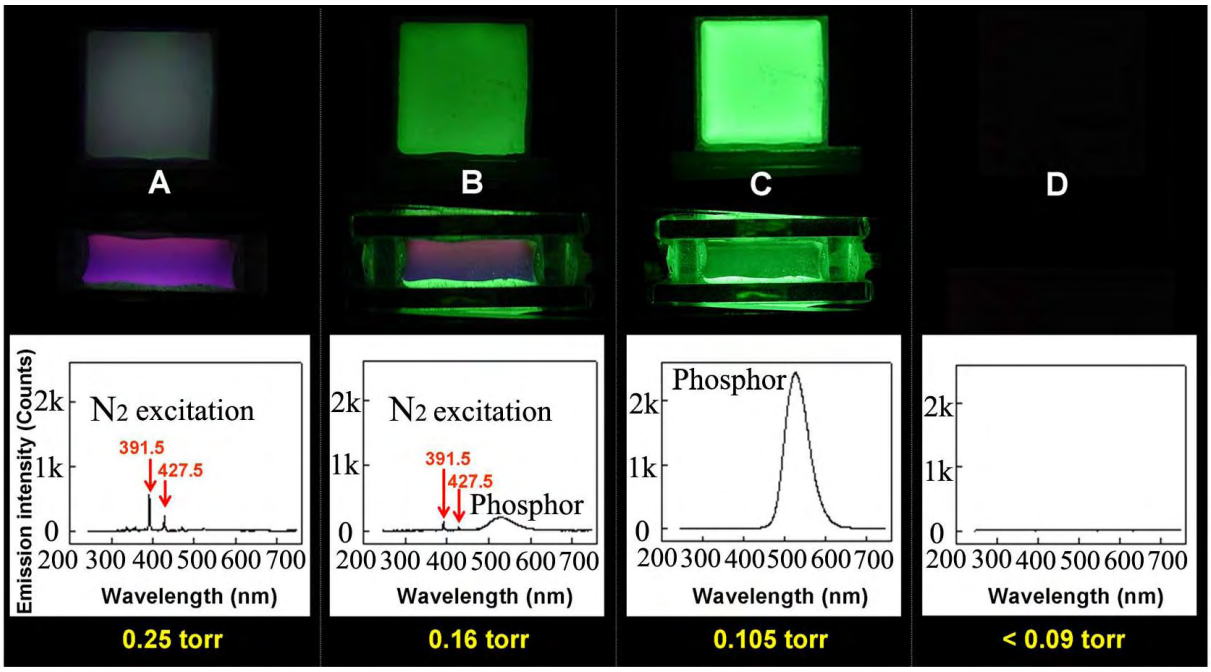

Fig.2.6 Photos and spectrum of N_2 flat electron emission lamp with different pressures

In the Fig. 2.6 the spectrum with the wavelengths respectively locating at 391.5 and 427.5 nm are originated from the nitrogen gas excitations belonging to the first negative system ($B_2\Sigma u+$—$X_2\Sigma g+$) (391.4 and 427.8 nm) [10]. The peak wavelength of the phosphor is around 530nm. As the N2 pressure is between 0.11 and 0.20 Torr (Fig. 2.6 (b)), the photo shows the emergence of phosphor emission with attenuating glow background. The spectrum evidently shows the weakened peak intensity from the N2 excitations, with an apparent peak centering at the characteristic wavelength (530 nm) of the phosphor. As the N2 pressure is between 0.10 and 0.11 Torr (Fig. 2.6 (c)), the spectrum displays only a strong peak at 530 nm reflecting the green light emitted from the anode phosphor and the characteristic peaks of the N2 glow excitations disappeared altogether. As the N2 pressure falls below P = 0.1 Torr, neither any lighting is seen in the images nor any peak is revealed in the spectrum.

From their experiment results, there should be a critical pressure for the gas discharge in such a region. When the pressure is higher, the elastic and inelastic collisions processes should dominate in the discharges volume, the light comes from the characteristic spectral line of the filled gas. The increase of the population of gas particles provide more chances for inelastic collisions which are mainly excitation process and help to transfer electrical power to spectral emission. More collisions provide more charged particles, and lower voltage is necessary, but lower energy of electrons makes the phosphor dimmer. In this domain the light emission intensity would increase with the pressure until it goes to an optimum value. That indicate the

reason that the glow from the N2 with 0.25 Torr is brighter than that with 0.16 Torr (Fig. 2.6 (a, b)), While on the other hand, more chances of collisions makes the mean free path decrease, which means the energy that particles get from the electrical field would decrease too. As well known, the excitation process is selective to the induced particle energy, and if the energy is below a threshold, the inelastic collision would not happen. So as the pressure continues to increase after the optimum value, the scattering energy loss in the elastic collisions become more and more outstanding and the light emission would trend to decrease.

While the pressure is below 0.09 Torr, the number of collisions is so limited. Electrons that arrive at the anode are not enough to make breakdown happen or maintain the discharge. Without electron avalanche few electrical particles will excite neither the gas nor the phosphor.

There should be a critical pressure for this kind of discharge, such as shown in Fig. 2.6(c). Although there is no nitrogen characteristic spectrum to attest the discharge exists in the chamber, we can believe the gas is broken down. Or the pressure below 0.09 Torr which leads to larger electron energy could have supported the phosphor excited. It demonstrates that the density of electrons that arrive at anode must reduce sharply. At this critical pressure, the gas discharge happens and mainly provides electrical particles into the space except for excitation of gas atoms, which means the ionization collisions exceed the excitation collisions. The density of gas is low and the population of charged particles is small, so the current is small. Besides the ionization, the secondary electron emission by ion bombardment at the cathode is also indispensable to maintain the discharge.

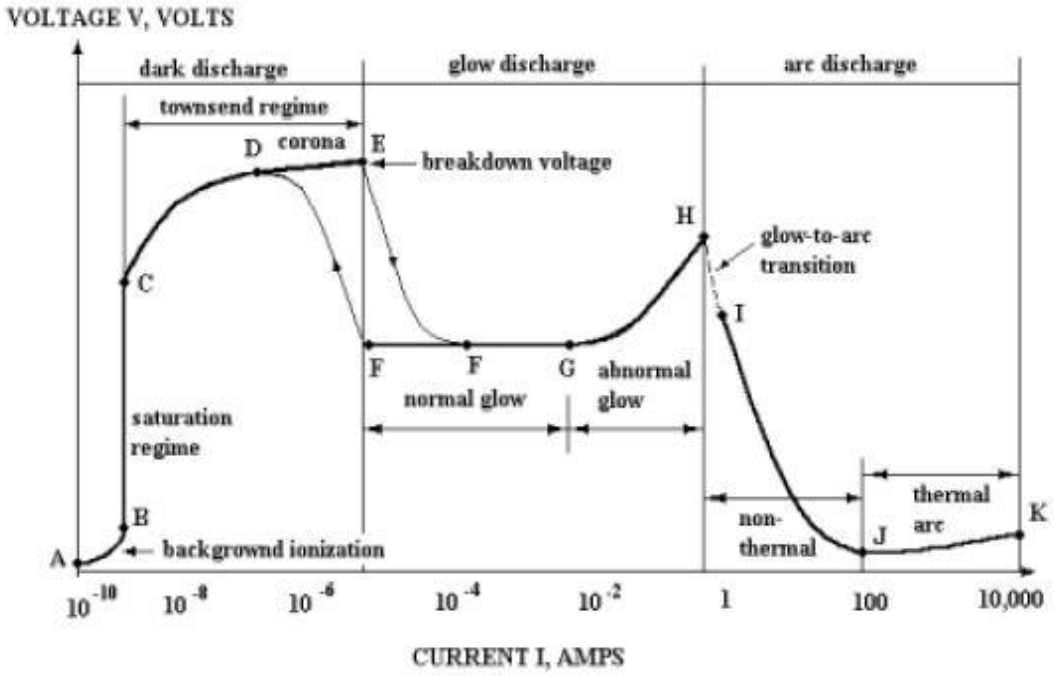

Fig. 1.4. Voltage v.s. current plot of discharge.

From Fig.1.4 in chapter I.2.2, the voltage current characteristic curve of a glow discharge, C-E represents the Townsend regime: the current rises exponentially and the point E represents the breakdown point. Then the process in this kind of condition should locate between the point E and G in the figure. Among this progress, area from E to F is a transition regime and area from F to G is the normal glow discharge regime, which would happen automatically. When the electron avalanche happens the lamp voltage will automatically decrease to a low value which is enough to sustain the multiplication of the current and corresponds to the stable voltage in the regime from F to G. The current would be decided by the ballast resistor in the outer circuit, while the stable voltage would be related to the pressure if gas species and discharge equipment are same. The lower pressure require higher self- sustain voltage. So when the pressure is low enough to make the self-sustain voltage close to the breakdown voltage, we would get the working condition for the FDDL. If the electric field becomes even stronger, the secondary electron may also ionize another neutral atom leading to an avalanche of electron and ion production.

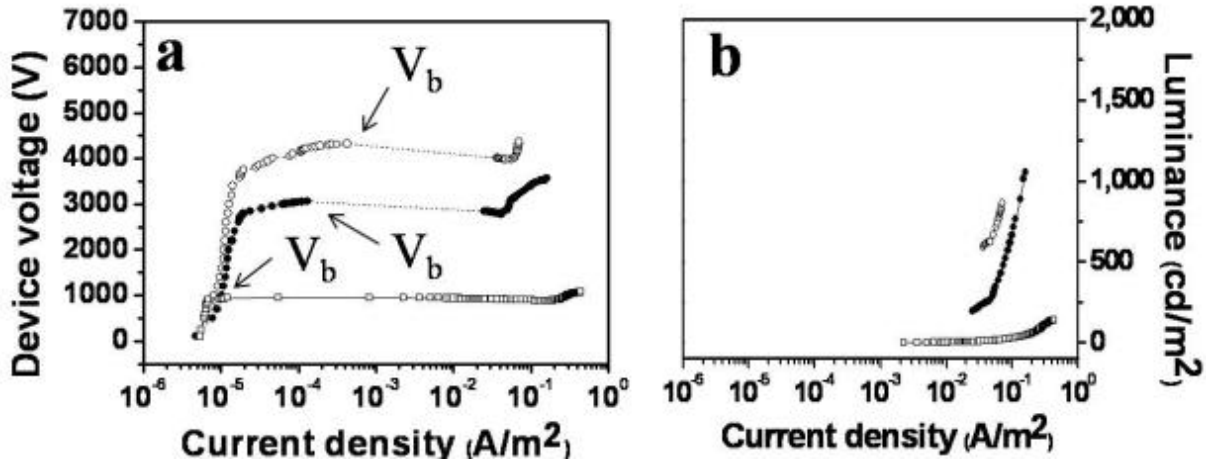

Fig. 2.7 (a) The current density-voltage characteristics of devices operated at various gas pressures. (○, p = 0.110 Torr; ●, p = 0.130 Torr; □ , p = 0.210Torr); (b) Photo-luminance versus current density (L-J) for the corresponding devices shown in (a).

Fig. 2.7 [11] and 2.8 is the voltage current plot of nitrogen FDDL from Energy and Environment Research Laboratories, Industrial Technology Research Institute of Taiwan. Comparing the Fig. 1.4 and Fig. 2.8, we can easily find their common features. As Townsend discharge, FEEL also works under high voltage and its discharge current is small only in μA scale but rises exponentially. This kind of discharge shows features of a Townsend discharge. If continue increase the current the discharge may go to the glow discharge area. As showed in Fig. 2.7, the breakdown voltage V_b and the voltage plateau are decided by the pressure (the higher pressure, the lower voltage). For this cold electrode discharge it is hard to gain extra electrons from the conductive film electrode like what happens in the abnormal glow region. That is why at the end of the lines the voltage will go upside.

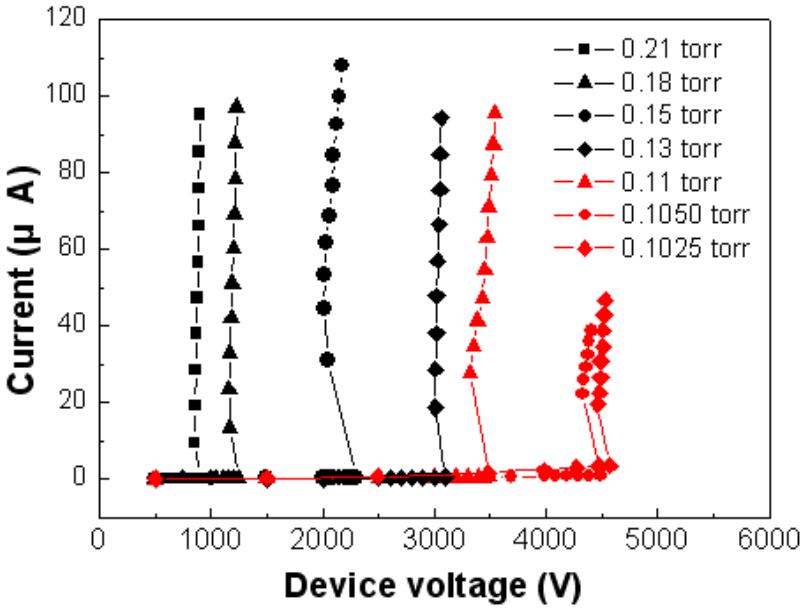

Fig. 2.8 V-I curve of FEEL

II.3 Physics of discharge theory

II.3.1 Mean free path

European nuclear society defines the Mean free path as the medium length of a path covered by a particle (photon, atom or molecule) between subsequent impacts [12].

Imagine a beam of particles A (with density n and radius r_a, the direction of mobility is positive x axis direction) being shot through a target particles B (with density N and radius r_b), and consider an infinitesimally thin slab of the target. In the distance between x and x + dx, the number of the particles A collided per unit time and per unit cross area is dn.

$$\frac{dn}{dt} = -N\pi(r_a + r_b)^2 n \frac{dx}{dt} \qquad (2.1)$$

After integration of equation 2.1, we can get 2.2.

$$n = n_0 \exp[-N\pi(r_a + r_b)^2 x] \qquad (2.2)$$

n_0 is the density of particle A at x=0, and $\sigma = \pi(r_a + r_b)^2$ is defined as effective cross sectional area. Q=N*σ means the total effective cross sectional area, which also means number of collisions per unit length and per unit time for single particle A [13]. So we can get mean free path λ as:

$\lambda=1/(N^* \sigma)$ (2.3)

The number of molecules per unit volume N can be determined from Avogadro's number N_A and the ideal gas law, leading to:

$$N = \frac{m*N_A}{V} = \frac{m*N_A}{\frac{m*R*T}{p}} = \frac{N_A*p}{R*T} = \frac{p}{k_B*T} \quad (2.4)$$

Then from 2.3 and 2.4 we could get:

$$\lambda = \frac{k_B*T}{\pi(r_a+r_b)^2*p} \quad (2.5)$$

In kinetic theory the target particles B are not resting. Considering the molecular mean free path, if the velocities of the identical particles B have a Maxwell distribution, the following relationship applies [14]:

$$\overline{v_{relative}} = \sqrt{2}\bar{v} \quad (2.6)$$

and it may be shown that the mean free path, in meters, is:

$$\lambda = \frac{k_B*T}{\sqrt{2}\pi d^2*p} \quad (2.7)$$

where k_B is the Boltzmann constant in J/K, T is the temperature in K, p is pressure in Pascals, and d is the diameter of the gas particles in meters.

When it is on, the lamp voltage is high and the temperature is low (about 300K). The velocity of gas atoms in the chamber could be neglected compared with that of the electrons and the size of electrons could be neglected compared with that of gas atoms. So we can use formula 2.5 to calculate the mean free path. The results show in table 2.1.

pressure(Pa)	He	Ne	Ar	Kr	Xe	N2
20	68,6	45,7	13,1	8,5	5,7	22,6
30	45,7	30,4	8,7	5,7	3,8	15,1
60	22,9	15,2	4,4	2,8	1,9	7,5

Table2.1 Mean free path (in mm) of gases at different pressure

The mean free path of the gases at low pressure is comparable with the distance between electrodes (10 mm). It demonstrates only some of the electrons in the discharges space have an opportunity to collide with the gas atoms or molecular before they arrive at the anode. These electrons will transfer the energy from the electrical field to the gas atoms by the elastic or inelastic collisions, which have the atoms or molecular ionized or excited and make the gas breakdown. The other electrons will not lose their energy by collisions, which will excite the CL phosphor on the anode.

II.3.2 General diffusion

When we study gas discharge, it is always limited by an insulating wall (such as glass) and by electrodes (metals or conductive film). These materials, whose properties are different from those of the plasma, lead to the emergence of differences in density (matter or radiation), temperature and potential. This will result in a displacement of matter (or radiation) that will tend to restore the homogeneity of the medium. During this displacement, the electron cloud will get power from the source and the electrical particles will move to the boundary of the discharge space.

If we accept the approximation that the electrons' movement should follow the rules for the binary distribution of a type of minority particles in a homogeneous gas, then we can get the the following expression for the current distribution:

$$n_e V_e = -\frac{\nabla(n_e k_B T_e)}{m_e \nu_{el}'} \qquad (2.7)$$

where ν_{el}' is the effective collision frequency.

If the temperature of electrons Te varies quite little, we can get the diffusion flux as:

$$n_e V_e = -\frac{k_B T_e}{m_e \nu_{el}'} \nabla n_e = -D_e \nabla n_e \quad \text{with} \quad D_e = \frac{k_B T_e}{m_e \nu_{el}'} \tag{2.8}$$

At the microscopic level, in the absence of electric field, if one seeks to study the Boltzmann equation the evolution of a non-uniform electron cloud density in a homogeneous neutral gas, we can have diffusion current as:

$$n_e V_e = -\frac{1}{3} \nabla \int_0^{\infty} \frac{\nu_e^2}{\nu_{el}} 4\pi \nu_e^2 \emptyset_0 \, d\nu_e = \frac{1}{3} \nabla \left[n_e \left\langle \frac{\nu_e^2}{\nu_{el}} \right\rangle \right] \tag{2.9}$$

where ν_{el} is the collision frequency for the transfer of momentum. If the distribution function is homogeneous, $\left\langle \frac{\nu_e^2}{\nu_{el}} \right\rangle$ can leave the operator and get

$$n_e V_e = -D_e \nabla n_e \quad \text{with} \quad D_e = \frac{1}{3} \left\langle \frac{\nu_e^2}{\nu_{el}} \right\rangle \tag{2.10}$$

The comparison of the relationship (2.8) and (2.10) leads to the expression of the effective collision frequency

$$\nu_{el}' = -\frac{\nabla [n_e \langle \nu_e^2 \rangle]}{\nabla \left[n_e \left\langle \frac{\nu_e^2}{\nu_{el}} \right\rangle \right]_e} \tag{2.11}$$

If the ν_{el} is constant, then we can get $\nu_{el}' = \nu_{el}$ and

$$D_e = \frac{k_B T_e}{m_e \nu_{el}} \tag{2.12}$$

We assumed that the diffusion of electrons and ions were free and independent of each other. It would not happen in the plasma which obeys the electrical neutrality condition. If the species of ions and electrons were independent from each other in the plasma, they would separate from each other at very different speeds. It shows that:

$$\frac{D_e}{D_i} \sim \sqrt{\frac{m_i}{m_e}}$$

In mercury discharge the number should be 600 and in the argon discharge the number should be 270.

Given the importance of electrostatic forces, any separation between the ion cloud and the electron cloud will bring up a restoring force tending to restore intense neutrality. This force is related to the field of ambipolar diffusion Ea. Under these conditions, at the boundary of plasma, under the double influence of density gradients and ambipolar diffusion field Ea, all charges will travel at a speed greater than ions but lower than expected electron.

For solving this problem completely, we should take into account the balance of creation and destruction of ions and electrons (with speed Vi and Ve), the movement of these particles under the double influence of the field Ea and density gradients of ions and electrons and finally the Poisson equation linking electrical field and the charges in the space. In general we will simplify the resolution by admitting that $\mathbf{n_i = \varepsilon n_e}$ and $\mathbf{n_i V_i = n_e V_e}$. With this simplification the Poisson equation is no longer needed and we obtain:

$$n_i \mathbf{V_i} = n_e \mathbf{V_e} = -D_s \nabla n_e = D_s \nabla n_i \qquad \text{with} \qquad D_s = \varepsilon \frac{\mu_i D_e - \mu_e D_i}{\varepsilon \mu_i - \mu_e} \qquad (2.13)$$

When ε = 1 this diffusion is called ambipolar diffusion and Ds = Da. Taking into account the Einstein relation as

$$D = \frac{\mu k_B T}{e} \qquad (2.14)$$

where D is the diffusion constant; μ is the "mobility", or the ratio of the particle's terminal drift velocity to an applied force, $\mu = V_d / F$; T is the absolute temperature. For the given species the diffusion coefficient is obtained:

for Te»Tg: $D_a = \frac{\mu_i k_B T_e}{e}$ and for Te = Tg: $D_a = \frac{2\mu_i k_B T_e}{e}$ (2.15)

This ambipolar diffusion approximation is only checked if the diffusion distance is very large compared to the Debye length.

II.3.3 Townsend discharge theory

The **Townsend discharge** is a gas ionization process where free electrons, accelerated by a sufficiently strong electric field, give rise to electrical conduction through a gas by avalanche multiplication. When the number of free charges drops or the electric field weakens, the phenomenon ceases. The Townsend discharge is named after John Sealy Townsend, and is also commonly known as a "Townsend avalanche".

The avalanche is a cascade reaction involving electrons in a region with a sufficiently high electric field. This reaction occurs in a medium that can be ionized, such as air. Following the ionization of an atom or molecule of the medium in a device which exerts an electric field, the positive ion drifts towards the cathode, while the free electron drifts towards the anode of the device. If the electric field is strong enough, electrons gain sufficient energy to free a further electron by collision with another atom/molecule. The two free electrons then travel together some distance and gain energy from the electric field before another collision occurs, and so on. This is effectively a chain reaction of electron generation. The number of electrons travelling towards the anode is multiplied by a factor of two for each collision, so that after *n* collisions, there are 2^n free electrons. The limit to the amount of multiplication in an avalanche is known as the Raether limit [15].

Townsend proposed three coefficients: the first Townsend ionization coefficient α, the second Townsend ionization coefficient β and the third Townsend ionization coefficient γ.

The first Townsend ionization coefficient α expresses the number of electron-ion pairs generated per unit length (e.g. meter) by an electron moving from cathode to anode. Townsend described it as 2.16.

$$\frac{I}{I_0} = e^{\alpha * d} \qquad (2.16)$$

I is the current flowing through the device. I_0 is the photoelectric current at cathode. d is the distance between electrodes.

Considering the meaning of mean free path λ and ionization possibility, the first Townsend coefficient α is a function of pressure and accelerating field. The coefficient α is expected to behave conform [16]

$$\alpha = \frac{const}{\lambda_e} \exp\left(-\frac{E_{ion}}{E\lambda_e}\right) \qquad (2.17)$$

where λe is the mean free path for electron scattering off neutrals, $E_{\lambda e}$ is the energy gain in the electric field generally between collisions, and E_{ion} is the energy needed to ionize the atoms. Note that the mean free path for electron scattering is inversely related with pressure (seen in 2.5). Further, voltage V equals the electric field times gap distance d. That yields

$$\alpha = A * p * \exp\left(-\frac{B*p*d}{V}\right) \qquad (2.18)$$

where A and B are constant in a confirmed condition determined experimentally [17] and found to be roughly constant over a range of voltages and pressures for any given gas [16].

Subsequent experiments revealed that the current I rises faster than predicted by the formula 2.17. Two different effects were considered in order to explain the phenomenon. The second Townsend coefficient β expresses the number of electron-ion pairs generated per unit length by an ion moving from anode to cathode, and the third Townsend coefficient γ expresses the number of electrons generated from the cathode by the impact of an ion.

In one dimensional model [18], particle balance for these species is expressed by the continuity equations:

$$\frac{\partial n_e}{\partial t} + \frac{\partial \Phi_e}{\partial x} = S_e \qquad (2.19)$$

$$\frac{\partial n_i}{\partial t} + \frac{\partial \Phi_i}{\partial x} = S_i \qquad (2.20)$$

where ne and ni are the electron and ion densities, Φ_e and $\Phi_i$are the electron and ion fluxes and Se and Si are the source functions of slow electrons and ions. The fluxes are calculated on the basis of the drift-diffusion approximation:

$$\Phi_e = -\mu_e n_e E - D_e \frac{\partial n_e}{\partial x} \qquad (2.21)$$

$$\Phi_i = \mu_i n_i E - D_i \frac{\partial n_i}{\partial x} \qquad (2.22)$$

where μ_e and μ_i are the mobilities of electrons and ions. De and Di are the diffusion coefficients of electrons and ions. In Townsend theory the electrons and ions comes from the electron-atom (α process) and ion-atom (β process) ionization collisions. Then we can get the source function as below.

$$S_e = S_i = \alpha\Phi_e + \beta\Phi_i \qquad (2.23)$$

The electrical flux has relationship with the circuit current as

$$\Phi = \frac{I}{e} \qquad (2.24)$$

Then we could get the relationship between circuit current density I and the particles flux.

$$\Phi_{total} = \Phi_e + \Phi_i = \frac{I}{e} \qquad (2.25)$$

We only discuss the stable and uniform discharge, so the time part in the 2.20 and 2.21 could be deleted. In the low pressure condition, we assume the diffusion part could be neglected too. The initial condition is

At cathode, x=0, V_0=0, $\Phi e=I_0/e+\gamma\Phi_i=I_0/e+\gamma(1-\Phi e)$

At anode, x=d, $V_d=U_{lamp}$, $\Phi_i=0$, $\Phi_e=\Phi$

From 2.20-2.26 and the initial condition we can get the electron current per unit area ie(x) at the position x as below [13]:

$$i_e(\mathrm{x}) = \frac{(\alpha-\beta)I_0+(\alpha\gamma+\beta)\mathrm{I}}{(1+\gamma)(\alpha-\beta)}\mathrm{e}^{(\alpha-\beta)\mathrm{x}} - \frac{\beta\mathrm{I}}{(\alpha-\beta)} \qquad (2.27)$$

We know that at the anode the ie(x) equals I. So we can get:

$$I = \frac{i_0(\alpha-\beta)e^{(\alpha-\beta)d}}{\alpha(1+\gamma)-(\alpha\gamma+\beta)e^{(\alpha-\beta)d}} \qquad (2.28)$$

where i_0 is the initial or background current. It is decided by the density of space free charges. Generally speaking is quiet small in the magnitude about 10^{-12} A [13]. Because generally the ions need thousands of eV energy to ionize other atoms, the possibility is small for them to achiever that before collision. When β is neglected, 2.21 will turn to:

$$I = \frac{i_0 e^{\alpha d}}{1-\gamma(e^{\alpha d}-1)} \qquad (2.29)$$

In Towsend's theory, if the discharge could sustain by themselves, that means I_0 could be zero. In 2.23, when the numerator is zero, the denominator should be zero too, which could keep I sustain. And then we get the criterion of self-sustained discharge as below:

$$\frac{1}{\gamma} = e^{\alpha d} - 1 \qquad (2.30)$$

Combining 2.18 with the breakdown condition [16], [19], [20] yields

$$V_{breakdown} = \frac{\mathrm{B}*\mathrm{p}*\mathrm{d}}{\ln(\mathrm{A}*\mathrm{p}*\mathrm{d})-\ln(\ln(1+\frac{1}{\gamma}))} \qquad (2.31)$$

Formula 2.31 relates the breakdown voltage $V_{breakdown}$ with the product p*d, which is called the Paschen curve. It should be noticed that the Paschen curve has a minimum below which breakdown cannot occur (seeing Fig. 1.5.a). The Paschen curve is a function of the gas and weakly of the electrode material [21].

The electrode material is fluorine-doped tin-oxide film. The equation 2.30 and 2.31 offer a method to measure the secondary electron emission coefficient γ. There is a inear fit to the experimental data is shown as below in previous research [22],

$$\gamma = \ 1.2 \times 10^{16} \times \frac{E}{n} - \ 0.0043 \qquad (2.32)$$

in which the breakdown voltage is measured for argon discharge with tin oxide electrodes, for three different electrode distances (0.01 cm, 0.025 cm and 0.05 cm) and for pressure between 1.3 kPa and 13.3 kPa. In Phelps' paper [1] this coefficient in argon and in high reduced electrical field with copper electrodes was also discussed.

The ITO films covered with FTO particles of 7 nm in average size show an ionization potential of 5.01 eV, as compared with ~4.76 and ~4.64 eV in ITO and FTO films, respectively, which decreases as the FTO particle size increases. Here we assume the secondary electron emission coefficient is 0.2.

The first and second Townsend ionization coefficients α and β could be calculated by their definition such as 2.18.

II.4 Theoretical Analysis on the FDDL

II.4.1 Ions and electrons current distribution with x position

In our discharge condition we could assume parameter of discharge as below:

- The distance between the film electrodes d is 1cm.
- The temperature of working lamp is 300K
- The pressure of gas p is 18 Pa.
- The voltage on the discharge gap V_{lamp} is 1 kV.
- The current through the lamp is 1mA.
- The surface area is 100 cm2

According to 2.4 the density of gas N is $4.35*10^{+21}$ m^{-3}. So the reduced electrical field E/N is $2.30*10^{+04}$ Td (1Td =10^{-17} Vcm^2). The current density I is 10^{-5} A/cm^2.

As the mean free path is larger than the gap distance d, the collision should be rare. For example, when λ=40 mm, the electron-atom collision portion is only about 22%. We assume

the ionization collision is the main process and the excitation and elastic collision could be neglected. Only one pair of electron and ion would be produced in each ionization collision.

Poisson equation is as below:

$$\frac{\partial^2 V}{\partial x^2} = -\frac{\partial E}{\partial x} = -\frac{e}{\varepsilon_0}(n_i - n_e) \qquad (2.33)$$

We could get the electrical field and the density of electrons and ions from 2.18 and 2.24. Ve and Vi are considered as the function of reduced electrical field (E/N), and e is the elementary charge and ε_0 is the permittivity of free space.

The diffusion coefficients De and Di are calculated from the Einstein relation 2.14.

According to Townsend theory [14], α is first Townsend coefficient and γ is secondary emission coefficient. α means the number of electrons created in the gas per length and it is the function of E/P. In Townsend discharge there is the relation as below:

$$i = \frac{i_0 e^{\alpha d}}{1 - \gamma(e^{\alpha d} - 1)}$$

I_0 is the initial current in scale of 10^{-12} A, i is the discharge current and d is the gap distance between electrodes. We could get the electron and ion current distribution along x axis, as is in Fig. 2.9.

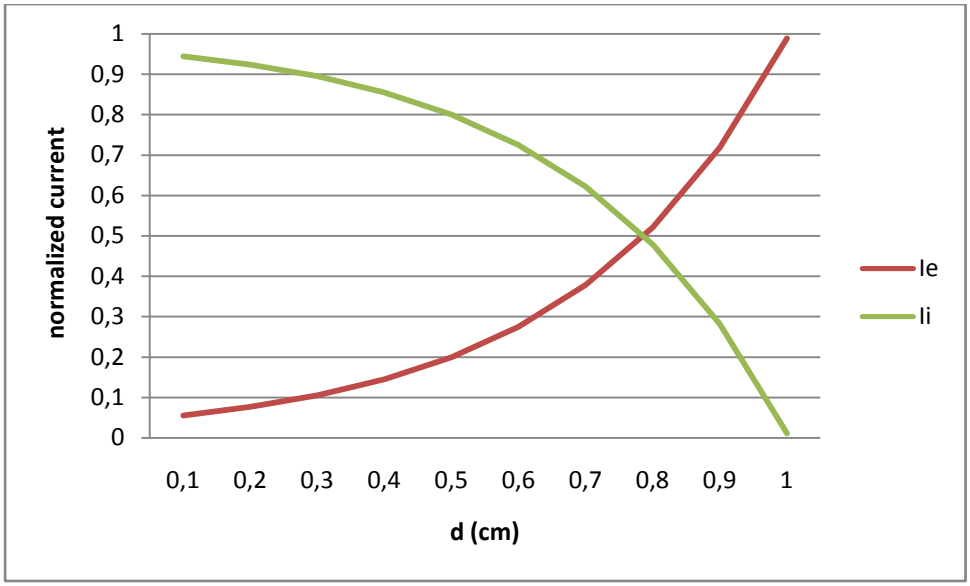

Fig. 2.9 The normalized electron current (i_e) and ion current (i_i) distribution. X is the distance from cathode in cm, and anode is at x=1 cm.

II.4.2 Analyses by mean free path of ionization and excitation collision

According to Table 2.1, we know that at low pressure mean free path of electrons in the gases is comparable with the discharge gap of the FDDL, which explains the high working voltage for this lamp. Fig 2.6(c) demonstrates that there is a critical pressure at which the phosphor luminance is strong while the excitation emission is quite rare.

Assuming the velocity distribution of electrical particles insides obeys the Maxwell–Boltzmann distribution:

$$f(v) = \sqrt{\left(\frac{m}{2\pi kT}\right)^3} 4\pi v^2 \exp\left(-\frac{mv^2}{2kT}\right) \qquad (2.34)$$

we could calculate the mean cross section as below:

$$\bar{\sigma} = \int_0^\infty \sigma(v) f(v) dv \qquad (2.35)$$

Combing with the formula 2.3 and 2.4, we could get:

$$\lambda = \frac{k_B T}{\bar{\sigma} p} \qquad (2.36)$$

where T is the ambiance temperature during filling the working gas, P is the filling pressure. Then from the database of the excitation and ionization cross section [23], the energy distribution of the excitation and ionization mean free path (λ_{ex} and λ_i) of each kind of gases at certain pressure could be calculated as shown from Fig 2.10-2.15.

$$\lambda_{ex} = \frac{k_B T}{\bar{\sigma}_{ex} p} \qquad (2.37)$$

$$\lambda_i = \frac{k_B T}{\bar{\sigma}_i p} \qquad (2.38)$$

The horizontal axis shows the energy of electrons in eV and the vertical axis is length in m.

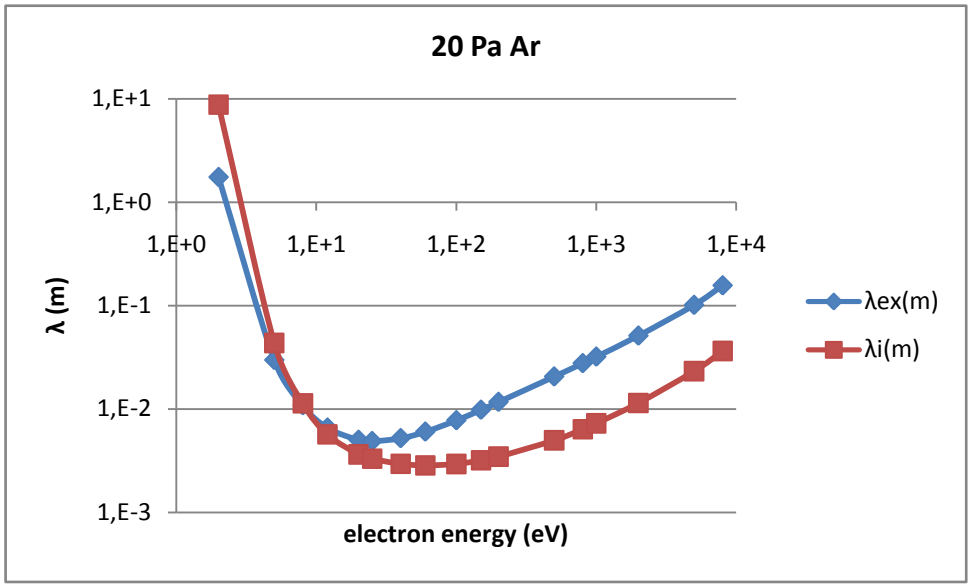

Fig. 2.10 Energy distribution of the excitation and ionization mean free path in 20 Pa Ar.

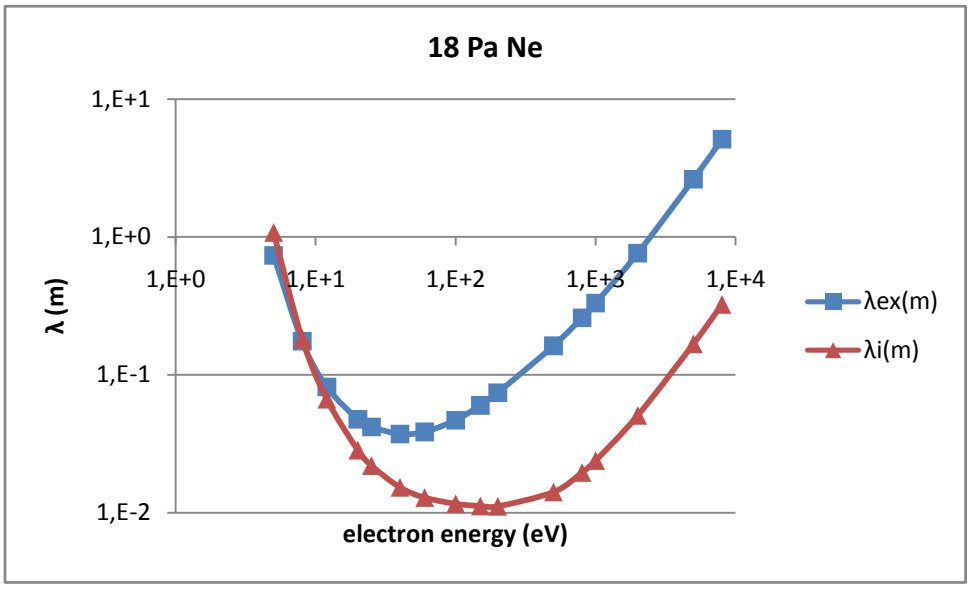

Fig. 2.11 Energy distribution of the excitation and ionization mean free path in 18 Pa Ne.

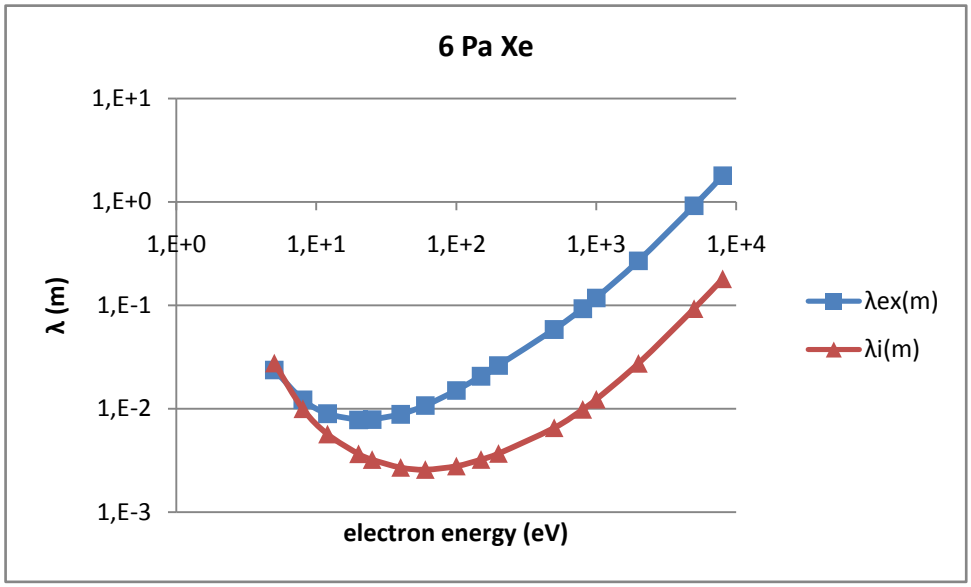

Fig. 2.12 Energy distribution of the excitation and ionization mean free path in 6 Pa Xe.

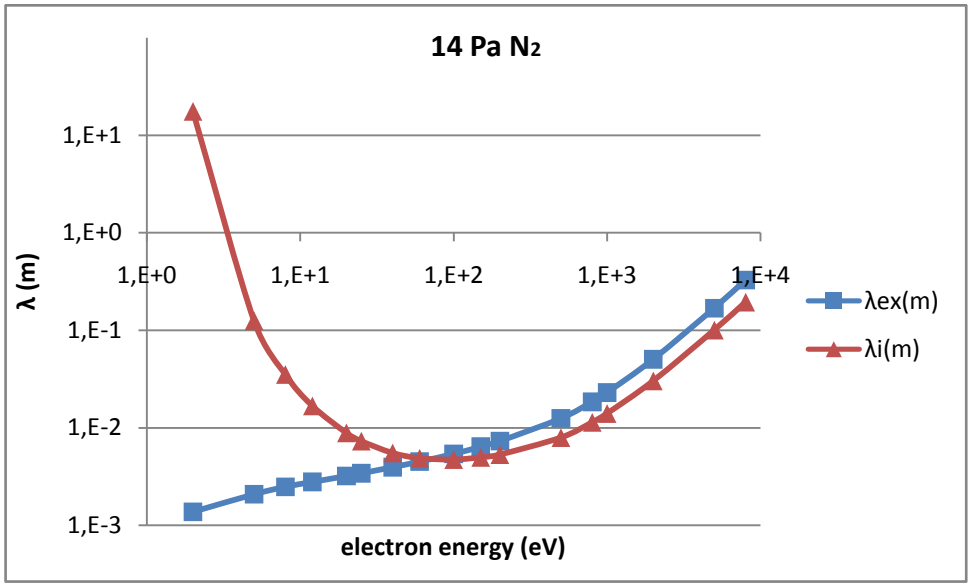

Fig. 2.13 Energy distribution of the excitation and ionization mean free path in 14 Pa N2.

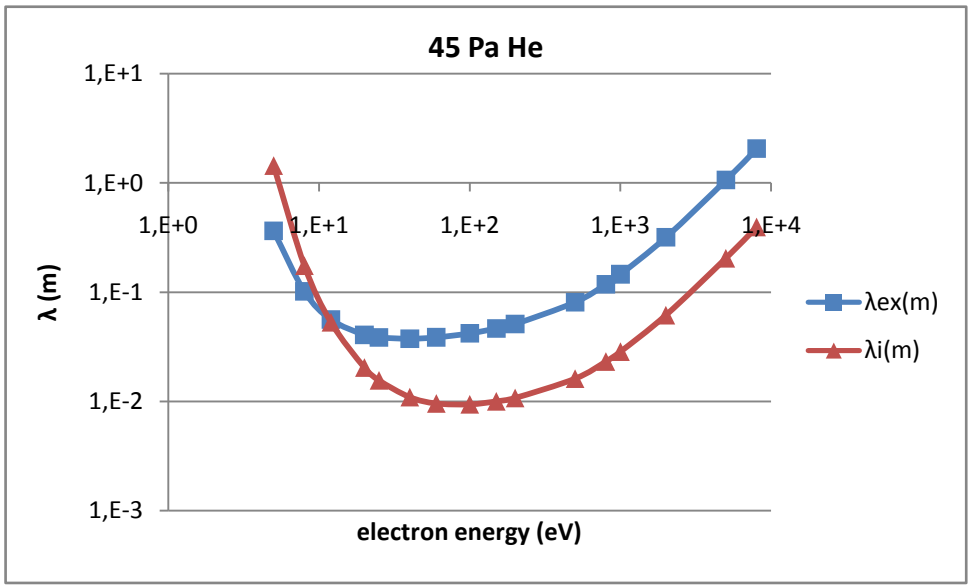

Fig. 2.14 Energy distribution of the excitation and ionization mean free path in 45 Pa He.

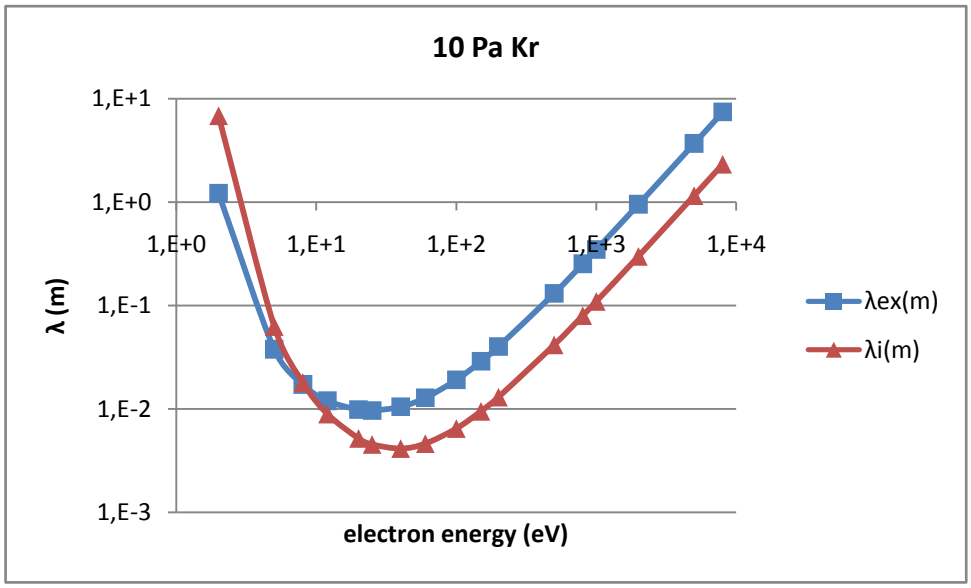

Fig. 2.15 Energy distribution of the excitation and ionization mean free path in 10 Pa Kr.

Mean free path of excitation λ_{ex} predicts the mean length between the electron excitation collisions, and λ_i defines the mean length between the electron ionization collisions. When $\lambda_{ex} > \lambda_i$, it means in the same space the times of excitation collisions are fewer than the ones of the ionization collisions. As the discharge distance for our application is 0.01m, when $\lambda_{ex} > 0.01 > \lambda_i$, it means ionization collisions could provide the electrons to hit the anode phosphor while the seldom excitation collisions would happen in the space, which relates to phenomenon that only the phosphor luminance could be observed in the Fig 2.6(C).

Pressure will decide the vertical position of the free path lines. Lower pressure will make the lines move upward. Generally speaking when the electrons energy is lower than 10 eV, the excitation collisions could be more frequent than the ionization collisions. In the application of N_2 gas the energy of the electrons should be between 100 and 1000 eV. If we use interpolation method we could get a further range between 372 and 703 eV on the Fig 2.13.

Actually the Maxwell–Boltzmann distribution assumption may not be so reliable for our condition, as it is hard for the electrical particles to experience enough collisions to reach the equilibrium state. However the shape of the lines in the figure is consistent with the qualitative analysis: (a). when electron energy is low, possibility of excitation is higher than ionization; when electron energy is high enough, possibility of excitation is lower than ionization. (b). according to the quantization of the energy transfer in the inelastic collisions,

the possibility for excitation and ionization should have a maximum. It would be helpful for understanding the physical procedure in the FDDL.

1. The minimum of the λ_i means the maximum of ionization collisions possibility. The ionization collision will create more electrons and good for the phosphor luminance. λ_{ex} can present the possibility of excitation collision which consumes the energy of electrons before they arrive at anode.

2. There is a minimum for the ionization free path of each kind of gas. It means that there should be a threshold pressure below which no ionization collision would happen between the electrodes no matter how much voltage is applied on the device. Otherwise, the electrons that hit the anode should come from the cathode instead of gas ionization, such as the FED or the CRT.

3. From Fig. 2.16, the pressure will influence the vertical position of the λ_{ex} and λ_i curve. The curve move upwards as the pressure reduces, and move downwards as pressure increases. Obviously bigger density would increase the possibility of ionization collisions and so the mean free path would also be shorter.

4. Excitation collisions transfer energy from electrons to the gas characteristic emission, which would reduce the energy flux at the anode. It would be better to choose the discharge gap between the λ_{ex} and λ_i. So if the pressure is fixed we could adjust the gap distance to have the same results. If the pressure is higher, the gap distance should be lower, which means lower voltage is required to maintain the same electrical field. The lamp may be thinner too.

5. The horizontal position on the plot is the electrons energy, which is decided by the applied voltage as the FDDL temperature is almost stable. If the pressure is a bit high and both the radiation from the gas and from the phosphor could be observed, increasing the voltage on the device would be a possible way to get the phosphor luminance higher and excitation emission lower theoretically.

6. The threshold pressure is different with the gas species. The sequence from high to low is He, Ne, N2, Ar, Kr, Xe.

These quantitative results could point the direction for improvement of the application as people's demand.

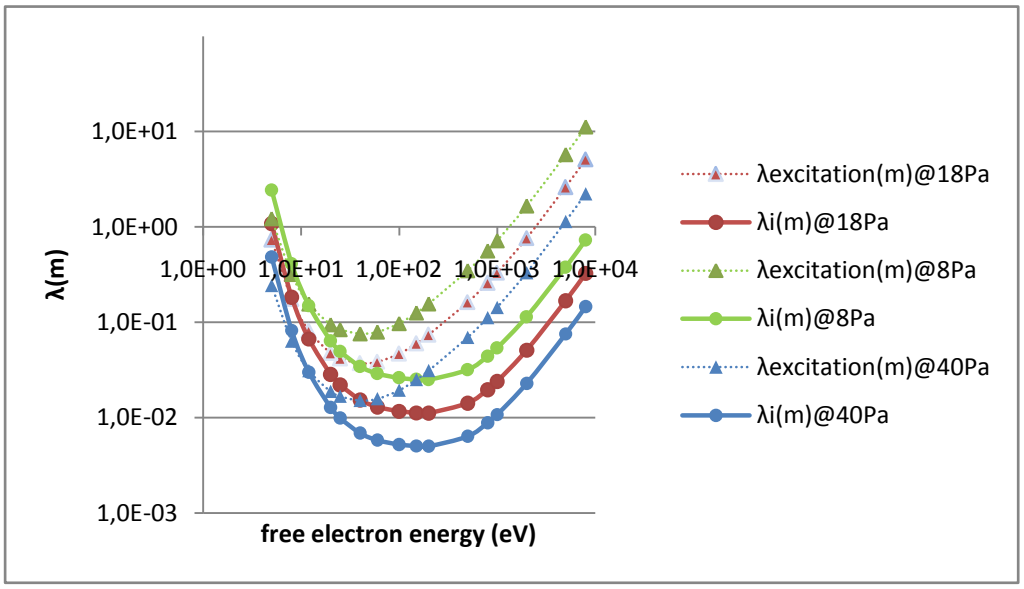

Fig. 2.16 Energy distribution of distribution of the excitation and ionization mean free path in Ne at 8Pa, 18Pa and 40Pa.

II.5 Conclusion

The FDDL works in low pressure, narrow discharge gap and high reduced electrical field. In such a condition it has some common feature with the Townsend discharge, which could help us to make some simple calculation. The narrow discharge gap is even smaller than the thickness of the cathode-fall region [15]. As no sufficient collisions happen before the electrons hit anode phosphor, I use the mean free path of excitation and ionization to predict the relation between the gas species, gas pressure, discharge gap distance and applied voltage, which could give some quantitative guide for improving the FDDL lamp. Further and preciser calculation requires some kind of tracing model to be used, which is not included in this work.

Reference

[1] Phelps, A V, et Z Lj Petrovic. Cold-cathode discharges and breakdown in argon: surface and gas phase production of secondary electrons. *Plasma Sources Science and Technology* 8, no. 3 (août 1, 1999): R21-R44.

[2]Li, Jung-Yu, Shih-Pu Chen, Chia-Hung Li, Yi-Ping Lin, Yen-I Chou, Ming-Chung Liu, Po-Hung Wang, Hui-Kai Zeng, Tai-Chiung Hsieh, et Jenh-Yih Juang. A lighting mechanism for flat electron emission lamp. *Applied Physics Letters* 94, no. 9 (2009): 091501.

[3] C.E Hunt, High-Quality, Energy-Efficient and Affordable Light Source using Cathodoluminescent Phosphors, *Proceedings of the 13th international symposium on the science and technology of lighting*,P395

[4] Weber, L.F. History of the plasma display panel. *IEEE Transactions on Plasma Science* 34, no. 2 (avril 2006): 268 - 278.

[5] Myers, Robert L. *Display interfaces: fundamentals and standards*. John Wiley and Sons. pp. 69–71. ISBN 978-0-471-49946-6. 2002.

[6] Yen, William M.; Shionoya, Shigeo; Yamamoto, Hajime. P*hosphor handbook. CRC Press*. ISBN 978-0-8493-3564-8. (2007)

[7] J. G. Eden, Plasma science in the limit of the small: recent advances in microcavity plasmas and their applications, *The 39th IEEE International Conference on Plasma Science*,2012

[8] Cao, Mitchell M., Rebecca J. Chacon, et Charles E. Hunt. A Field Emission Light Source Using a Reticulated Vitreous Carbon (RVC) Cathode and Cathodoluminescent Phosphors. *Journal of Display Technology* 7, no. 9 (septembre 1, 2011): 467-472.

[9] Li, Jung-Yu, Shih-Pu Chen, Chia-Hung Li, Yi-Ping Lin, Yen-I Chou, Ming-Chung Liu, Po-Hung Wang, Hui-Kai Zeng, Tai-Chiung Hsieh, et Jenh-Yih Juang. A lighting mechanism for flat electron emission lamp. *Applied Physics Letters* 94, no 9 (2009): 091501. doi:10.1063/1.3093802.

[10] R. W. B. Pearse, A. G. Gaydon, The *Identification Of Molecular Spectra*, (Chapman & Hall LTD, London, 1965) third edition, pp.209-220.

[11]Li, Chia-Hung, Ming-Chung Liu, Chang-Lin Chiang, Jung-Yu Li, Shih-Pu Chen, Tai-Chiung Hsieh, Yen-I Chou, et al. Discharge and photo-luminance properties of a parallel plates electron emission lighting device. *Optics Express* 19, no S1 (décembre 17, 2010): A51. doi:10.1364/OE.19.000A51.

[12] http://www.euronuclear.org/info/encyclopedia/m/mean-fee-path.htm

[13]X.Xu. *Gas Discharge Physics*. Fudan University Press, Shanghai, 1996. ISBN7-309-01669-6/O.165

[14] S. Chapman and T.G. Cowling, *The mathematical theory of non-uniform gases*, 3rd. edition, Cambridge University Press, 1990, ISBN 0-521-40844-X, p. 88

[15] Heinz Raether, *Electron avalanches and breakdown in gases*. Butterworths 1964

[16] M. Lieberman, *A. Lichtenberg, Principles of plasma discharges and materials processing*, (Wiley & Sons, New York, 1994).

[17] J. Cobine, *Gaseous conductors*, (Dover, New York, 1958)

[18] P. HARTMANN, H. MATSUO, Y. OHTSUKA, M. FUKAO, M. KANDO and Z. DONKO, Heavy-Particle Hybrid Simulation of a High-Voltage Glow Discharge in Helium, *Jpn. J. Appl. Phys*. Vol. 42(2 003) pp. 3633–3640

[19] F. Chen, *Introduction to plasma physics and controlled fusion*, (Plenum Press, New York, 1984).

[20] R. Bartnikas, E. McMahon, *Engineering dielectrics, Vol. 1, Corona measurement and interpretation*, (ASTM, STP 669, Philadelphia, 1979).

[21] Burm, K. T. a. L. Calculation of the Townsend Discharge Coefficients and the Paschen Curve Coefficients. *Contributions to Plasma Physics* 47, no. 3 (2007): 177–182.

[22]Mariotti, D, J A McLaughlin, et P Maguire. Experimental study of breakdown voltage and effective secondary electron emission coefficient for a micro-plasma device. *Plasma Sources Science and Technology* 13, no. 2 (mai 1, 2004): 207-212.

[23] PHELPS database, http://www.lxcat.laplace.univ-tlse.fr, retrieved Oct. 10, 2012.

CHAPTER III:

Experiment Results on FDDL

III.1 Introduction

Experiments are operated on the sample and empty FDDLs. From the sample tests, some characteristics of the FDDL have been revealed in chapter III.2 including the phosphor performance (the response of the phosphor to different wavelength incident photons) and the uniformity of the lamp. It will help to fully understand the characteristics of this type of brand new light sources. In chapter III.3, the empty lamps are filled with different pressure neon to present the lamp behavior with different pressures and input powers. Low pressure and high input power would help to improve the lamp application. Xenon is also filled as buffer gas to compare the turn on voltage with that of Neon. The V-I plot could help to prove its difference from the field emission. In the commentary chapter, some failures and problems are revealed and possible reasons are discussed.

III.2 Measurement of Basic Quality

III.2.1 Phosphor response to the laser

The phosphor in the lamp is the vacuum phosphor which is also widely used in the vacuum electron emission lamps, such as CRTs. Its component is **(**ZnS:Cu,Al)+In_2O_3. In the phosphor the main luminescent material is ZnS doped Cu and Al. The mechanism of luminescence is similar with semiconductor in which photon emission comes from the recombination of negative free electrons and positive holes. The donor Al^{2+} supply the free electrons and the accepter Cu^{2+} create holes. However, the phosphors are difficult to be used at low voltages due to the presence of the non-emissive layer on the surface of the phosphors and/or the charging-up on the surface of the phosphors with high resistivity. Here the In_2O_3 powder adhered to the surface of ZnS phosphor particle helps it work in lower voltage. It was found

that the conductive coating retarded or eliminated charging-up on the phosphor surface and improved the cathodoluminescent (CL) brightness. However, on the other side, the non-emissive conductive coating also degraded the CL brightness when it was too thick. A study said that phosphors with a 10 wt.% InCl coating (In_2O_3 conductive layer derived from the hydrolysis of indium chloride) would increase the brightness by 20% at 500 V and 1 μA [1]

A band model [2] can be used to demonstrate that process, shown in Fig. 3.1:

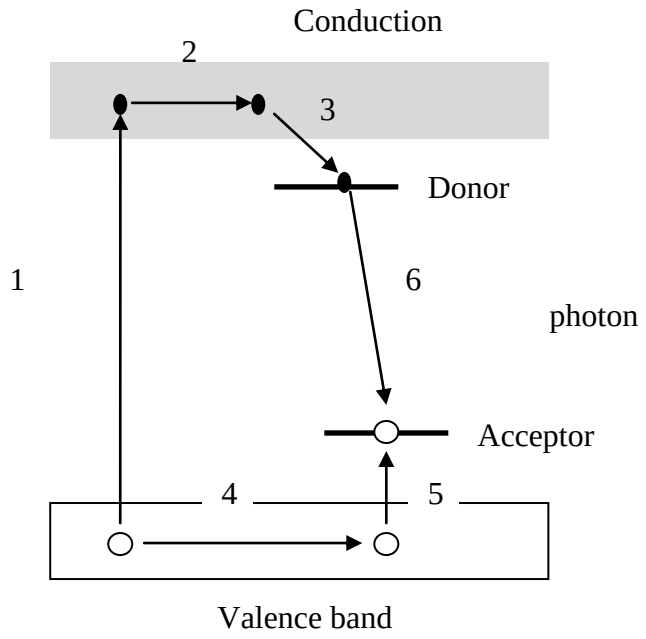

Fig. 3.1 The band model of the ZnS:Cu:Al phosphor

A valence band (In solids, the valence band is the highest range of electron energies in which electrons are normally present at absolute zero temperature [3] .) and a conduction band (The conduction band is the range of electron energies enough to free an electron from binding with its atom to move freely within the atomic lattice of the material as a 'delocalized electron'.) is usually used in discussing the luminescent properties of the ZnS:Cu:Al phosphor. Figure 3.1 shows the luminescence process from (1) excitation of electron from the valence band, (2) migration of the excited electron in the conduction band, (3) the trapped electron in the donor level (Al^{2+}), (4) migration of the hole in the valence band, (5) the trapped hole in the acceptor level (Cu^{2+}), and (6) the electron transition (radiative) from the donor to the acceptor. The green luminescence of the ZnS:Cu:Al phosphor has the peak center wave length at around 530nm(as shown in Fig3.3) which could be well explained by the band model.

The incident electrons or photons could excite the electrons from the conductive band to the valence band. When the electrons are trapped by the donor, they can transit back to the accepter and radiate photons.

From the Fig. 3.1, the minimum energy of incident electrons should equal band gap energy E_g, which is given by 3.1:

$$Eg = E_A + E_D + Ev \qquad (3.1)$$

where E_D is the depth of the Doner level below the conduction band (0.03 eV) and E_A is the depth of the Acceptor level above the valence band (1.2 eV). From equation 3.2, to excite the 530nm photon with the energy of 2.34eV, the minimum energy of incident particle is about 3.57eV in ZnS .

$$E = hv = h\frac{c}{\lambda} \qquad (3.2)$$

But generally electrons may need more energy to penetrate the insulator layer (such as ZnO) to excite the phosphor particles, which makes the necessary electron energy is about $3*E_g$. So the theoretical excitation energy for this phosphor is about 11eV. Its energy conversion efficiency is about 0.21 [4].

According to equation 3.2 if the incident particle is photon, its wavelength should be below 348nm (respond to 3.57ev) and efficient wave length should be below 113nm (respond to 11eV). The realistic value also relates with the concentration of Cu, Al and In_2O_3, the anode voltage Va, particle size, thickness of phosphor and so on.

But as shown in Fig. 3.3, the green luminescence of the ZnS:Cu:Al phosphor is a broad band of Gaussian shape instead of line spectrum. The band model cannot explain this, we should think of the special atomic model in the ZnS crystal. The separation distance (r) distribution of Al^{2+} and Cu^{2+} in ZnS crystal lattice creates this bell shape spectrum. The energy of the emitted photon E(r) could be expressed by 3.3:

$$E(r) = Eg - (E_A + E_D) + \frac{e^2}{\varepsilon * r} \qquad (3.3)$$

where e is the electron charge, and ε is the dielectric constant of ZnS in vacuum.

III.2.2 FDDL sample tests

Thanks to Professor M.C. Liu from Industrial Technology Research Institute of Taiwan. We have 3 neon FDDL sample lamps for the characteristics test. The main structure of the lamps is made of glass. A layer of fluorine-doped tin-oxide (FTO) film is deposited on the inner surface of the main glass as the flat electrode. The phosphor is coated uniformly on the film which works as anode of the lamp. The distance between the electrodes is 1cm. We can see them in Fig. 3.2. The lamps works under DC power supply whose voltage output range is from 0-5.5kV. A resistor with rating of 1MΩ and 10kV is employed as ballast. The other specifics of the sample are in table 3.1.

	Size(inch)	Phosphor	Pressure(Torr)	Voltage(kV)	Current(mA)
Sample 1 and 2	4*4	ZnS:Cu,Al+In_2O_3	0.13-0.15	2.5-3.5	1-2
Sample Small	2*2	ZnS:Cu,Al+In_2O_3	0.13-0.15	3.5-5	0.4-1

Table 3.1 Specifics of sample 1, sample 2 and sample small.

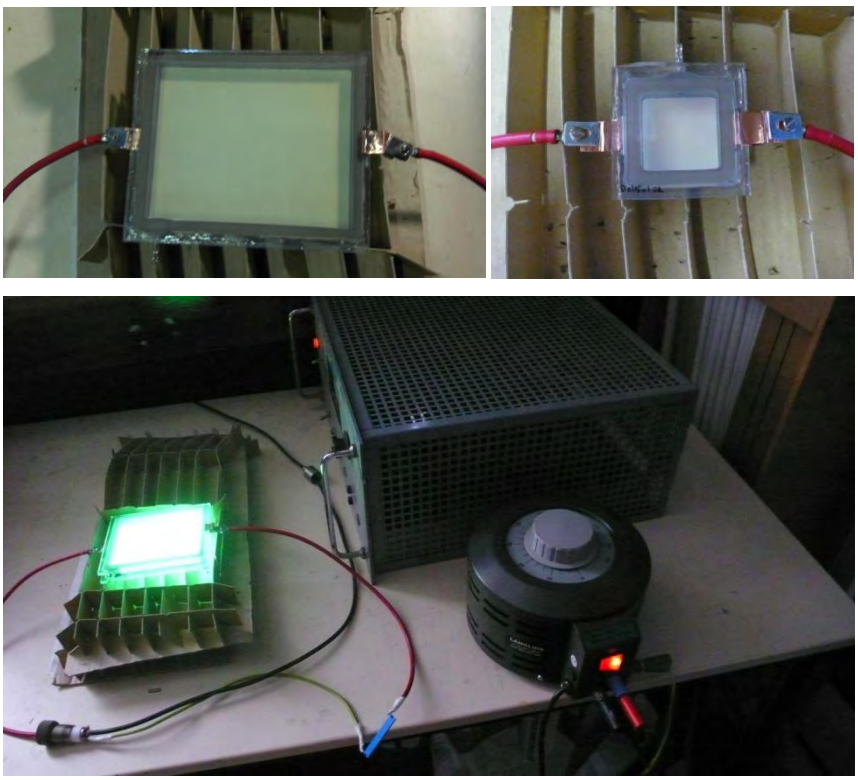

Fig. 3.2 Photos of the sample 4 inches and 2 inches and the experiment setup.

III.2.2.1 Spectrum

The spectrum profile of the sample lamps is shown in Fig. 3.3. A JETI spectroradiometer (specbos 1201) is used to measure the spectrum of the lamp. The peak wavelength is 530nm.

The emission mainly comes from the contribution of Vacuum Fluorescent Display Phosphors. The peak position and profile of this spectrum are quite near that of luminous efficacy function. The luminosity function, as shown in Fig. 3.4, describes the average visual sensitivity of the human eye to light of different wavelengths. This may predict the high visual efficiency of the lamp in further real applications.

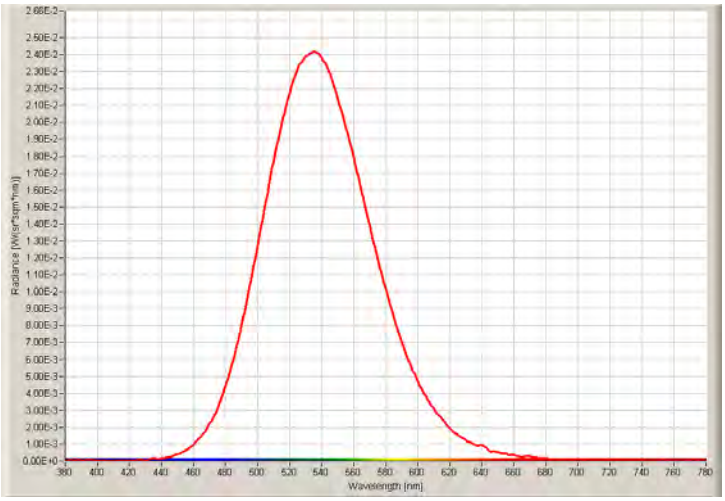

Fig. 3.3 The Spectrum of the sample FDDL with the ZnS:Cu:Al phosphor

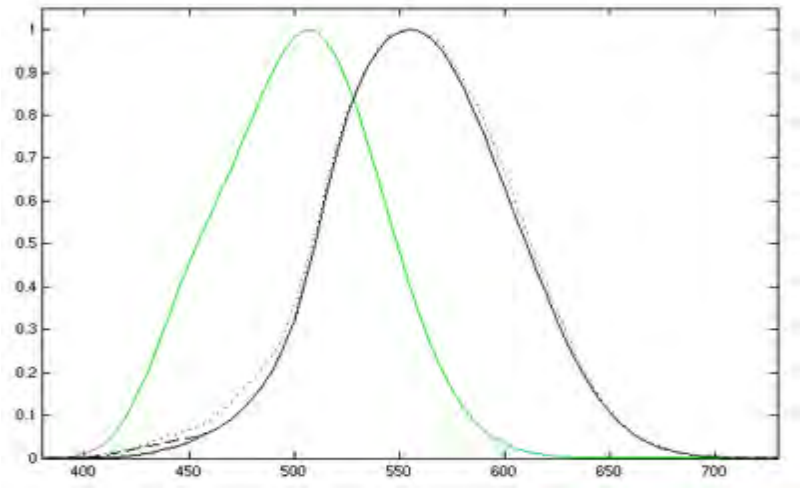

Fig. 3.4 Photopic (black) and scotopic (green) luminosity functions.

Neon works as the buffer gas in the lamps. We can find that in the wave length around 600nm the profile of the spectrum is not so flat. They are the neon characteristic spectral lines [5] (585nm: Three-body production of dimmers; 609nm: Chemoionization; 614nm: Electron

impact ionization of the ground-state and metastable atoms; 640nm: Electron impact de-excitation to the ground state and the $2p^5$ 3s states; 650nm: Spontaneous emission of radiation). However, there is no visible pink light emitted by Neon discharge in the volume. The characteristic radiation is so weak that it could be ignored. That is the reason we name the lamp as dark discharge lamp. The significance of the radiation from the buffer gases could be decided by the pressure of the gas as well as the input power in the operation, which we will discuss in the next chapter.

III.2.2.2 Laser excitation of phosphors

For testing the excitation of the phosphor by different wavelength photon radiation, three laser diode sources are used. The setup of the measurement is as Fig. 3.5. A JETI specbos 1201 is used as the detector in the direction normal to the anode surface of the lamp. The incident angle of the laser is 45 degree. The laser sources can emit red (650nm, <5mw), green (532nm, <5mw) and violet (405nm, <20mw) radiation.

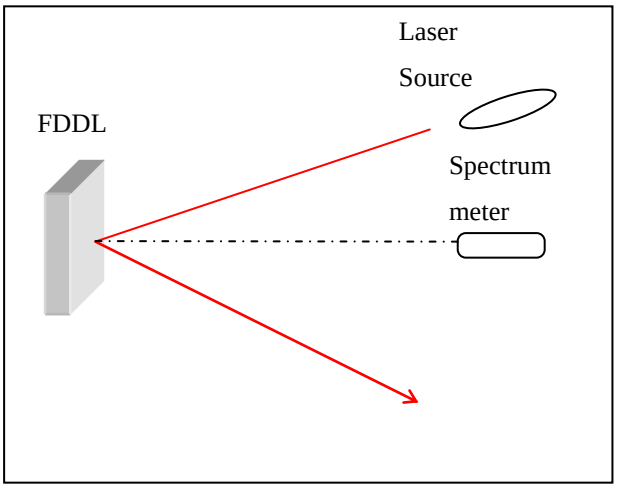

Fig. 3.5 Schematic diagram of measurement

Fig. 3.6 and Fig. 3.7 show the outcome of this measurement. With the green and red laser the spectrum shows only the laser radiation peaks. But with the violet laser the spectrum also shows that there is a weak and broad violet peak at 530 nm. This is the radiant spectrum of the phosphor which only the violet photon managed to excite. However the peak at the 530 nm is nearly two orders of magnitude lower than that at 405 nm. Considering the peak intensity of the three color lasers presents the scatter light intensity of each laser, the phosphor excitation efficiency for the 405nm photon could be much lower than 1%. This demonstrates that the

electron-excited phosphor is not sensitive to visible light and it needs higher energy particles to be excited. As the analysis in III.1, the threshold for ZnS:Cu:Al phosphor should be 336nm. But with the help of In_2O_3, the 405nm photon does excite the phosphor with low efficiency.

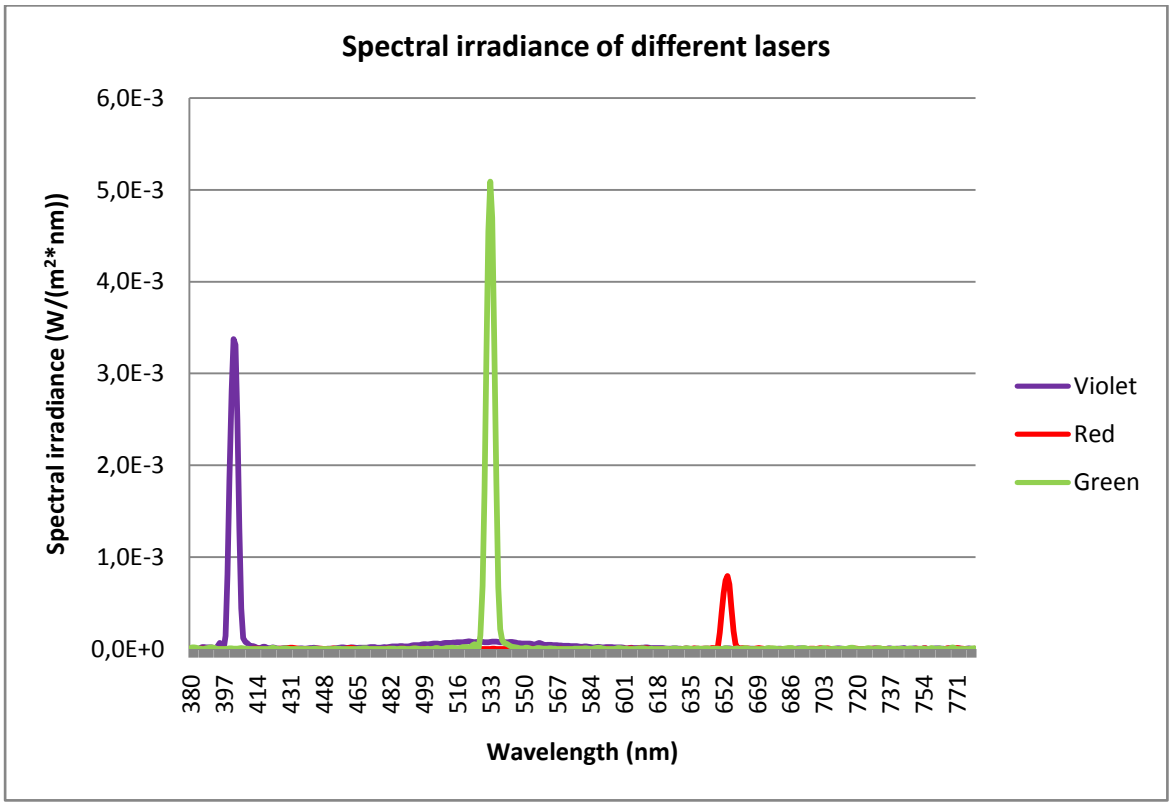

Fig. 3.6 Spectral irradiance of different lasers.

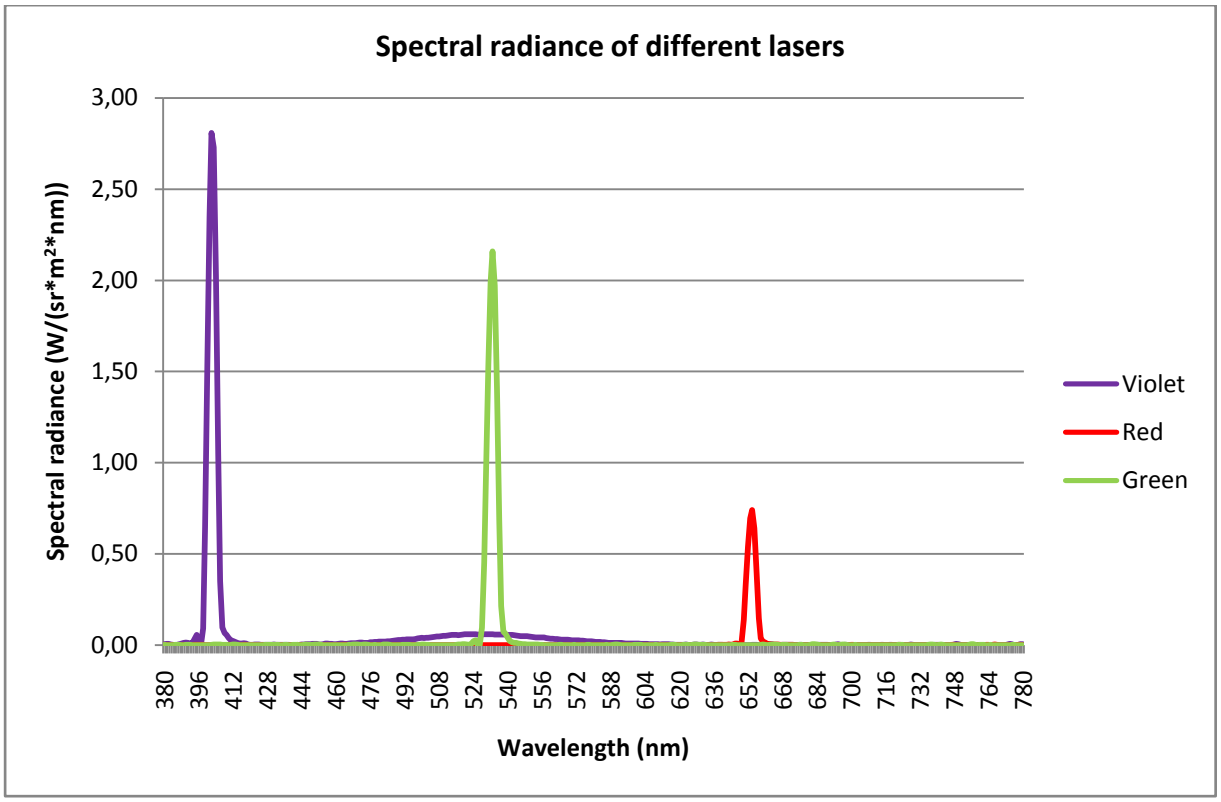

Fig. 3.7 Spectral radiance of different lasers.

III.2.2.3 Uniformity analysis

As the uniformity of such a lamp for future applications is very important we used a calibrated Canon E50 camera to acquire the luminance on the surface of the flat lamp (see Fig. 3.8). The distance between the camera and the lamp was about 150 cm, which is about ten times longer than the size of the lamp.

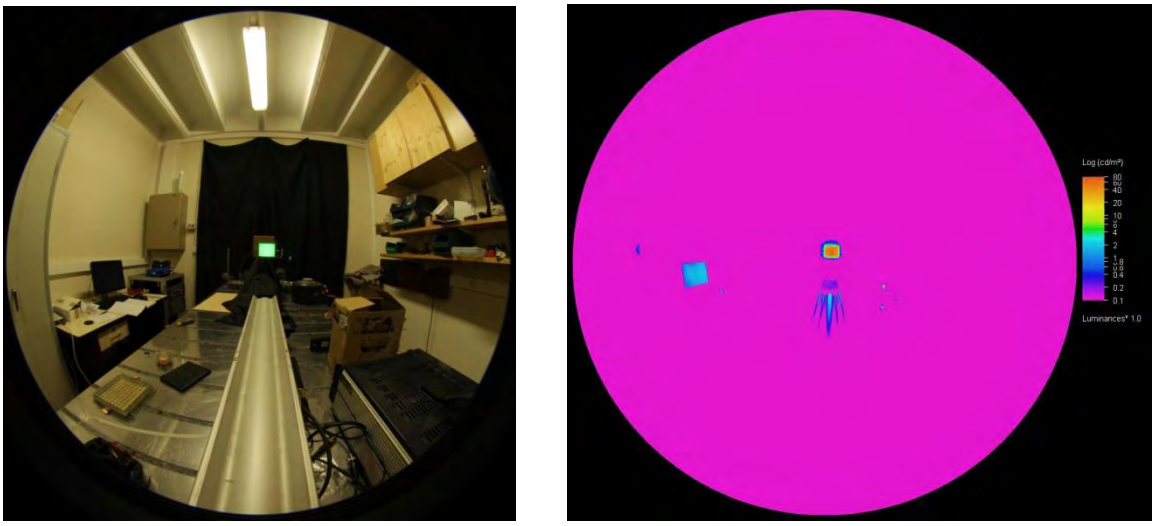

Fig. 3.8 photo shot by camera and the calibrated luminance map.

We can zoom out the lamp area and get the luminance distribution maps of the samples. In these Figures (Fig. 3.9-3.11) we can find out the luminance on major part of the lamp surface is uniform, though the central circle part on the flat lamp is about twice brighter than the peripheral edge area. The uniformity of the sample 2 is shot about every half an hour. As it works, the luminance decreases but the central bright area still exist.

The luminance on the uniformity map presents the plane distribution of incident energy on the phosphor surface, which involves in both the density and velocity of the input particles (electrons and photons). The round central brighter part should relate with the square shape of the lamp. Firstly, it is not infinite large plate, so the electrical field E at the edge is weaker than that in the center. Secondly, the ambipolar diffusion near side glass would create a sheath area.

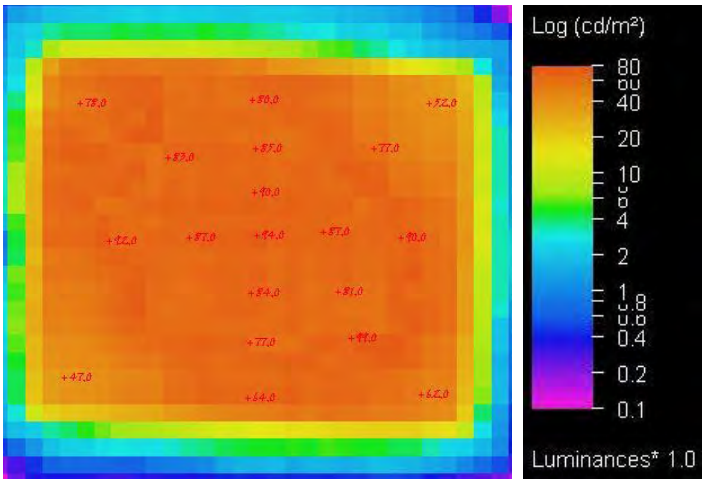

Fig. 3.9 Luminance distribution of Sample 1

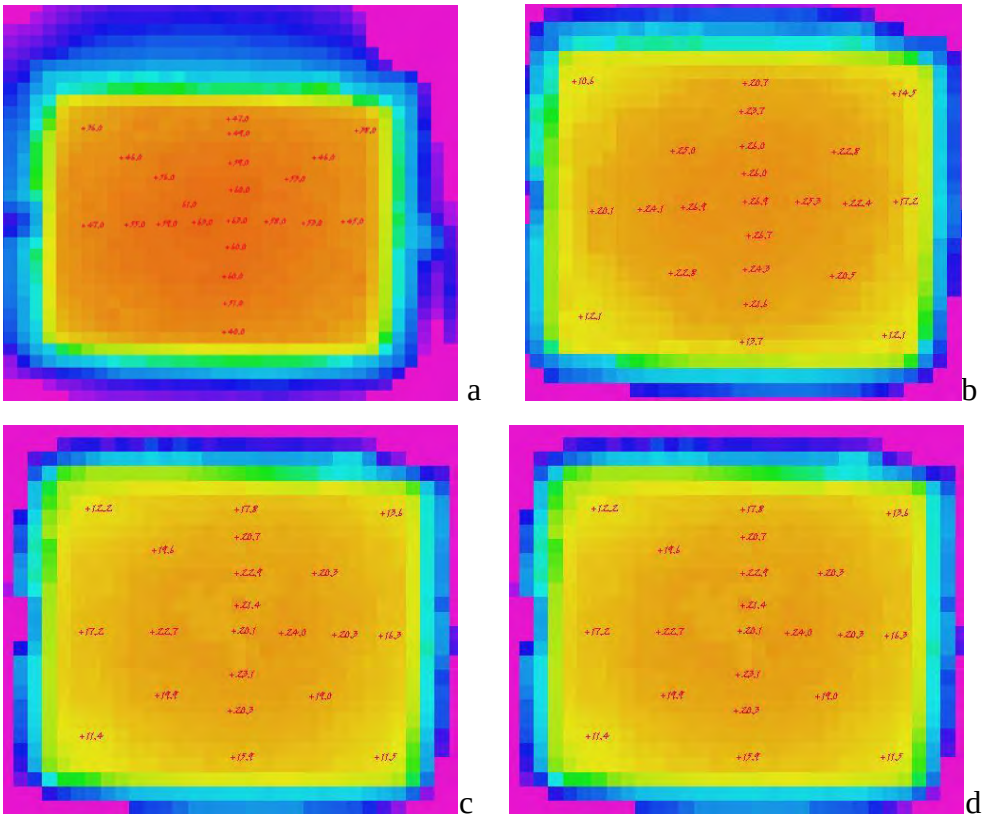

Fig. 3.10 Luminance distribution of Sample 2. a:at t=0; b:at t=0.5h; c:t=1h;d:t=1.5h

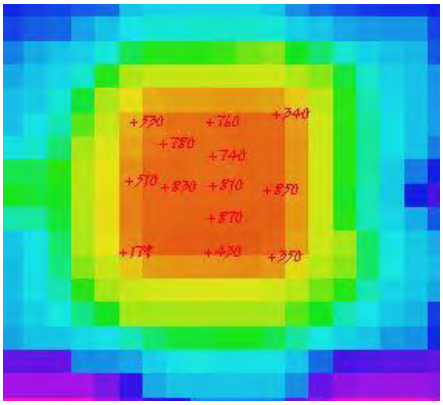

Fig. 3.11 Luminance distribution of Sample Small

From the shape of the central bright aera, It could be reasonable to guess that the efficiency could increase if the surface of the lamp could be changed from square to round.

Fig. 3.10 shows the automatic dimming of the sample lamp with the time, then the self-extinguish happened before next measure point arrived. As time goes by, the breakdown

voltage increases. It illustrate that initial electrons turn fewer or that productions of secondary electrons are more difficult. The initial electrons may be absorbed to the inside wall. Similar problem could also be found in a test result from Taiwan in Fig. 3.12. The self-extinguish demonstrate the electrons insides or the current is too rare to maintain the discharge.

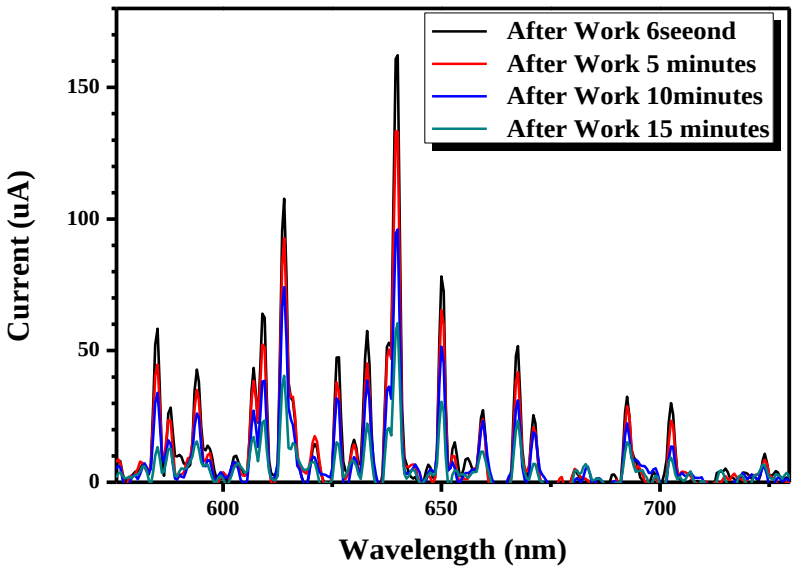

Fig. 3.12 Spectral distribution of FDDL sample without phosphor inside at different working time.

III.3: Lamp Character at Different Pressures

In this part of experiment we filled the empty FDDL lamps with neon. The empty FDDL has the same size and structure with the samples as above. The empty lamp is connected with the vacuum pumping system for adjusting the pressure of buffer gas. Given the pressure we start to increase output of the DC power supply from 0 to 5kV.After the lamp is turned on, the radiance intensity and spectrum is measured by the spectrometer and the electrical parameter is tested by current and voltage meters . we also fill the lamp with Xenon to compare the start voltage with buffer gas neon.

III.3.1 Experiment setup

Fig. 3.13 Photoes of the equipment

The setup of equipments for the experiment shows in Fig. 3.13 and Fig. 3.14. List of the equipment are as following:

Power supply: voltage regulator (output 0-240V)+ALIMENTATION DE POMPE IONIQUE (RIBER Model 401-350, output range 0-5.5kV).

Current meter: PSY30uA-LANGLOIS ampéremètre agnétoélectrique, 100mV, 30-100-300μA- 1-3-10-30-100-300mA- 1-3A, precision :1.5%.

Voltage meter : KEITHLEY 175A autoranging multimeter, DCV range: 200mV-20V-200V-1000V, accuracy: ±0.03%+1 digits.

Spectrometer: JETI spectroradiometer (specbos 1201), Luminance accuracy: ± 2 %.

Pumping System: AUPEM SEFLI, BATI DE POMPAGE MANUEL.Pump:ALCATEL PASCAL 2005I. Vacuum Gauge: ALCATEL CA III pirani (10^{-3}mbar-1ATM), ALCATEL FA III penning (10^{-7}mbar-10^{-2}mbar), MKS instruments PR4000 and Baratron® Manometers (0.01-155,000 Torr).

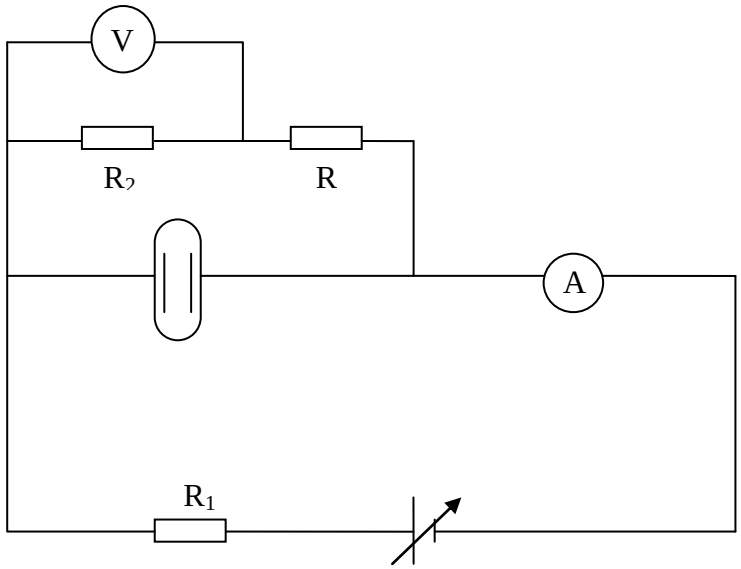

Fig. 3.14 Experiment setup

III.3.2 Neon at 0.19 mbar and 0.20 mbar

In this part the experiment circuit is shown in Fig. 3.14. In the circuit the resistance of the resistors are as below : R1=1MΩ, R2=10.3MΩ, R3=0.99MΩ. The voltage regulator's output is connected to the input of the power supply and controls the total voltage from 0 to 5kV.

The pressure of the neon is set at 0.19mbar (about 0.14Torr). By changing the current and voltage, the radiance of the lamp was measured and shown in Table 3.2 and Fig. 3.15.

I (mA)	*U_{lamp}(V)*	*P(W)*	*R_{lamp}(MΩ)*	*Radiance (W/sr*m2)*
0,5	1726,6	*0,86*	*3,45*	*2,50E-02*
0,6	1748,2	*1,05*	*2,91*	*3,06E-02*
0,7	1837,2	*1,29*	*2,62*	*4,05E-02*
0,8	1899,9	*1,52*	*2,37*	*5,22E-02*
0,9	1995,7	*1,80*	*2,22*	*6,79E-02*
0,5	2235,2	*1,12*	*4,47*	*3,97E-02*
0,6	2274,0	*1,36*	*3,79*	*5,71E-02*
0,7	2340,1	*1,64*	*3,34*	*7,53E-02*

0,8	2340,1	*1,87*	*2,93*	*1,01E-01*
0,9	2530,6	*2,28*	*2,81*	*1,27E-01*
0,5	2799,7	*1,40*	*5,60*	*6,53E-02*
0,6	2856,7	*1,71*	*4,76*	*9,28E-02*
0,7	2984,4	*2,09*	*4,26*	*1,33E-01*
0,8	3135,0	*2,51*	*3,92*	*1,81E-01*
0,9	3318,6	*2,99*	*3,69*	*2,52E-01*
0,5	3357,3	*1,68*	*6,71*	*8,27E-02*
0,6	3406,4	*2,04*	*5,68*	*1,33E-01*
0,7	3536,4	*2,48*	*5,05*	*2,02E-01*
0,8	3786,1	*3,03*	*4,73*	*2,50E-01*
0,9	4024,5	*3,62*	*4,47*	*3,03E-01*

Table 3.2 electrical parameters of the test lamp.

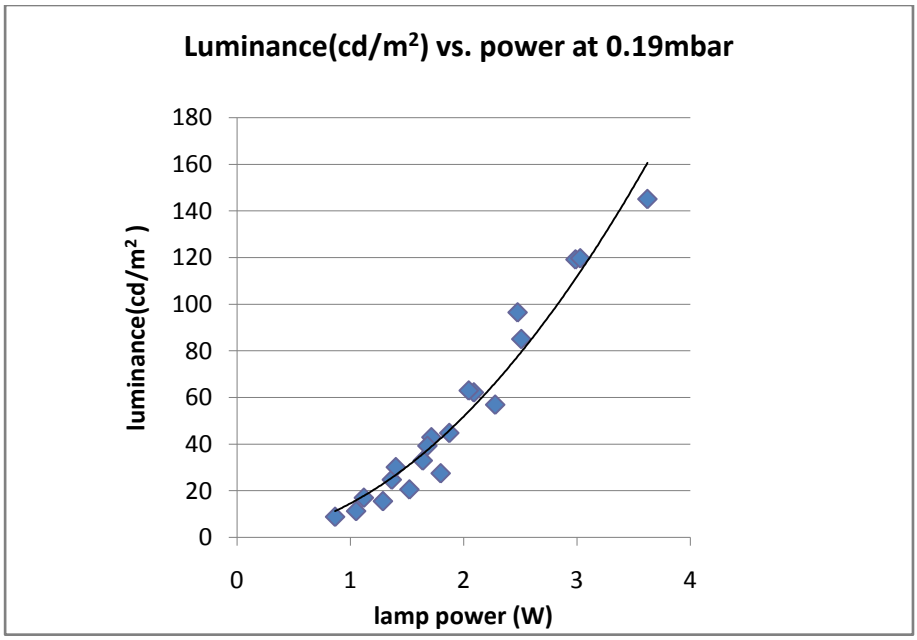

Fig. 3.15 Luminance vs. lamp power, pressure is 0.19mbar

The data of radiance with neon at a pressure of 0.19 mbar is shown in Fig. 3.15. The figure reveals the positive correlation of the lamp radiance to the lamp power. The radiation intensity is proportional to the input electrical power. The energy efficiency of the phosphor is constant. More input power means larger energy and density of the incident particles which would help to excite more photons from the phosphor. It is consistant with the energy conservation.

But the spectra are different under different input power. When the power is low, the characteristic spectral line of the buffer gas is more obvious, which is shown in Fig. 3.16.

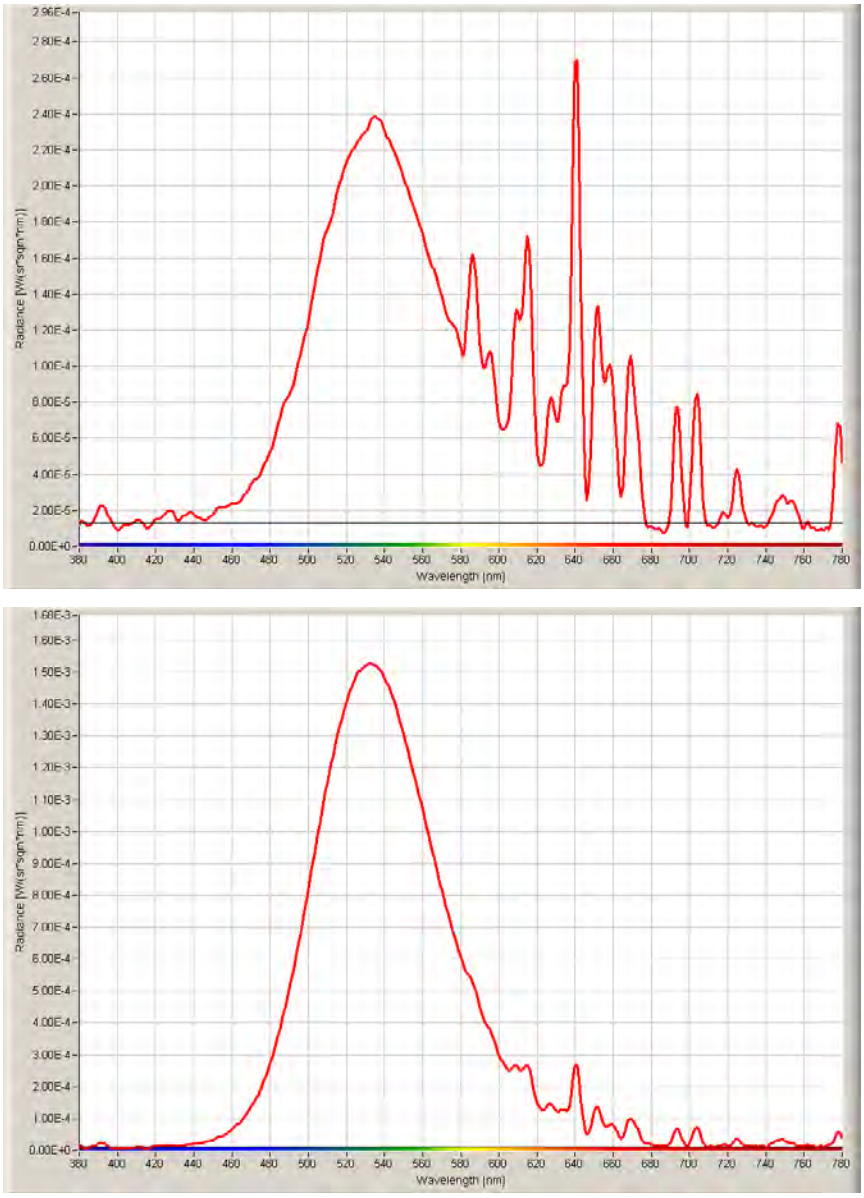

Fig. 3.16 Left: P = 0.14 Torr, I = 0.6 mA, Ulamp = 1748.2 V; Right: P = 0.14 Torr, I = 0.6 mA, Ulamp = 3406.4 V.

As mentioned in **III.1.2.1**, the 640nm is one of neon characteristic spectral wavelength. The Fig. 3.15 shows that the peak spectral radiance values at 640 nm are close ($2.69x10^{-4}$ and $2.67x10^{-4}$[W/(sr*sqm*nm)]), which demonstrates the intensity of neon discharge is same and not proportional to the lamp voltage. However, the spectral radiance of the phosphor will rise by one order of magnitude (radiance peak value varied from $2.4x10^{-4}$ to $1.5x10^{-3}$[W/(sr*sqm*nm)]), when the lamp voltage is increased from 1748V to 3406V. It is reasonable to believe that the neon discharge is limited by pressure. High lamp voltage helps to give more visible emission. It could increase the energy of electrical particle inside the discharge chamber. However as the current is the same, the density of electrons that collide on the anode phosphor should be lower.

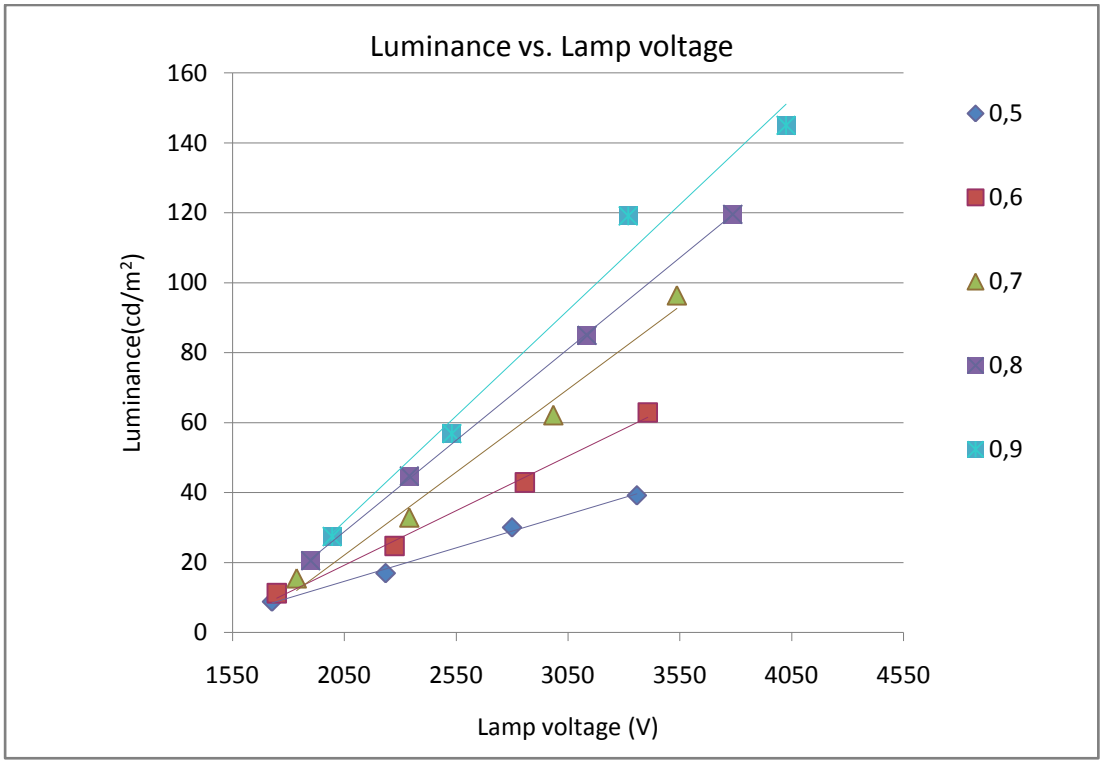

Fig. 3.17 Luminance vs. Lamp voltage, at I = 0.5, 0.6, 0.7, 0.8, 0.9 mA. Pressure is 0.19 mbar.

Both voltage and current would contribute to the luminance of the FDDL. As shown in Fig. 3.17, when voltage is the same, higher current will provide higher luminance too.

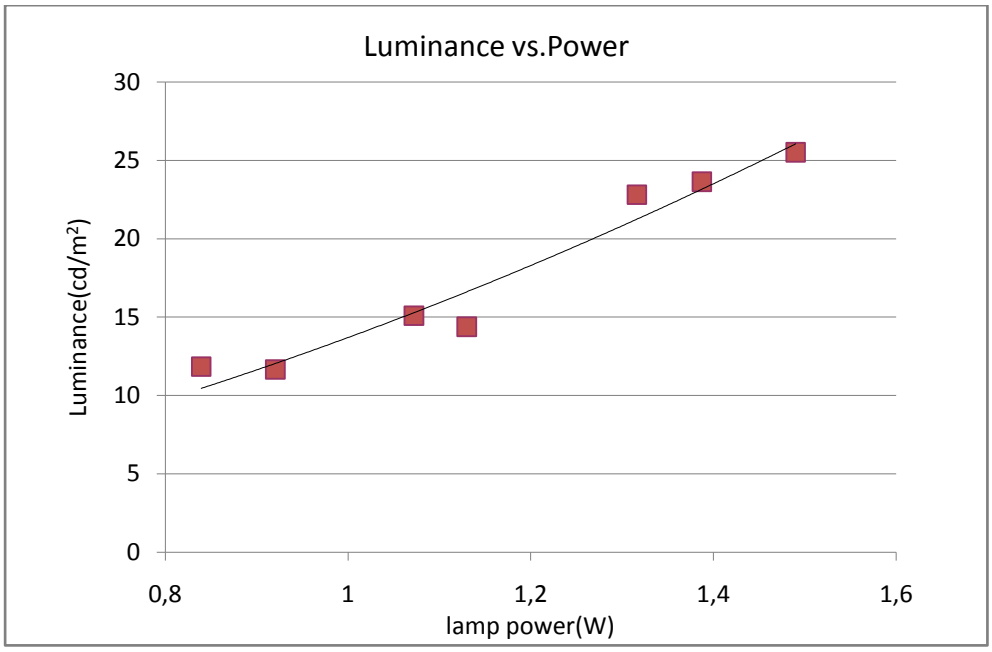

Fig. 3.18 Luminance vs. lamp power, pressure is 0.20mbar

When the pressure of Ne is increased to 0.20 mbar. The relation between the Lamp luminance and the power is the same as shown in Fig. 3.18. The luminance will increase with the lamp power. When the current is constant, the luminance will increase with the lamp voltage as shown in Fig. 3.19.

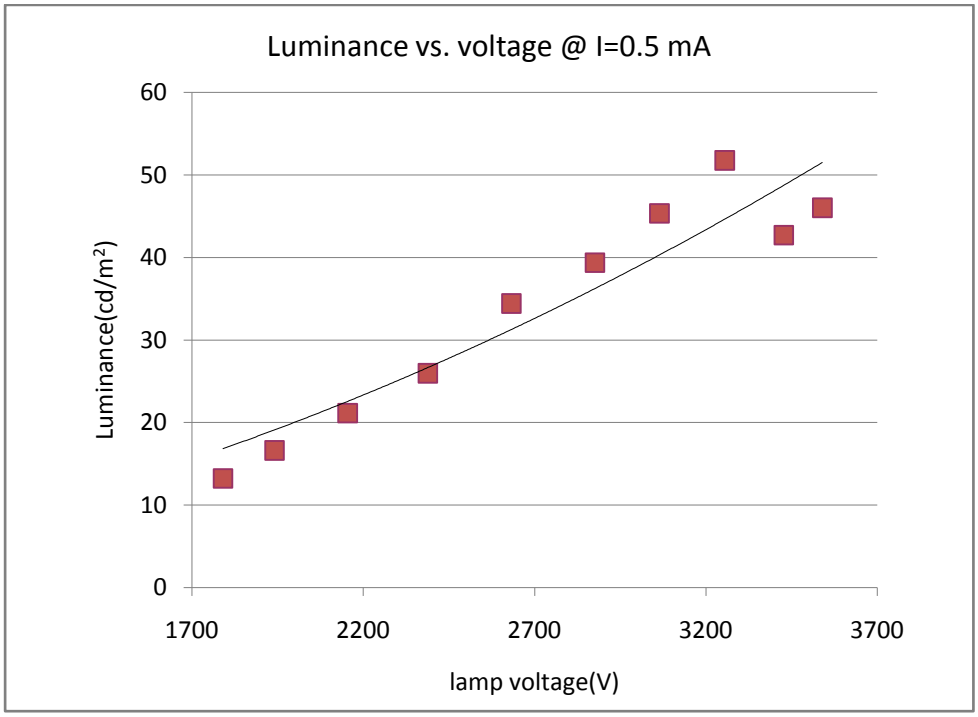

Fig. 3.19 Luminance vs. lamp voltage, pressure is 0.20mbar and I =0.5mA

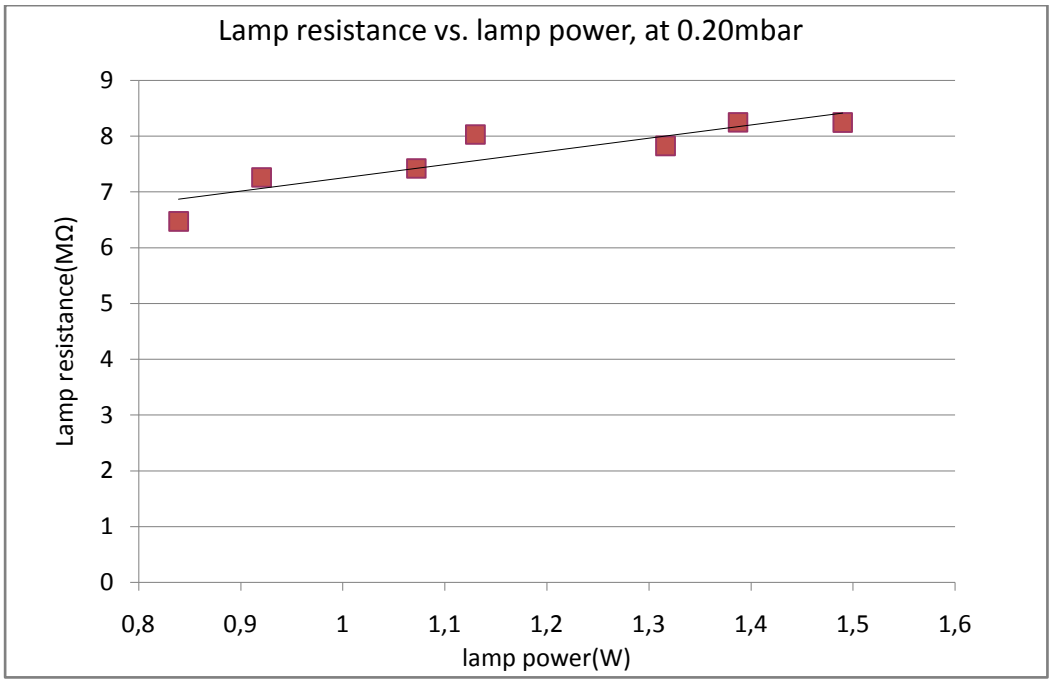

Fig. 3.20 Lamp resistance vs. lamp power, pressure is 0.20mbar

The lamp resistance is quite high and tends to increase with the power, as shown in Fig. 3.20. The resistance presents the charge transport capacity inside the discharge chamber. When the power of each charged particle becomes larger, it would be harder to create new free electrons. The number of colisions is limited by the low pressure and narrow gap distance. This would lead to the extinguish in the end.

III.3.3 Neon at different pressure

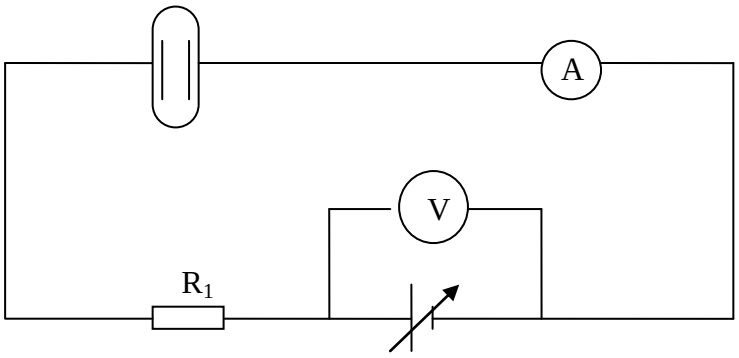

Fig. 3.21 The circuit of experiment

For this part the circuit is shown in Fig. 3.21. The FDDL is connected with the pumping system. After several hours' pumping the vacuum could reach to 10^{-4} mbar. The operation is as below: 1. Flush the system twice with Ne before I fill in the Ne to one pressure. 2. Adjust the voltage regulator to increase the total voltage from 0 to 5 kV until the lamp is turned on. 3. Set the total voltage and record the current and measure the spectral parameter several times. 4. Turn down the voltage and turn off the lamp. 5. Release the valve and pump the lamp to high vacuum. Repeat the operation 1-5 and fill in Ne to 0.20mbar, 0.21mbar,0.22mbar and 0.25 mbar. The R_1 =1MΩ works as ballast resistor.

Stable state

JETI specbos 1201 was employed to measure the luminance of the lamp at around 15 minutes after the FDDL was turned on. It is believed that the lamp could reach to relative equilibrium state. First we could find that the brightness of the FDDL goes down as the pressure is increased from 0.2 mbar to 0.25 mbar as shown in Fig. 3.22.

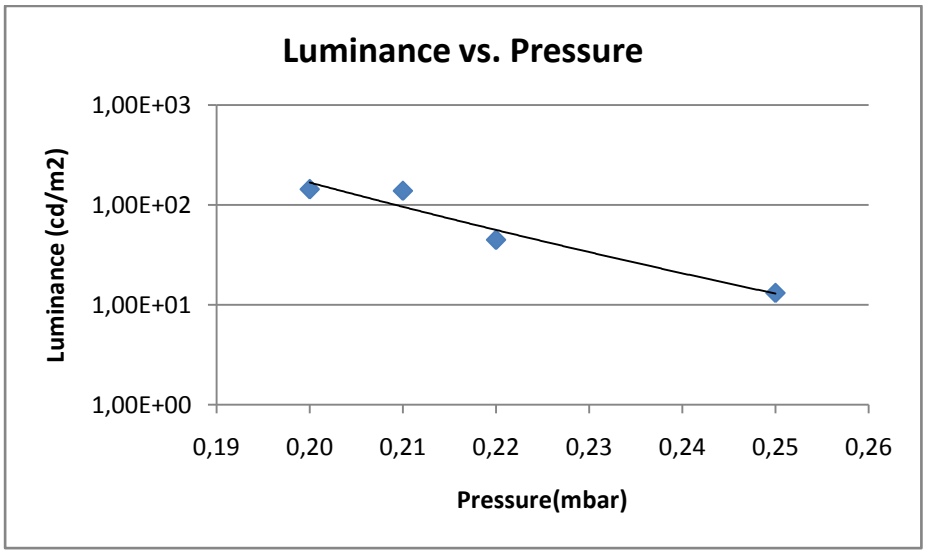

Fig. 3.22 Luminance vs. Pressure

Higher pressure means more atom particles inside and also reduced the lamp voltage. Although more atoms would help to provide more charged particles to excite the phosphor and to increase current which is good for the brightness, the charged particles are accelerated to lower energy by the lower lamp voltage which goes against the brightness. The luminance has positive relation with the lamp voltage as shown in Fig. 3.23, which demonstrate the lamp should work under higher lamp voltage. Though the lower pressure would limit the lamp current to a low level, we still need it to keep the lamp voltage at high level.

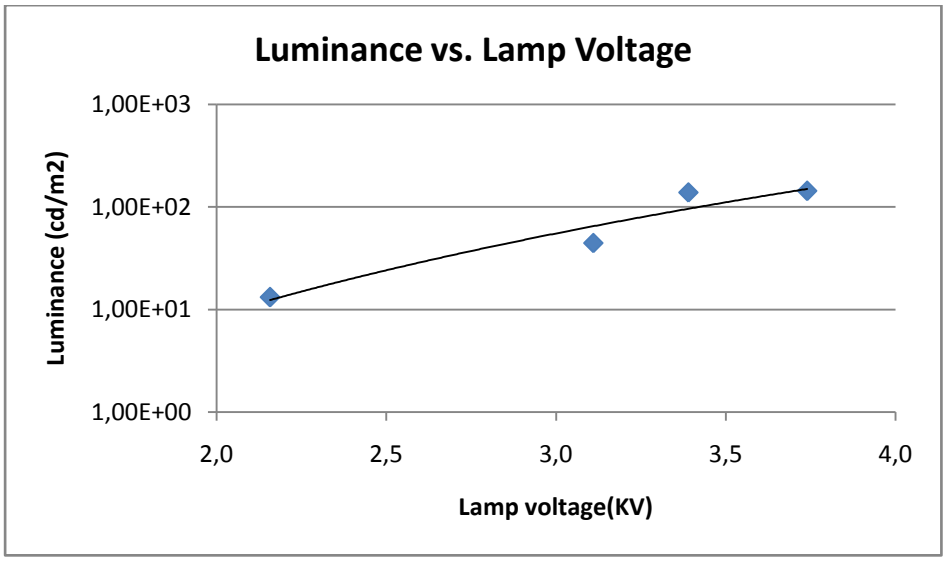

Fig. 3.23 Luminance vs. Lamp Voltage

As the 640nm is one of neon characteristic spectral wavelength and the peak wavelength of the phosphor is around 530nm, the Spectral Radiance Ratio between 534nm and 640nm would present the luminance ratio between phosphor emission and neon emission. From Fig. 3.24 we could find when pressure is low the phosphor emission dominate the total luminance, because less excitation collisions and more ionization collisions would happen in lower pressure. Little energy wasted in excitation collision is good for this kind of application.

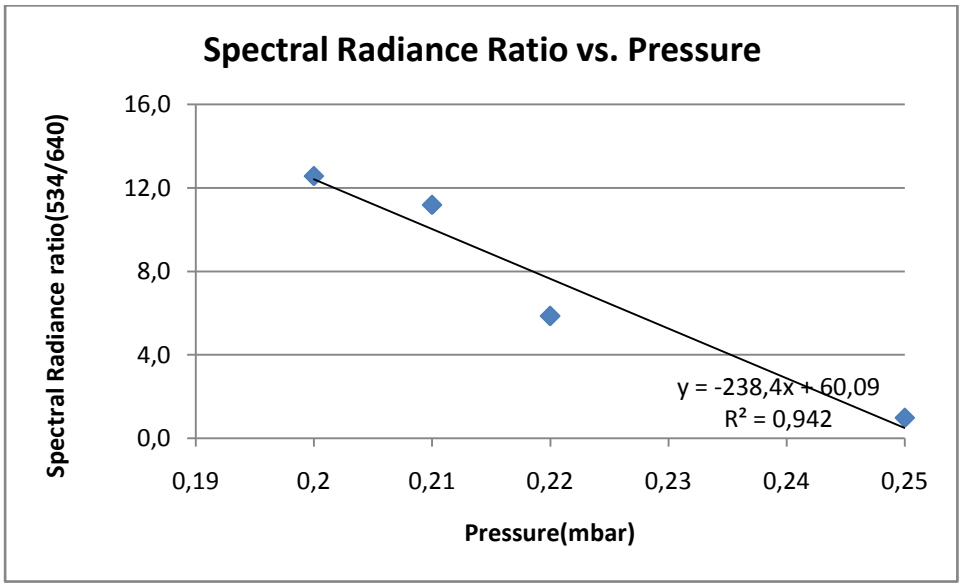

Fig. 3.24 Spectral Radiance Ratio vs. Pressure

Non- stable state

Spectral and electrical parameter have been measured every two minutes since the lamps were turned on at different pressures. Fig. 3.25 is the current-voltage curve of FDDL, which show the negative resitance behavior of gas discharge lamps.

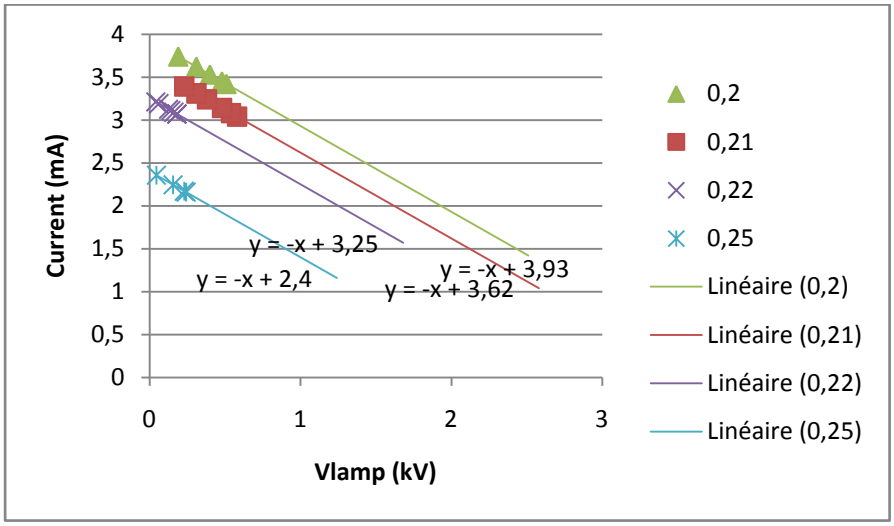

Fig. 3.25 I-V curve for the FDDL at different pressure (0.20mbar, 0.21mbar, 0.22mbar, 0.25mbar)

In the Figure 3.25, the line of 0.20mbar is far from the origin point while the line of 0.25mbar is close to the origin. So when the pressure is lower, the resistance capacity should be stronger. It is helpful to maintain the high lamp voltage in application.

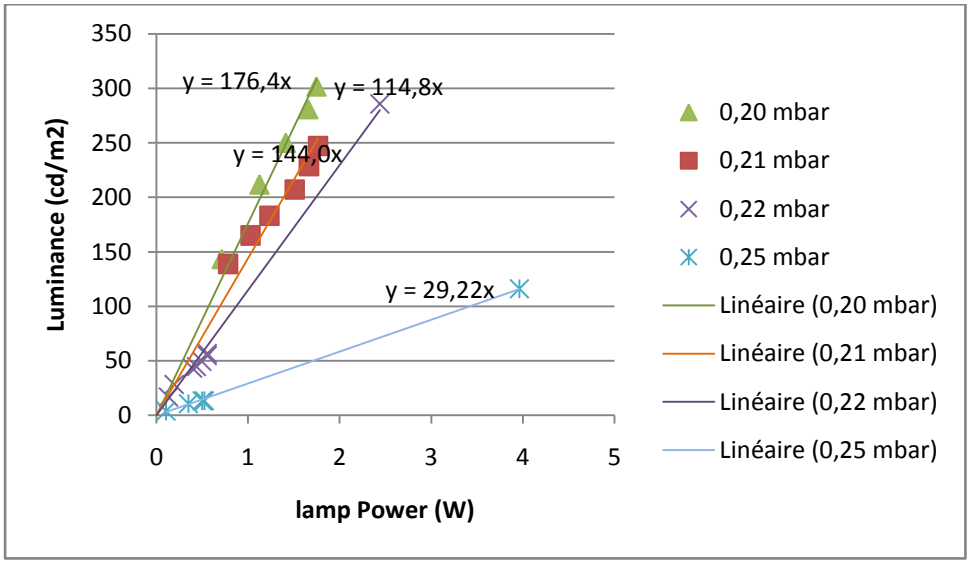

Fig. 3.26 Luminance vs. Lamp power at different pressure.

From Fig. 3.26, we can find that at different pressure the luminance is almost proportional to the lamp power, and the low pressure is good for the light efficacy because less energy would

be wasted in the excitation collisions. If we assume that the luminance behavior of FDDL at different pressures follow the proportion relationship with the lamp power, we could get the lamp luminance under different power which is shown in Fig. 3.27. It shows when the lamp power is higher the pressure influence to the lamp performance would also be greater. Low pressure and high lamp voltage would be better working condition for this kind of application.

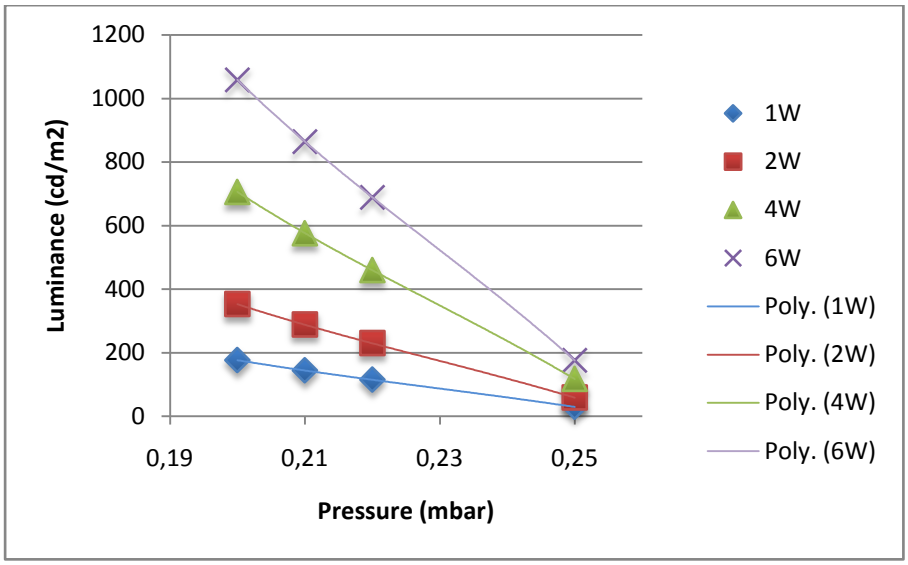

Fig. 3.27 Luminance vs. Pressure under different Lamp power.

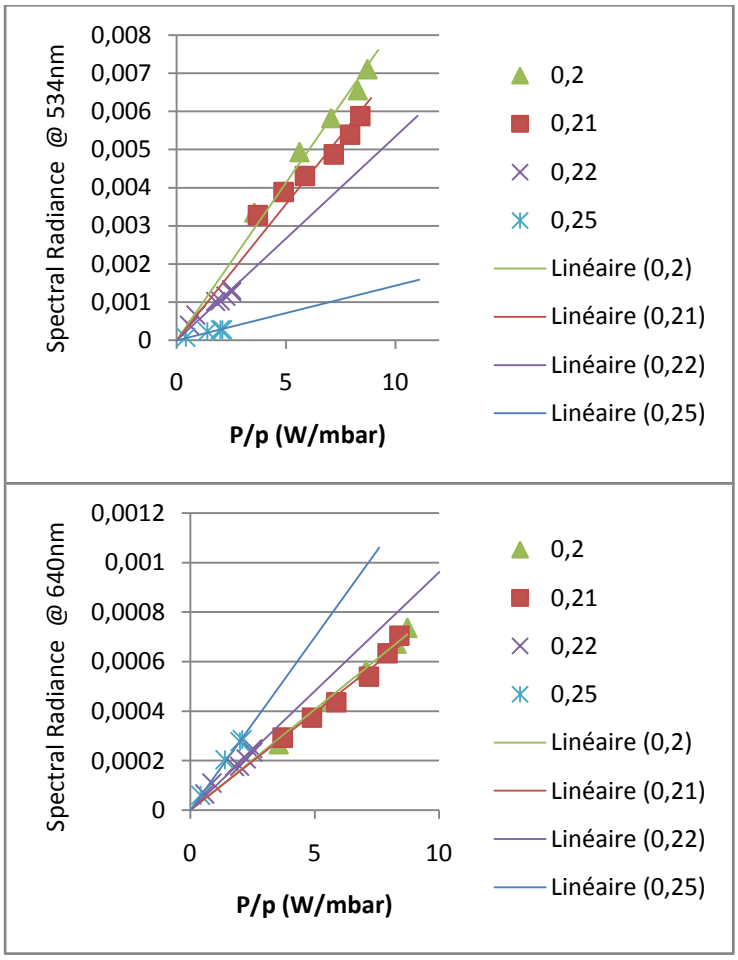

Fig. 3.28 Spectral Radiance at 534nm and 640nm vs. Power/pressure

When the FDDL is on, the temperature would keep moderate (generally in the range from 30°C to 70°C). If we neglect the heat consumption, the power divided by pressure could present the mean energy of each particle inside the lamp. The spectral radiance at 534nm and 640 nm could present separately the light emission intensity from the phosphor and the neon. Fig. 3.28 shows that both the phosphor and buffer gas excitation emission are proportional to the mean energy inside the lamp, but have different relation with the pressure. The phosphor emission goes down as the pressure grows while the neon excitation emission goes up. This demonstrates that the effective particles exiting the phosphor for this application is not photon but fast charged electrons.

Fig. 3.29 shows the spectral radiance ratio variation with P/p (the mean energy per particles). Firstly , we can find when the mean energy is the same, lower pressure is better for phosphor excitation which agree with the result above. Secondly , the neon excitation emission could became obvious as the mean energy increase.

For different pressure there is a mean energy over which only the emission from the buffer gas exits and no phosphor excitation. We can calculate these threshold position from Fig. 3.29 and plot them on Fig. 3.30. It shows that when the pressure grows the neon excitation emission is easier to dominate the total luminance from the FDDL.

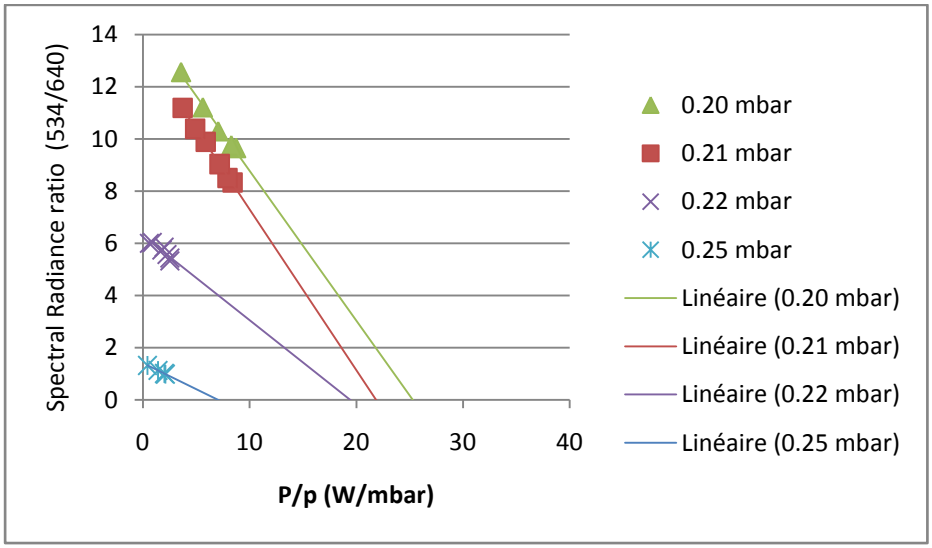

Fig. 3.29 Spectral Radiance Ratio vs. Power/pressure

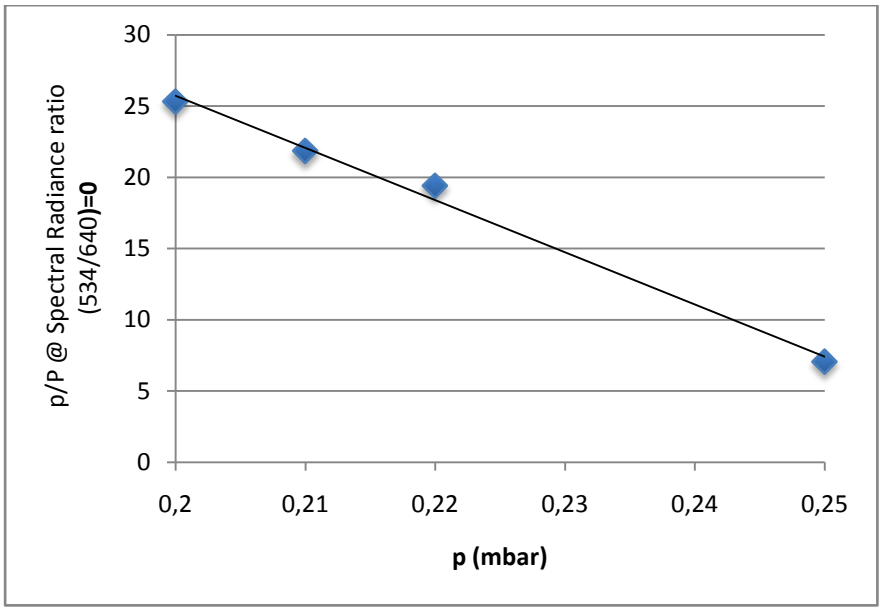

Fig. 3.30 Threshold mean energy VS. Pressure

III.3.4 Start voltage

The output voltage is controlled by the voltage regulator and grows up from zero until the FDDL is turned on. This voltage value is recorded as the start voltage. The result of Xenon and Neon shows in Fig. 3.31. it is apparent that the turn on voltage reduce while the pressure increase. It agrees with the left wing of Paschen curve as the gap distance is constant. Higher pressure would offer better possibility of inelastic collision when the pressure is low.

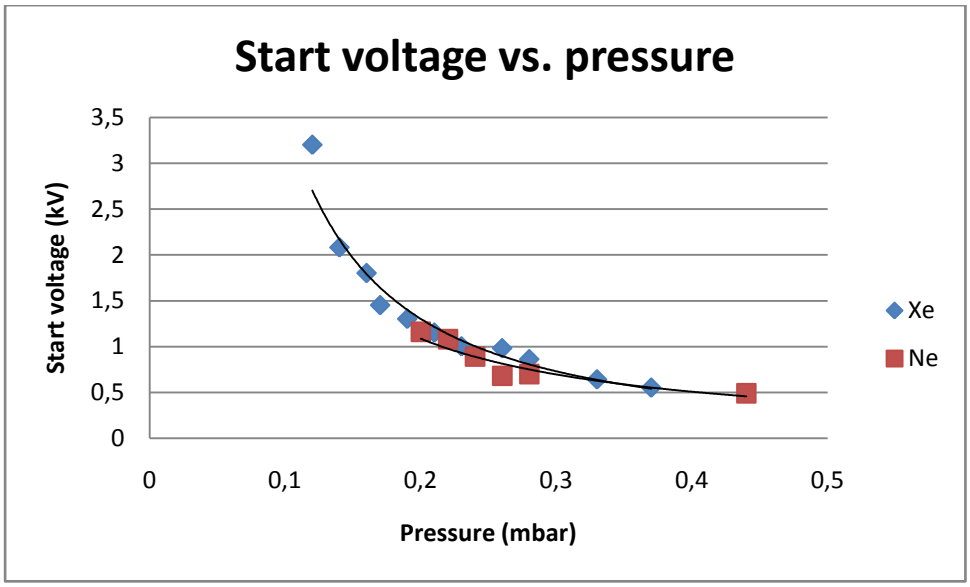

Fig. 3.31 The start voltage vs. pressure.

In the experimental condition, the threshold pressure to turn on the Ne FDDL is 18 mbar. If the Ne pressure is lower the lamp could not be excited under the total voltage from 0 -5.5KV. But it is possible to turn on the FDDL filled with Xe at much lower pressure. In Table 3.3 the calculated radii of inert gases are listed which are based on the theoretical models, as published by Enrico Clementi and others[6]. The larger size of Xe will promise lager possibility of inelastic collision and lower ionization energy. This would allow the Xe works in lower pressure than Ne. We could also understand this effect from the Fig. 2.6 and 2.7. Fig. 2.6 shows that for the Ne at 18 mbar, almost all particles' ionization mean free paths are higher than the gap distance, while for the Xe at 6 mbar the electrons with the energy range from 8 to 800 eVcould have good chance to ionize the atoms in less than 1cm gap distance.

gas	He	Ne	Ar	Kr	Xe	N2
calculated radii (in A)	0,31	0,38	0,71	0,88	1,08	0,54

Table 3.3 [6] calculated radius of inert gases

III.3.5 Voltage-Current plot analysis

In the chapter I we discussed the difference between FDDL and FED (field emission display). Its structure could be quite similar with that of FDDL, as shown in Fig. 3.32[7]. Carbon nanotubes (CNTs) are used as the electrons emitter and coated on the surface of the cathode. However their working mechanisms are different. The difference can be proved in this part by voltage –current plot analysis and the Fowler-Nordheim theory.

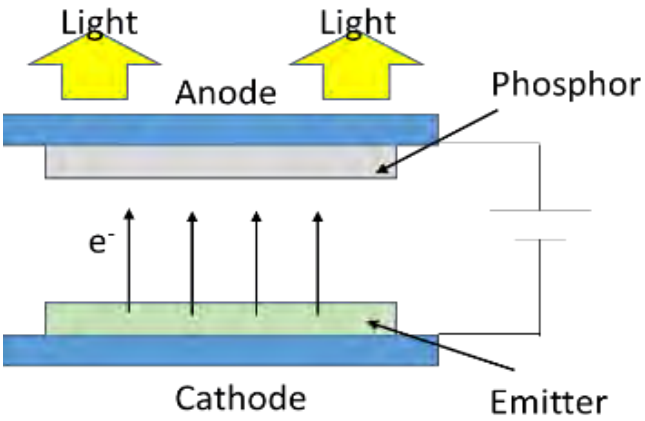

Fig.3.32 Schematic diagram of the FED lighting

The theory of cold field emission of electrons from metals into vacuum is often called Fowler-Nordheim (FN) theory, after the first authors to treat this effect as wave-mechanical

tunneling through a triangular potential barrier [8]. When the electric field is very large, the barrier becomes thin enough for electrons to tunnel out of the atomic state, leading to a current that varies approximately exponentially with the electric field. As an exact solution of the Schrodinger equation, it predicts that when field emission dominates, the J-V characteristics are described by [9]

$$J = AF^2 \exp\left(-\frac{8\pi\sqrt{2m^*}\emptyset_B^{3/2}}{3hqF}\right) \quad (3.1)$$

where m* is the effective charge carrier mass, Φ_B is the potential barrier height, F is the applied electric field, and A is a rate coefficient given by

$$A = \frac{q^3}{8\pi h \emptyset_B} \quad (3.2)$$

Equation 3.1 can also be written as

$$J = AF^2 \exp\left(-\frac{\kappa}{F}\right) \quad (3.3)$$

Where

$$\kappa = \frac{8\pi\sqrt{2m^*}\emptyset_B^{3/2}}{3hq} = \text{constant} \quad (3.4)$$

Equation may be rewritten as

$$\ln\left(\frac{J}{F^2}\right) = \ln A - \kappa\left(\frac{1}{F}\right) \quad (3.5)$$

As the shape of the device is set, equation 3.5 could also be written as

$$\ln\left(\frac{i}{V^2}\right) = C - B\left(\frac{1}{V}\right) \quad (3.6)$$

FN theory demonstrates that the voltage and current of field emission device should follow the liner relationship in equation 3.6 with negative slope.

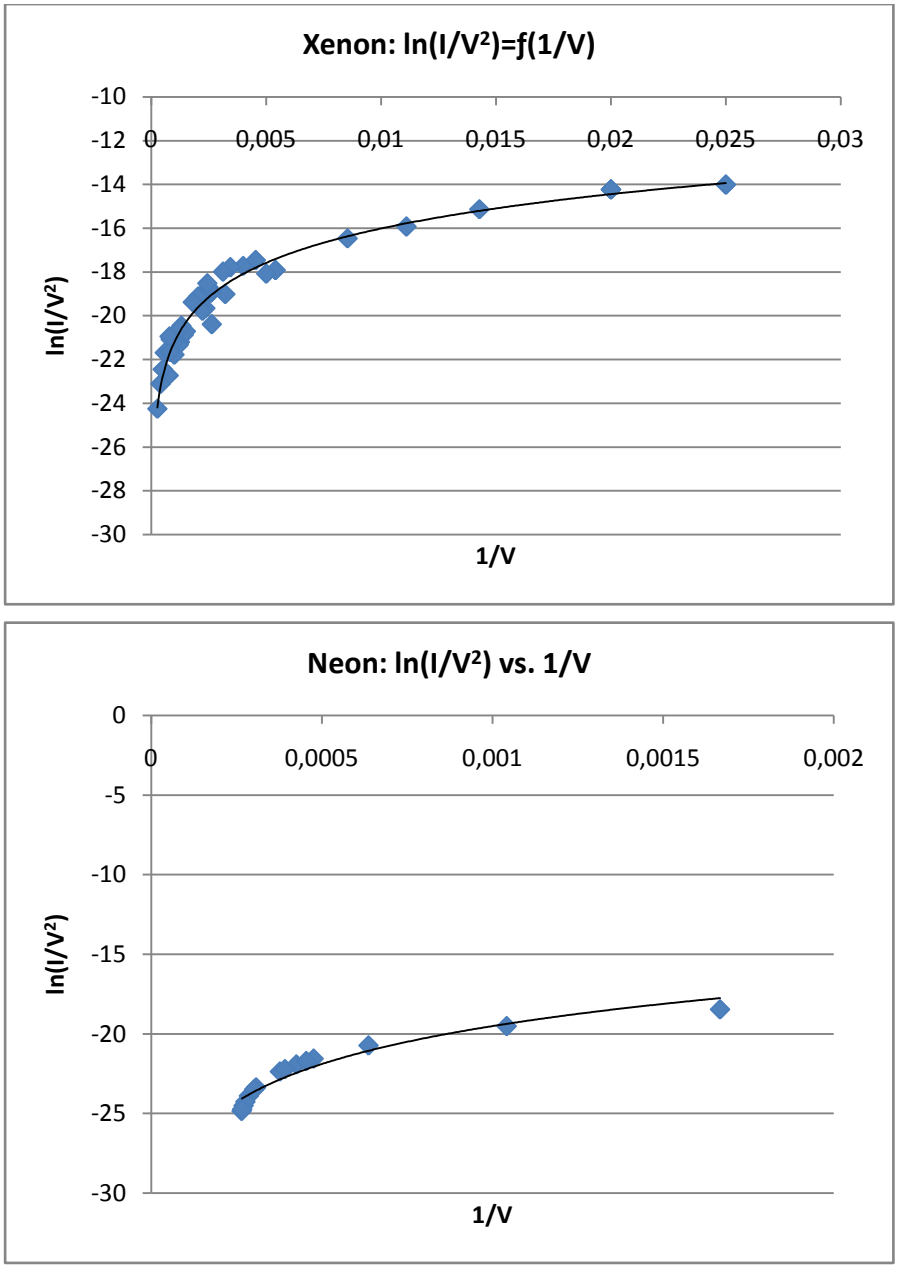

Fig. 3.33 the FN plot of FDDL filled with Xe and Ne

Fig. 3.33 is the FN plot of FDDL filled with Xe and Ne. The pressures of Ne are 0.18mbar, 0.22mbar, and 0.25mbar. The pressures of Xe range from 0.05mbar to 0.20mbar. It is easy to tell that they do not follow the liner relation with negative slope but agree with logarithmic curve in some level, which means the electrons are not extracted from the cathode by high electrical field for this application.

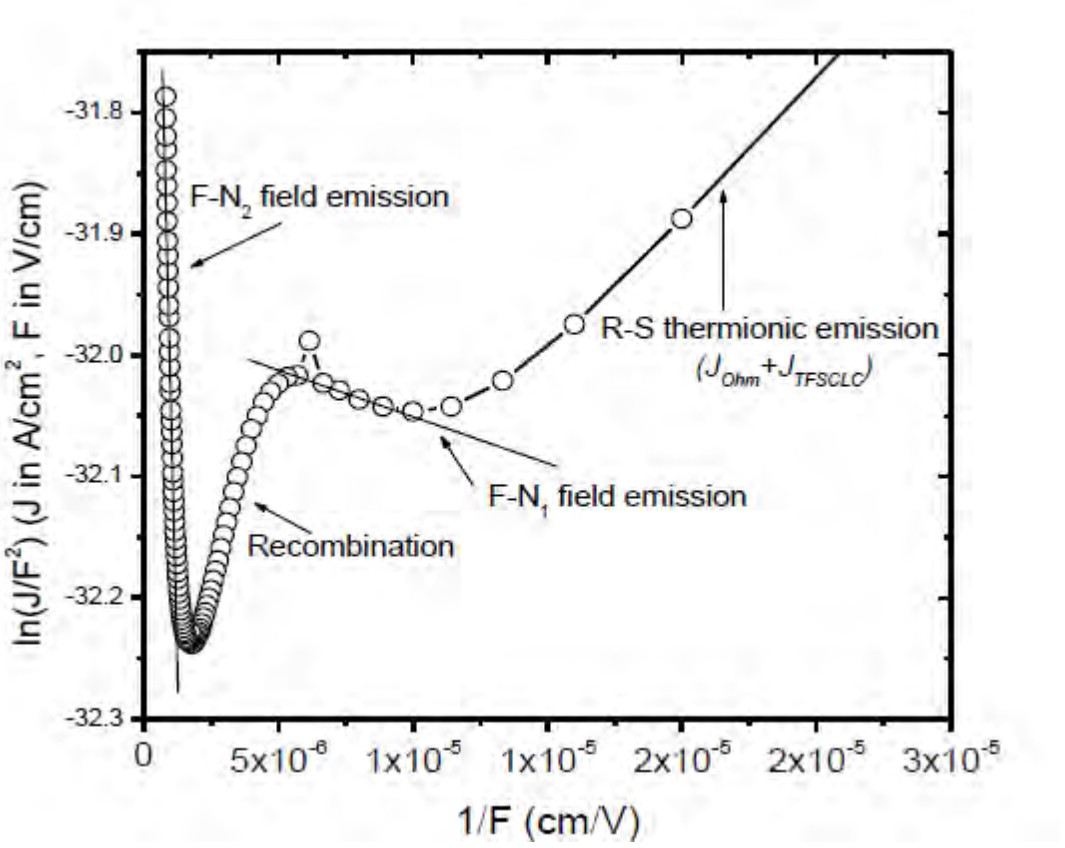

Fig. 3.34: 300 K F-N plot for Al/P3HT:PCBM/Al device, showing the four different regimes: R-S thermionic emission, electron tunneling through the lower barrier electrode, recombination regime, and hole tunneling through higher barrier electrode.

According to Chiguvare's work[9][10], charge injection in the metal/polymer/metal devices such as OLEDs would mainly employ two mechanisms: the thermionic emission (electrons have sufficient kinetic energy to escape from metal electrode to some transport level in the polymer) and the field emission (the quantum mechanical tunneling of charge carriers at high enough applied electrical fields). The essential assumption of the Richardson-Schottky (RS) model of thermionic emission is that an electron from the metal can be injected once it has acquired sufficient thermal energy to cross the potential maximum that results from the superposition of the external and the image charge potential. This model usually is valid at lower fields and higher temperatures, which could be expressed as $kT>>\Phi_B$. In the other hand, the high bias voltage will reduce the potential barrier in the metal (due to image charge), the only field emission mode is usually valid at lower temperature and higher field, which could be expressed as $kT<<\Phi_B$. When the value of kT is near Φ_B, the both mechanisms would contribute to the current.

The field emission current follows equation 3.1, and the thermionic emission current is decided by Ohm's law:

$$J_{ohm} = qn\mu\frac{V}{d} \qquad (3.7)$$

where q is the electronic charge, n the charge carrier density, m the carrier mobility, V the applied voltage, and d the thickness of the sample. In the absence of traps, or when all traps are filled, the trap free space limited current J has a quadratic dependence on V, and follows the Mott-Gurney law:

$$J_{TFSCL} = \frac{8}{9}\varepsilon_0\varepsilon_r\mu\frac{V^2}{d^3} \qquad (3.8)$$

Here, $\varepsilon_r$and ε_o are relative permittivity and permittivity of free space, respectively.

Fig. 3.34[10] is the typical FN plot for the organic diodes device at the room temperature, which use aluminum as electrodes. Two negative slope regions with straight line tendencies are clearly observed, which suggests two tunnelling regimes in these devices. FN curve has variable positive slope at low applied electric fields, which is dominated by thermionic emission mechanism and becomes negative close to the highest applied fields dominated by field emission mechanism. The first minimum as voltage rising is due to significant tunnelling of electrons from Al electrode into the LUMO of the PCBM. A second point of inflexion again changes the slope to positive, suggesting a reduction in the rate of increase of charge carriers available for current conduction. It is attributed to recombination of charge carriers within the bulk of the film.

For the FDDL application the intermedium is replaced by low pressure gas and phosphor rather than polymer. As the work function of FTO is around 5.0 eV [11] and the lamp works in the room temperature (no exceeding 360K), the electrons kinetic energy kT is much lower than the potential barrier height Φ_B. It is hard for the electrons escaping from the cathode by thermionic emission. However the gas discharge will provide new electrons and ions. When heavy ions hit on the cold cathode electrons get the energy from the ions could transit the potential barrier to the space. The current is not limited by charge injection from electrodes to the intermedium but by the ionization and transportation of the charges in the discharge space. Though we can find it quite similar to the thermionic emission plot with strong recombination, it is not possible to deduce the same mechanism. As it is in accordance with the logarithmic curve in some extent, the relationship between $\ln(I/V^2)$ and $\ln(1/V)$ is explored in Fig 3.35 .

$$ln(I/V^2) = ln(1/V) - lnR \qquad 3.9$$

Here R is the lamp resistance. From Fig 3.35 we can tell that in the experiment pressure values for Xe the resistance variation with pressure should be low, while that is higher for Ne in the pressure range from 0.18 mbar to 0.25 mbar. This is because the diameter of Xe is larger than that of Ne. In the same variation of pressure, the mean free path change of Xe is much lower than that of Ne as shown in Table 2.1.

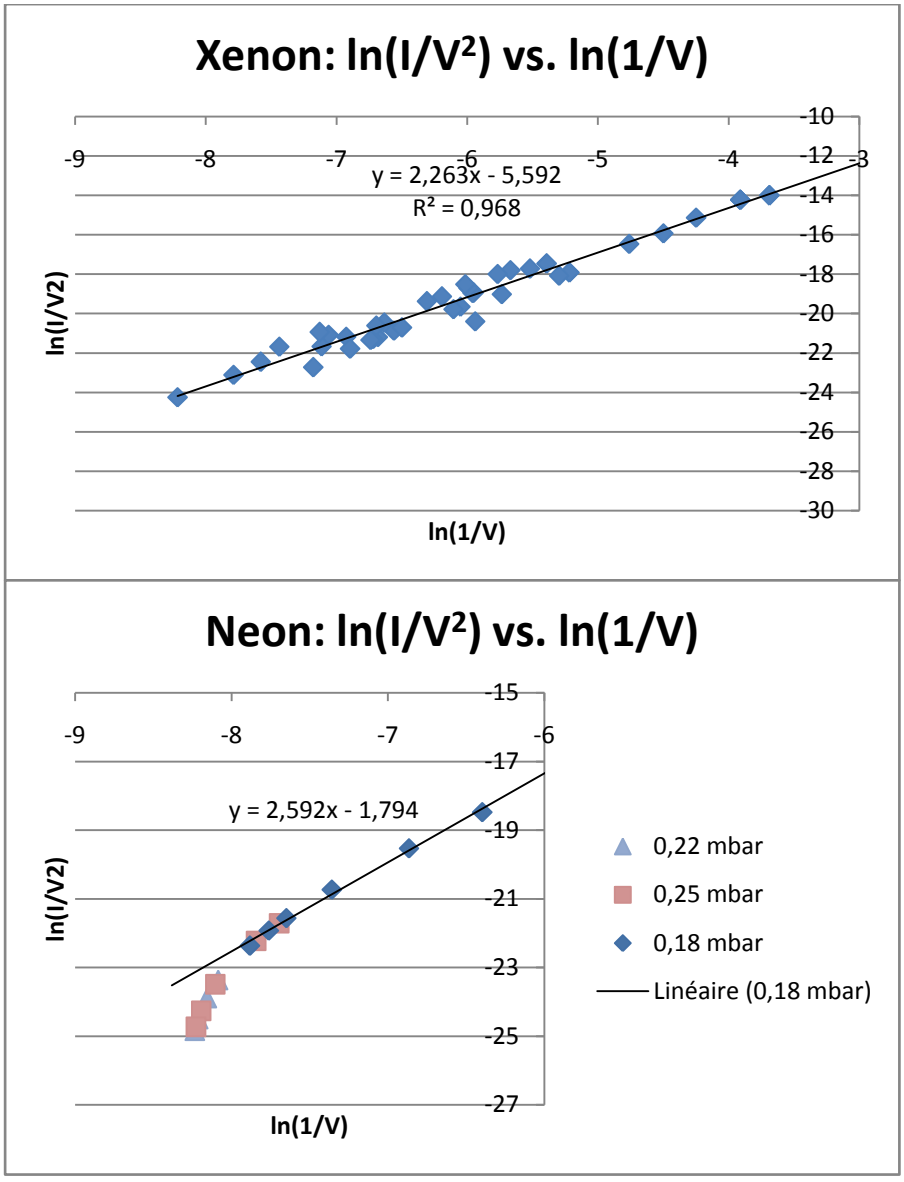

Fig. 3.35 The relationship between $\ln(I/V^2)$ and $\ln(1/V)$ for FDDL with Xe and Ne.

III.4 Commentary

The lamp maintains low current and cold electrodes, the high reduced electrical field E/N is the specialty of this discharge. Some problems for the FDDL applications would be discussed in this part.

III.4.1 Stability

The FDDL does not maintain stable output for long time. The radiances of the lamp may drop quickly by time. We can find that from sample test. Two of the three sample lamps can only work for several minutes after they are turned on, and then they will extinguish automatically. The other one can last working for hours, but after about 10 minutes the brightness turns weak and fluctuating. Their radiance variation with time (minutes) are shown in Fig. 3.36.

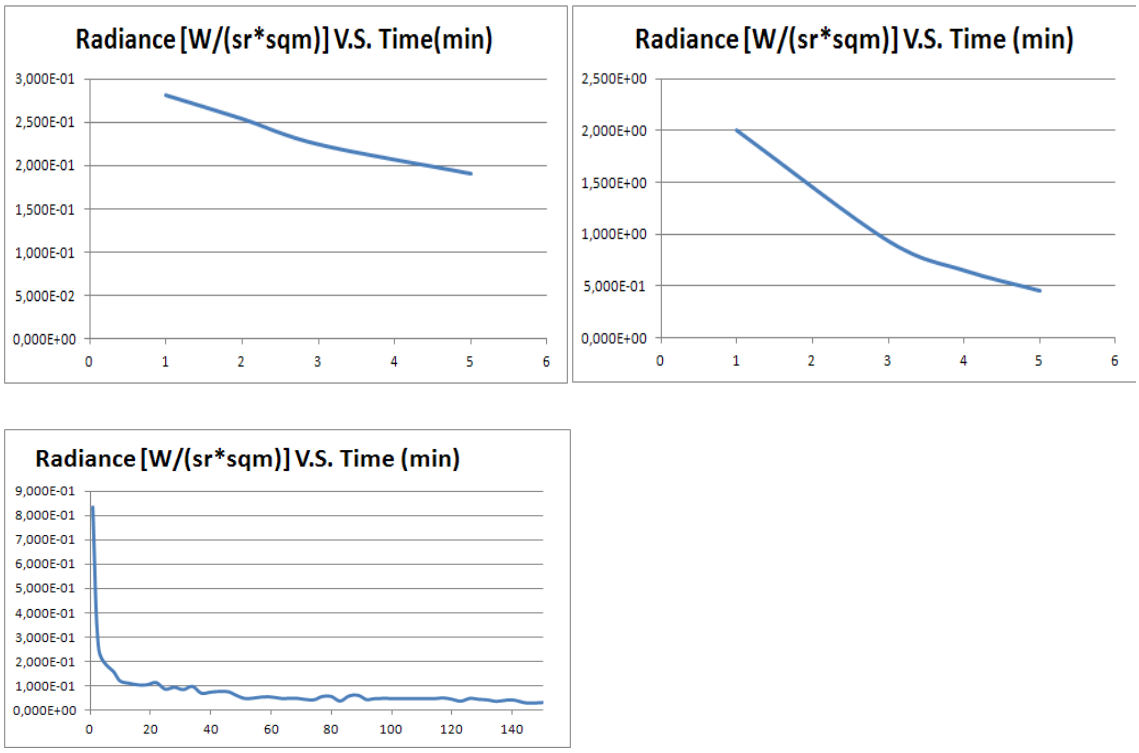

Fig. 3.36 Maintenance diagram of the Sample FDDLs.

For the filling lamps there is similar phenomenon. The current goes down while the lamp voltage goes up gradually after breakdown. It demonstrates the maintenance of the discharge become harder, which will lead to extinguish instead of working stably. The breakdown can happen but the discharge is a little bit hard to sustain, which means the discharge cannot provide enough electrons and ions, and the disappear of the charged particles is faster than the production of them. It is quite different from the glow or arc discharge which has the so-

called “negative resistance characteristics”. This is unreasonable if nothing changed inside. Townsend theory told us the breakdown would happen because the secondary electrons are enough to maintain the discharge. So one possible reason could be the electrodes’ ability of secondary electrons emission degrades by time. The solution could be improving the cathode material and its electrons emission capacity. The carbon nanotube can be a good candidate[12],[13],[14].

Another possible reason could be the leak of the lamp, which makes the electronegative gas, such as H_2O or O_2, enter the discharge space. The molecule of these gases would absorb the free electrons inside the discharge chamber which could leads to the rise of the working voltage and eventually the quench. They may be adsorbed on the surface of the inner wall or phosphor, and released during the discharge. Besides they do quite harm to the organic material which could be used in the glue and phosphor. Actually when some lamps can not be turned on any more, some powder could be found inside the lamp chamber. Digital microscope KEYENCE VH-Z100 UR (100-1000x zoom range) could be used to observe the inside surface of the phosphor as shown in Fig. 3.37. On the photo we could find some blank areas which means lack of phosphor on these parts. When we use the laser experiment like the III.1.2.2 to test the performance of the phosphor we will also find the drop of the phosphor by comparison with the new lamp, as shown in Fig. 3.38. The peak value of the two spectrums at 405nm is normalized. There is almost no phosphor emission at around 530nm for the used lamp.

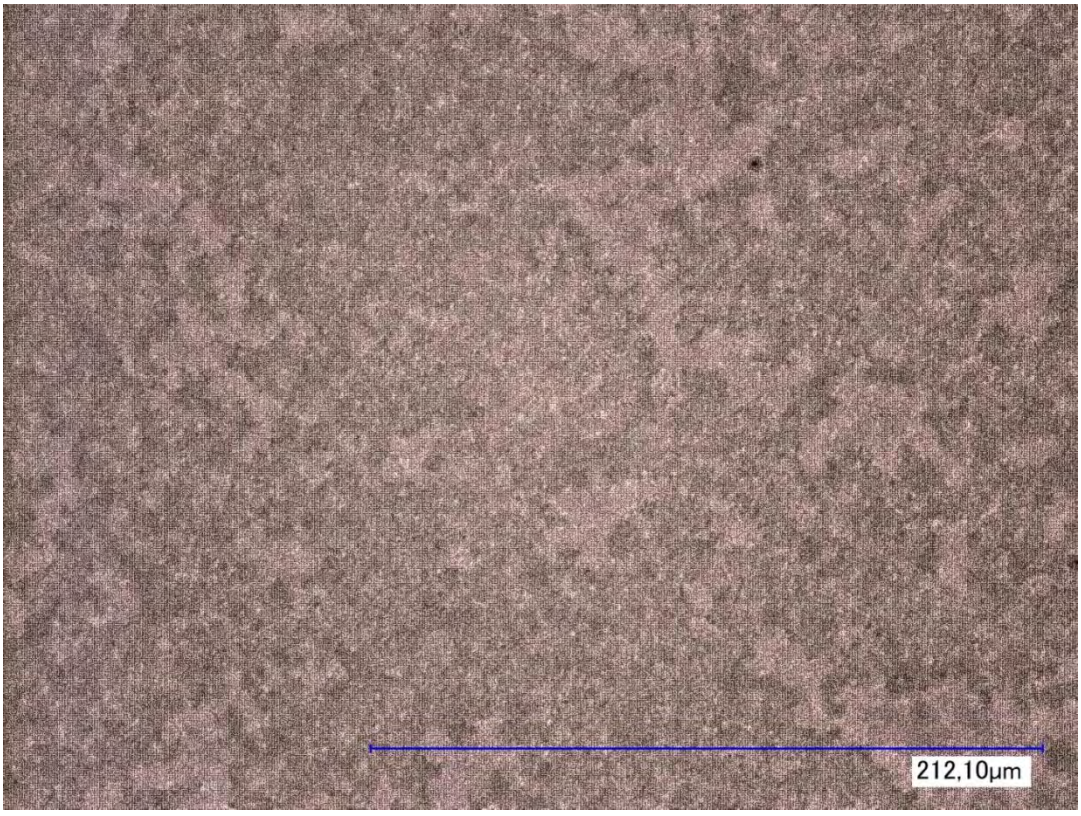

Fig. 3.37 Digital photo of the phosphor surface.

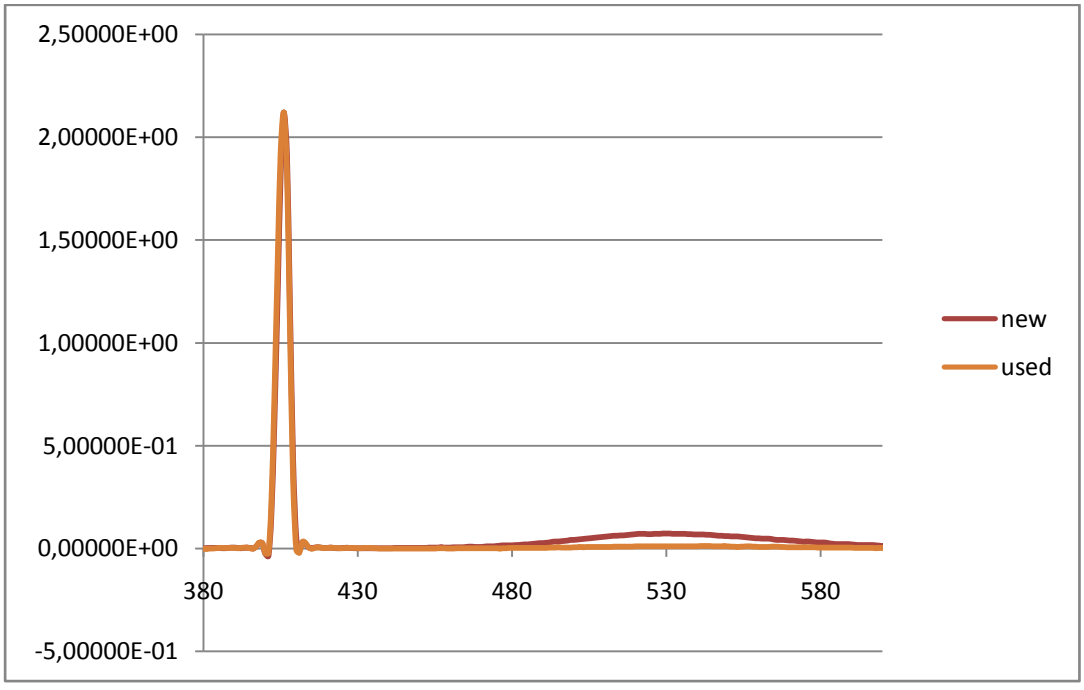

Fig. 3.38 Comparison of the laser test result between new lamp and one used lamp.

III.4.2 Infrared camera analysis

A FLIR infrared camera can be used to watch the surface temperature when the lamp is turned on as shown in Fig. 3.39. The lamp connects with the vacuum system, and it is filled with Neon at 0.19 mbar. We can find that when the lamp is working, the surface temperature is about 50℃. This temperature would be not enough to emit thermal electrons from cathode, which demonstrate that it works with cold cathode. When the ions hit on the cathode, some kinetic energy would be transferred to the cathode from the ions and converted to heat. In the center the temperature is higher than the surrounding part. First, as the electrode surface is not infinite, it is obvious that in the center the field should be stronger. Second, the inside wall of the glass would influence the space charge near the edge according to the ambipolar diffusion.

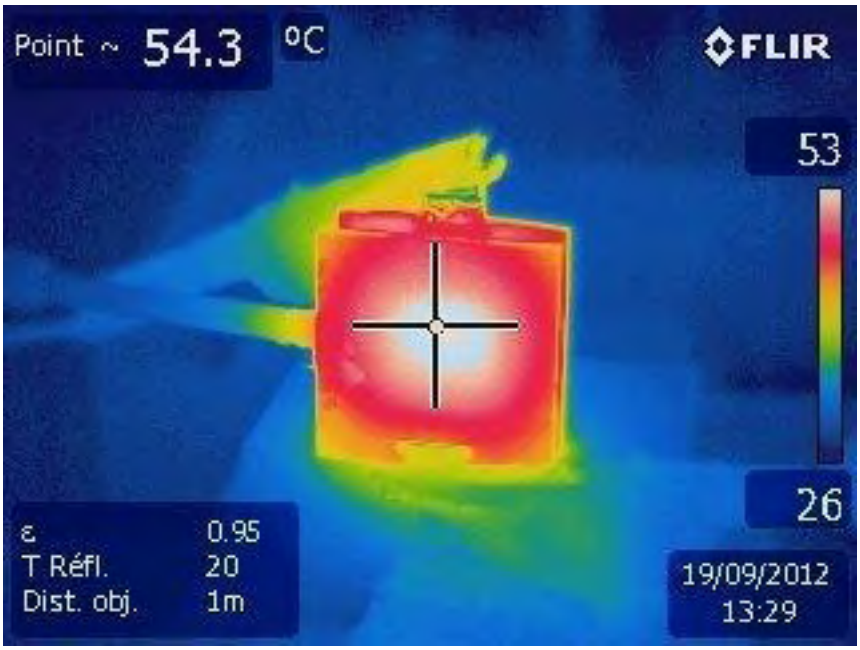

Fig. 3.39 Infrared photo of the lamp

When the lamps are damaged after working for some time, no uniform phosphor radiation could be achieved. Some spot near the edge seems easier to ignite the discharge as shown in Fig. 3.40. The voltage distribution on the cathode surface has been broken, which infer to the damage of the cathode. This damage could be caused by the ions bombardment

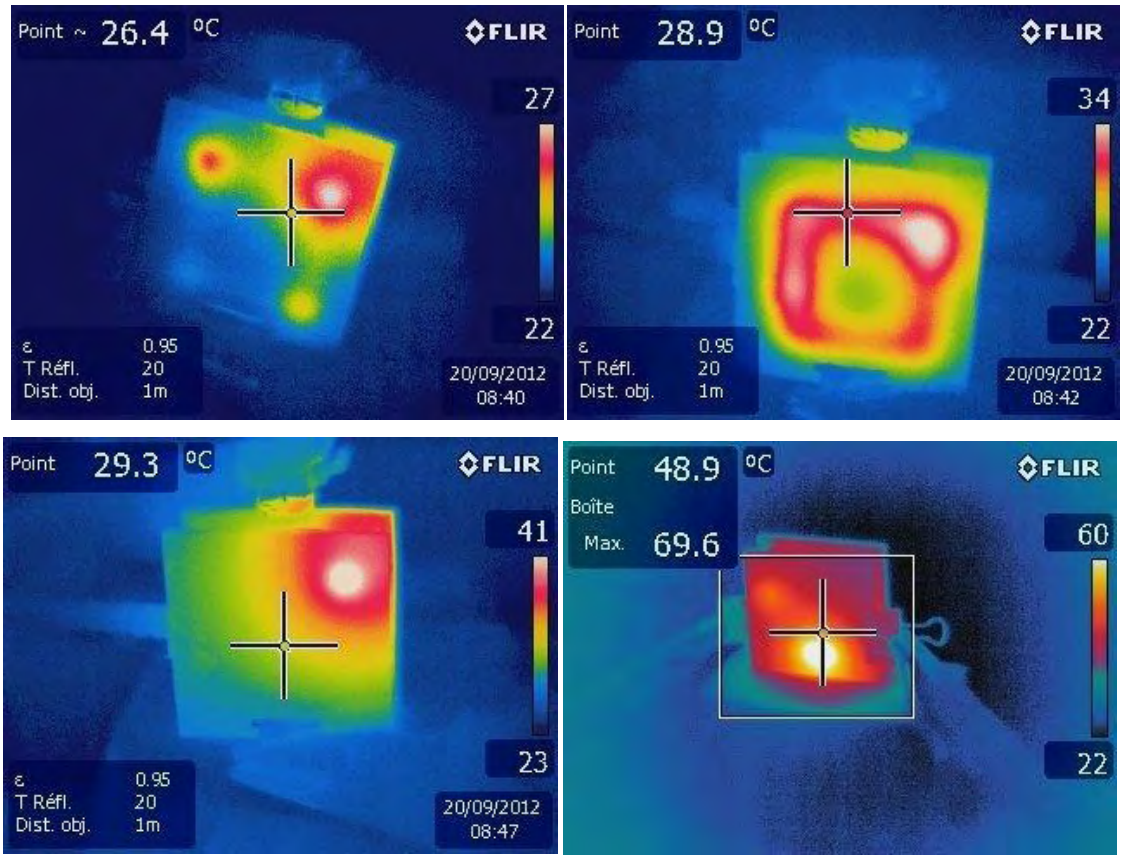

Fig. 3.40 Infrared photos of the damaged lamps

III.4.3 Scanning electron microscope (SEM) analysis

The phosphor surface is observed by the SEM (JSM-6060), after one lamp is broken. Fig 3.41 is the SEM photos of the piece of anode surface (x200, x500, x1000, x2000, x5000 and x15000). The phosphors show a cubic shape with an average particle size of about 3 μm, which has the smooth and clean surface. The structure of the FDDL phosphor appears similar with that of the normal ZnS phosphor from ITRI or some other reports [15] [16] [17] [18] [19] [20] has no difference with the SEM photo of the phosphor surface from ITRI is shown in Fig.3.42.

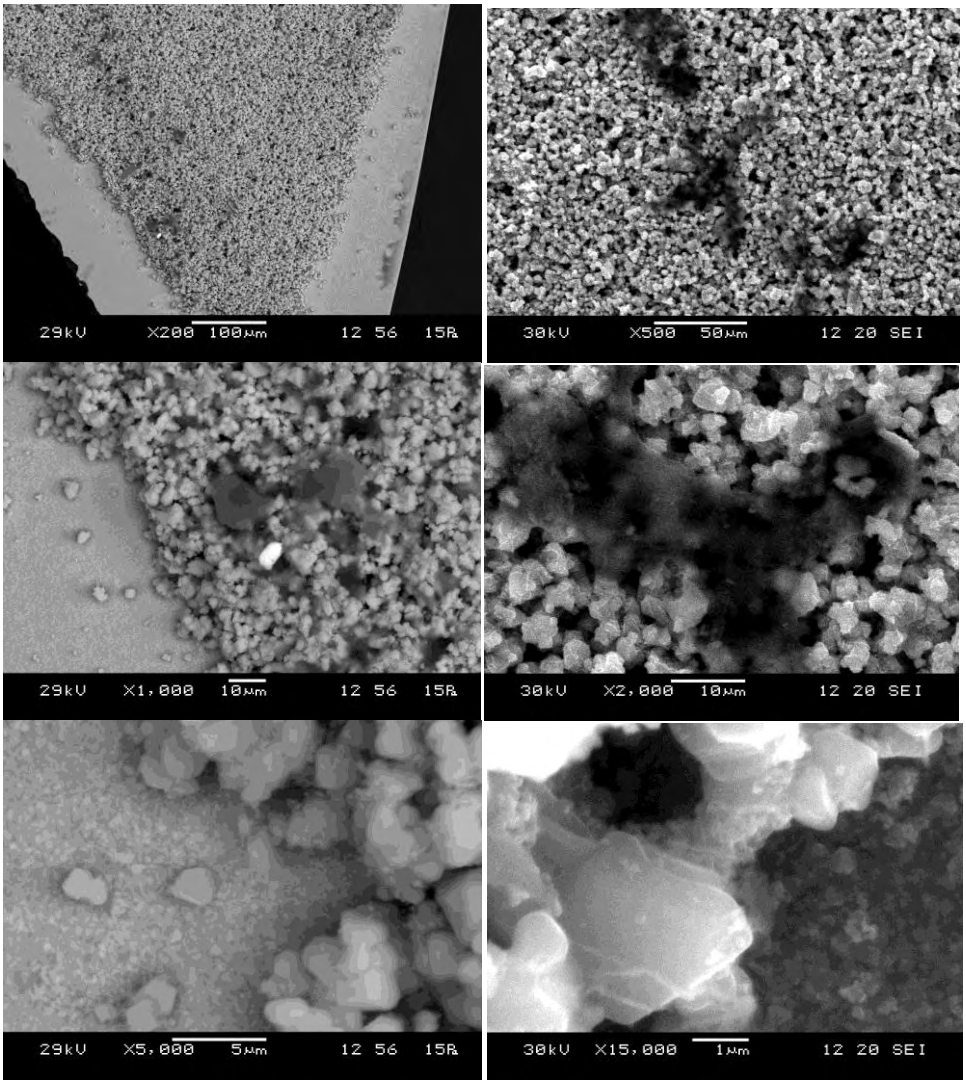

Fig. 3.41 SEM photos of the FDDL anode surface. (x200, x500, x1000, x2000, x5000 and x15000)

This kind of CL phosphor is wild used in CRT. When studying the effects of electron bombardment of CRT phosphors at low accelerating voltages (2 kV), it is found that surface chemical reactions were stimulated by the electron beam [21], [22]. These surface reactions could dramatically reduce the CL intensity from the phosphor. This phenomenon could be explained by ESSCR (electrons stimulates surface chemical reactions) model [21], [23]. This model is based on the postulate that the electron beam will dissociate surface-adsorbed molecular species (e.g. H_2O, H_2 or O_2) converting them into reactive atomic species. These reactive atomic species rapidly combine with S, forming products with high vapor pressures, such as SO_x or H_2S which desorbs from the surface.

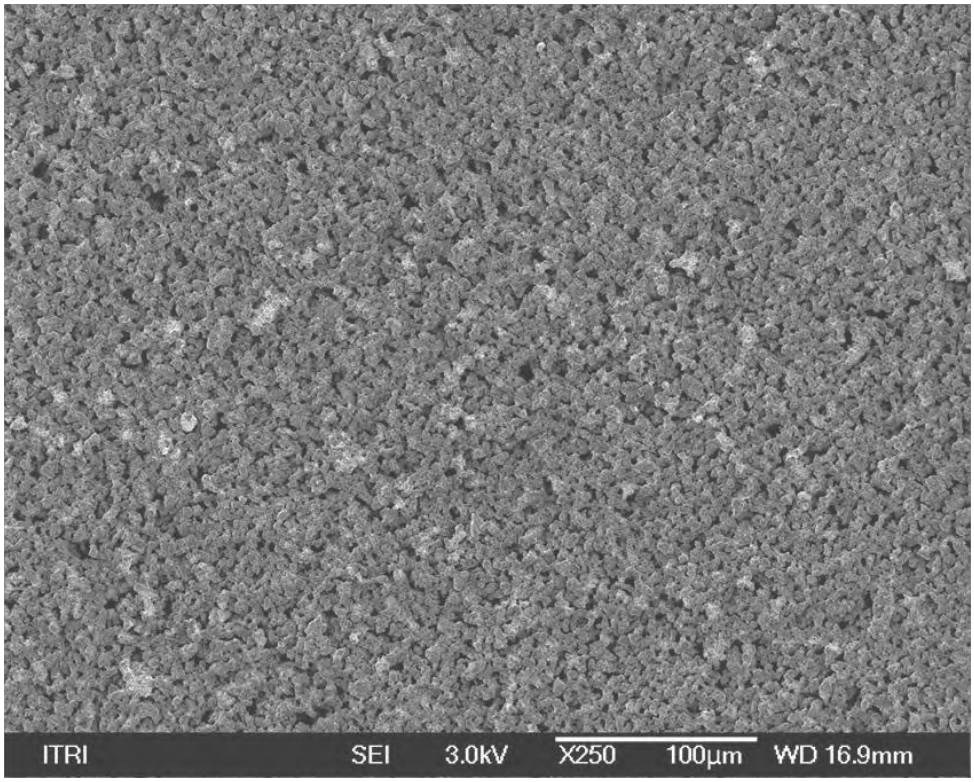

Fig. 3.42 SEM photo of phosphor (LDP-G1) from ITRI

When the vacuum ambient is reducing instead of oxidizing (such as H_2), there would not be an accumulation of O on the surface from the reaction. After S is removed as H_2S, a ZnS surface layer will remain exist. Some works [24] prove and explain that even Zn would also be removed by evaporation after ESSCR process, as the vapor pressure of elemental Zn is much higher than ZnS. The electrons beam at higher energy (for example at 5 keV) could cause rapid evaporation of the metallic Zn produced by ESSCR. Therefore SEM photos may show no change in surface morphology of uncoated particles after degradation [24]. When the ambient is oxidizing, the ZnS is converted to ZnO, a non-luminescent oxide.

The morphology of ZnS was cuboid as seen in the x15000 SEM photo. The smaller quasi-spherical particles could be In_2O_3 or ZnO. Since an oxygen atom is smaller than a sulfur atom, ZnO could not maintain the morphology and size of ZnS. Besides, a spherical particle has a smaller surface energy. The morphology of ZnO could be quasi-spheres with smaller sizes than that of ZnS particles and become more homogeneous [25].

III.5 Conclusion

In the experiment, Neon and Xenon are filled as buffer gas inside the FDDL lamp, in which Ne is the main target gas and Xe is used for the comparision on the start voltage. The radiance and electric parameter are measured when the pressure is controlled around 0.2mbar.

From the experiment results, we can find the luminance of the FDDL has positive relationship with the lamp power. When the lamp power is same, low pressure would help to increase the lamp luminance. Low pressure would keep the high lamp resistance and the high lamp voltage, which would help to enhance the phosphor excitation and reduce the neon excitation emission to make the phosphor dominate in the total luminance. Xe has lager atom radius and is easier to be breakdown. It could turn on the FDDL at lower pressure.

From the FN theory the electrons inside the FDDL does not come from field emission. Right now the lifetime and stable performance may be limited by the electrode material and the gas impurities inside the discharge chamber.

Reference

[1] Chang, Chia-Hao, Bi-Shiou Chiou, Kuen-Shian Chen, Chia-Cheng Ho, et Jia-Chong Ho. The effect of In2O3 conductive coating on the luminescence and zeta potential of ZnS:Cu, Al phosphors . *Ceramics International* 31, no 5 (2005): 635-640. doi:10.1016/j.ceramint.2004.04.011.

[2] Ozawa, Lyuji. *Cathodoluminescence and Photoluminescence: Theories and Practical Applications.* CRC Press, 2007.

[3] http://en.wikipedia.org/wiki/Valence_band

[4] Xiong, Qihua, G. Chen, J. D. Acord, X. Liu, J. J. Zengel, H. R. Gutierrez, J. M. Redwing, L. C. Lew Yan Voon, B. Lassen, et P. C. Eklund. Optical Properties of Rectangular Cross-sectional ZnS Nanowires. *Nano Letters* 4, no. 9 (septembre 1, 2004): 1663-1668.

[5] Z Navrátil et al Collisional–radiative model of neon discharge: determination of E/N in the positive column of low pressure discharge. *J. Phys. D: Appl. Phys*. 40 1037, 2007.

[6]Clementi, E., D. L. Raimondi, et W. P. Reinhardt. Atomic Screening Constants from SCF Functions. II. Atoms with 37 to 86 Electrons. *The Journal of Chemical Physics* 47, no 4 (15 août 1967): 1300-1307. doi:10.1063/1.1712084.

[7]Shimoi, Norihiro, Adriana Ledezma Estrada, Yasumitsu Tanaka, et Kazuyuki Tohji. Properties of a field emission lighting plane employing highly crystalline single-walled carbon nanotubes fabricated by simple processes. *Carbon* 65 (décembre 2013): 228-235. doi:10.1016/j.carbon.2013.08.018.

[8]Fowler, R. H., et L. Nordheim. Electron Emission in Intense Electric Fields. *Proceedings of the Royal Society of London*. Series A, Containing Papers of a Mathematical and Physical Character 119, no 781 (1 mai 1928): 173-181.

[9]Chiguvare, Zivayi. Electric field induced transition from electron—only to hole-only conduction in polymer—fullerene metal-insulator-metal devices. *Journal of Applied Physics* 112, no 10 (15 novembre 2012): 104508. doi:10.1063/1.4767455.

[10] Chiguvare, Z., J. Parisi, et V. Dyakonov. Current limiting mechanisms in indium-tin-oxide/poly3-hexylthiophene/aluminum thin film devices. *Journal of Applied Physics* 94, no 4 (15 août 2003): 2440-2448. doi:10.1063/1.1588358.

[11]Helander, M. G., M. T. Greiner, Z. B. Wang, W. M. Tang, et Z. H. Lu. Work function of fluorine doped tin oxide. *Journal of Vacuum Science & Technology* A 29, no 1 (1 janvier 2011): 011019. doi:10.1116/1.3525641.

[12] Bae, Na Young, Woo Mi Bae, An Na Ha, Masayuki Nakamoto, Jin Jang, et Kyu Chang Park. Low-voltage driven carbon nanotube field emission lamp. *Current Applied Physics, International Conference on Electronic Materials and Nanotechnology for Green Environment*, 11, no 4, Supplement (juillet 2011): S86-S89. doi:10.1016/j.cap.2011.07.014.

[13] Ryu, Je-Hwang, Gi-Ja Lee, Wan-Sun Kim, Han-Eol Lim, Mallory Mativenga, Kyu-Chang Park, et Hun-Kuk Park. All-Carbon Electrode Consisting of Carbon Nanotubes on Graphite Foil for Flexible Electrochemical Applications. *Materials* 7, no 3 (7 mars 2014): 1975-1983. doi:10.3390/ma7031975.

[14] Park, Kyu Chang, Je Hwang Ryu, Ki Seo Kim, Yi Yin Yu, et Jin Jang. Growth of carbon nanotubes with resist-assisted patterning process. *Journal of Vacuum Science & Technology B* 25, no 4 (1 juillet 2007): 1261-1264. doi:10.1116/1.2752513.

[15]Kao, Chih-cheng, et Yu-cheng Liu. Intense green emission of ZnS:Cu, Al phosphor obtained by using diode structure of carbon nano-tubes field emission display. *Materials Chemistry and Physics* 115, no 1 (15 mai 2009): 463-466. doi:10.1016/j.matchemphys.2009.01.013.

[16] Qi, Lai, Burtrand I Lee, Jong M Kim, Jae E Jang, et Jae Y Choe. Synthesis and characterization of ZnS:Cu,Al phosphor prepared by a chemical solution method. *Journal of Luminescence* 104, no 4 (août 2003): 261-266. doi:10.1016/S0022-2313(03)00079-6.

[17] Park, W., K. Yasuda, B. K. Wagner, C. J. Summers, Y. R. Do, et H. G. Yang. Uniform and continuous Y2O3 coating on ZnS phosphors. *Materials Science and Engineering: B* 76, no 2 (3 juillet 2000): 122-126. doi:10.1016/S0921-5107(00)00426-8.

[18] Feldmann, C., et J. Merikhi. Adhesion of Colloidal ZnO Particles on ZnS-Type Phosphor Surfaces. *Journal of Colloid and Interface Science* 223, no 2 (15 mars 2000): 229-234. doi:10.1006/jcis.1999.6648.

[19] Chang, Chia-Hao, Bi-Shiou Chiou, Kuen-Shian Chen, et Jia-Chong Ho. Characterization and conductive coating of phosphors for improved brightness. *Applied Surface Science* 243, no 1-4 (30 avril 2005): 55-61. doi:10.1016/j.apsusc.2004.07.069.

[20] Park, J. H., B. W. Park, K. W. Park, J. S. Kim, G. C. Kim, J. H. Yoo, et Il Yu. Cathodoluminescent and thermal properties of carbon nanotube–ZnS:Cu, Al phosphor composites. *Solid State Communications* 148, no 11-12 (décembre 2008): 573-576. doi:10.1016/j.ssc.2008.09.036.

[21] Swart, H. C., J. S. Sebastian, T. A. Trottier, S. L. Jones, et P. H. Holloway. Degradation of zinc sulfide phosphors under electron bombardment. *Journal of Vacuum Science & Technology A* 14, no 3 (1 mai 1996): 1697-1703. doi:10.1116/1.580322.

[22] Swart, H. C., T. A. Trottier, J. S. Sebastian, S. L. Jones, et P. H. Holloway. The influence of residual gas pressures on the degradation of ZnS powder phosphors. *Journal of Applied Physics* 83, no 9 (1 mai 1998): 4578-4583. doi:10.1063/1.367240.

[23] Darici, Y., P. H. Holloway, J. Sebastian, T. Trottier, S. Jones, et J. Rodriquez. Electron beam dissociation of CO and CO2 on ZnS thin films. *Journal of Vacuum Science & Technology A* 17, no 3 (1 mai 1999): 692-697. doi:10.1116/1.581688.

[24] Abrams, B. L., W. Roos, P. H. Holloway, et H. C. Swart. Electron beam-induced degradation of zinc sulfide-based phosphors. *Surface Science* 451, no 1-3 (20 avril 2000): 174-181. doi:10.1016/S0039-6028(00)00024-8.

[25] Ni, Yonghong, Xiaofeng Cao, Guangzhi Hu, Zhousheng Yang, Xianwen Wei, Yonghong Chen, et Jun Xu. Preparation, Conversion, and Comparison of the Photocatalytic and Electrochemical Properties of ZnS(en)0.5, ZnS, and ZnO. *Crystal Growth & Design* 7, no 2 (1 février 2007): 280-285. doi:10.1021/cg060312z.

General conclusions

In the modern life, artificial electrical light sources play an indispensible role in human's daily life. They could generally be divided into three categories: incandescent lamp, discharge lamp and solid state lamp, which have their own special lighting mechanisms and applications separately. The flat dark discharge lamp (FDDL) is a new discharge lamp whose lighting mechanism is different from the traditional discharge lamp, such as fluorescent lamp or metal halide lamp. The gas discharge is used to provide free charged particles rather than to produce photon emission.

The FDDL works in low pressure, narrow discharge gap and high reduced electrical field. In such a condition it has some common feature with the Townsend discharge, which could help us to make some simple calculation. As no sufficient collisions happen before the electrons hit anode phosphor, the mean free path of excitation and ionization is used to predict the relation between the gas species, gas pressure, discharge gap distance and applied voltage, which could give some quantitative guide for improving the FDDL lamp.

Some basic theoretical analyses are introduced in Chapter II, in which the excitation and ionization mean free paths are used to analyze the physics behind the threshold pressure for the FDDL. Mean free path of excitation λ_{ex} predicts the mean length between the electron excitation collisions, and λ_i defines the mean length between the electron ionization collisions. When $\lambda_{ex} > \lambda_i$, it means in the same space the possibility of excitation collisions is lower than that of the ionization collisions. As the discharge distance for our application is 0.01m, when $\lambda_{ex} > 0.01 > \lambda_i$, it means ionization collisions could provide the electrons to hit the anode phosphor while the seldom excitation collisions would happen in the space, which relates to phenomenon that only the phosphor luminance could be observed.

The plots of the mean free path of different gas species are present in Chapter II after calculation. As the density, diameters and collision cross section of different atoms or molecular are different, the position of the plots are not the same. Their collision cross section decides and the energy distribution will decide the shape and horizontal position. The Maxwell–Boltzmann distribution assumption is given for the energy distribution. Though it may not be so reliable for our condition, it is good enough to agree with the qualitative

analysis. Generally speaking when the electrons energy is lower than 10 eV, the excitation collisions could be more frequent than the ionization collisions. However in this application the electron energy should be larger. Pressure will decide the vertical position of the mean free path lines. Lower pressure will make the lines move upward.

Some feathers of the sample lamps are explored in chapter III, including the phosphor performance (the response of the phosphor to different wave length incident photons) and the uniformity of the lamp.

Besides, the experiment result of FDDL at different pressure filled with Neon and Xenon are present and discussed too. In the experiment, Neon and Xenon are filled as buffer gas inside the FDDL lamp, in which Ne is the main target gas and Xe is used for the comparison on the start voltage. The radiance and electric parameter are measured when the pressure is controlled around 0.2mbar. Based on the voltage –current plot analysis and the Fowler-Nordheim theory, we can distinguish the electrons emission mechanism between the FDDL and the field emission.

From the experiment results, we can find the luminance of the FDDL has positive relationship with the lamp power. When the lamp power is same, low pressure would help to increase the lamp luminance. Low pressure would keep the high lamp resistance and the high lamp voltage, which would help to enhance the phosphor excitation and reduce the neon excitation emission to make the phosphor dominate in the total luminance. Xe has lager atom radius and is easier to be breakdown. It could turn on the FDDL at lower pressure.

The maintenance and possible damage on the electrode and phosphor are also discussed at the end of chapter III. Elimination of impurity molecular (such as O_2 H_2O and H_2) is important to keep the lamp performance and lifetime.

AUTEUR : Yuan ZHANG
TITRE : Etude des lampes à décharge sombre dont le rayonnement provient des luminophores excités par électrons: Application au rétro-éclairage
DIRECTEUR DE THESE : M. Georges ZISSIS
LIEU ET DATE DE SOUTENQNCE : jeudi 4 décembre 2014, salle des colloques de LAPLACE, Toulouse

---

RESUME :
Les sources lumineuses électriques ont été développées il y a environ 200 ans. D'une manière générale, ils se décomposent en trois classes : lampe à incandescence, lampes à décharge et lampe à l'état solide. La FDDL (Flat Dark Discharge Lamp), qui fait l'objet de cette thèse, appartient à la famille des lampes à décharge dans laquelle le mercure n'est pas utilisé. Ainsi, elle est considérée comme une technologie très prometteuse pour l'environnement. Son fonctionnement repose sur le principe de la lampe à décharge basse pression et celui du CRT (Cathode Ray Tube).
Toutefois, son mécanisme d'allumage est nouveau par rapport aux lampes à décharge traditionnels, qui fonctionnent en régime d'arc ou en régime de luminescence. En outre, elle emploie le phosphore qui est largement appliquée dans le CRT. Il convient de souligner que la pression du gaz est inférieure à la pression du mercure dans les lampes basse pression et qu'elle est plus élevée dans le CRT ou FED (Field Emission Display). Cette pression permet de maintenir la lampe à une haute tension. C'est ainsi que les électrons, obtenus par l'ionisation des atomes dans le gaz, seront accélérés ce qui va exciter la substance fluorescente (phosphore). En tant que nouveau candidat, vert et sans mercure, pour l'application dans le domaine du rétro-éclairage, des recherches pour son optimisation doivent être envisagées.
La FDDL fonctionne en dépression, en espace de décharge étroit et dans un champ électrique élevé. Dans un tel état il existe certaines caractéristiques communes avec la décharge Townsend, qui pourront nous aider à faire de simples calculs. Le canal étroit de la décharge est d'autant plus petit que l'épaisseur de la région cathode chute. Comme il n'y a pas assez de collisions qui se produisent avant que les électrons interagissent avec le phosphore de la surface anodique, Le libre parcours moyen d'excitation et d'ionisation a été utilisé pour prédire la relation entre les espèces et la pression du gaz de décharge, la distance d'espacement et de la tension appliquée. Cette étude pourrait donner quelques indications quantitatives pour l'amélioration de la lampe FDDL.
Ajoutons également, des mesures sur des échantillons FDDL, remplis avec du néon, qui aident à connaître certaines caractéristiques de la lampe, y compris l'uniformité de la luminosité, la réponse de phosphore et de la distribution thermique à la surface. Le vert émit par le phosphore n'a pas de réponse aux longueurs d'ondes d'excitation 650 nm et 532 nm, mais pourrait être excité dans le violet (405 nm).
Par ailleurs, nous avons examiné l'influence de différents gaz tampon à différentes pressions, se trouvant à la sortie d'émission globale. De plus, on s'est intéressé à la région fine et inexplorés entre la décharge Townsend (excitation électronique des luminophores) et la décharge luminescente (excitation par collision des électrons avec gaz tampon). A ces régions, les deux mécanismes peuvent contribuer à la production globale et le contrôle pour les effets d'éclairage dynamique.

MOTS CLES :
- FDDL
- Décharge de gaz
- Basse pression
- Haute tension
- Néon

DISCIPLINE ADMINISTRATIVE : Génie Electrique
INTITULE ET ADRESSE DU LABORATOIRE :
Laboratoire plasma et conversion d'énergie (LAPLACE)
118, route de Narbonne, 31062 , Toulouse CEDEX 9

TITLE : A new flat dark discharge lamp for backlight applications based on electron-excited-phosphor luminescence

---

ABSTRACT :
Electrical light sources have been developed for about 200 years. There are three generation light sources: incandescent lamp, discharge lamp and solid state lamp. The flat dark discharge lamp (FDDL) lamp studied in this thesis is a new kind of discharge lamp in which no mercury is used. It borrows the ideas from the general low pressure discharge lamp and the cathode ray tube (CRT).
Its lighting mechanism is brand new compared with the traditional discharge lamps which generally work in the glow or arc discharge regime. It employs the phosphor which is widely applied in the CRT. The gas pressure is lower than the general low pressure mercury lamp and higher than that in the CRT or FED (Field Emission Display). This pressure can maintain high lamp voltage to accelerate electrons to excite the phosphor while the ionization of gas atoms produces electrons in the space. As a new candidate for the green backlight application, an optimum working condition needs to be explored.
The FDDL works in low pressure, narrow discharge gap and high reduced electrical field. In such a condition it has some common feature with the Townsend discharge, which could help us to make some simple calculation. The narrow discharge gap is even smaller than the thickness of the cathode-fall region. As no sufficient collisions happen before the electrons hit anode phosphor, in this study the mean free path of excitation and ionization are used to predict the relation between the gas species, gas pressure, discharge gap distance and applied voltage, which could give some quantitative guide for improving the FDDL lamp.
Measurements on FDDL samples which is filled with neon help to know about some characteristics of the lamp, including brightness uniformity, phosphor response and thermal distribution on the surface. The phosphor emitting green light has no response to 650 nm and 532 nm photon excitation but could be excited by violet (405 nm) light.
Moreover we have investigated the contribution of different buffer gases with different pressures to the overall emission output as we explored the fine and uncharted region between Townsend discharge (electron excitation of the phosphors) and glow discharge (electron impact excitation of the buffer gas) where both mechanisms can contribute to the overall output and controlled for dynamic lighting effects.

KEYWORDS :

- FDDL
- Gas discharge
- Low pressure
- High voltage
- Neon